SITE BLOCKING EFFECTS ON ADSORBED POLYACRYLAMIDE CONFORMATION

A Thesis
Presented to
The Academic Faculty

by

Brett A. Brotherson

In Partial Fulfillment
of the Requirements for the Degree
Doctor of Philosophy in the
School of Chemical and Biomolecular Engineering

Georgia Institute of Technology
December 2007

SITE BLOCKING EFFECTS ON ADSORBED POLYACRYLAMIDE CONFORMATION

Approved by:

Yulin Deng, PhD, Advisor
School of Chemical and Biomolecular Engineering/IPST
Georgia Institute of Technology

Peter Ludovice, PhD, Co-Advisor
School of Chemical and Biomolecular Engineering
Georgia Institute of Technology

Lawrence Bottomley, PhD
School of Chemistry and Biochemistry
Georgia Institute of Technology

James Frederick, PhD
School of Chemical and Biomolecular Engineering/IPST
Georgia Institute of Technology

Preet Singh, PhD
School of Materials Science Engineering/IPST
Georgia Institute of Technology

Date Approved: November 2, 2007

"Get your facts first, then you can distort them as you please."

Mark Twain

ACKNOWLEDGEMENTS

Throughout my work on this research project, I have been fortunate to have been helped by many people making the completion of this research possible. Of these people, the first I would like to thank are my advisors, Dr. Yulin Deng and Dr. Peter Ludovice. Dr. Deng gave me the flexibility in selecting any topic which I was interested in, allowing me to pick the fundamental project I have spent the last 4 years working on. Both Dr. Deng and Dr. Ludovice provided me with many thought provoking discussions which allowed me to remain on a feasible course throughout my work. I would like to thank Dr. Ludovice for helping to arrange for me to get help in my modeling work, an area I will readily admit is not my specialty. Secondly, I would like to thank all of my committee members, Dr. Lawrence Bottomley, Dr. James Frederick, and Dr. Preet Singh, who helped guide me when I needed extra assistance. I would like to thank Dr. Bottomley for many hours of thought provoking conversations which have helped me to develop a good fundamental approach towards solving problems and basic research involving scanning probe techniques. These conversations kept me thinking and never let me settle for anything short of the best work possible.

I owe many thanks to the following companies, who helped me accomplish this research. Ciba Specialty Chemicals synthesized the cationic polyacrylamide I used for my AFM work. MikroMasch performed the focused ion beam milling of my AFM cantilevers, which allowed this work to continue. SNF synthesized a cationic polyacrylamide, similar to that produced by Ciba, for use in the dynamic light scattering experiments. Asylum Research was extremely helpful in their suggestions, assistance, and provisions of code for working with their AFM.

I have been fortunate to have had enormous help from my friends and colleagues here at Georgia Tech. My group members from both advisors have been extremely helpful in assisting me with my work and providing suggestions. Se-Young Yoon, Zhaohui Tong, Ying Wang, Kim Nelson, Hongta Yang, Dr. Qunhui Sun, Dr. Yulin Zhao, Dr. Myung-Chul Park, and the rest of Dr. Deng's group have all helped me with my research here. Andrew Swann and John Melnyczuk were extremely helpful in writing my dissipative particle dynamics code and troubleshooting it throughout my time here. Without their help I would most likely still be attempting to write the code for this work. Kane Barker and Karen Meloy of Dr. Bottomley's group were very helpful in providing me with insight into my research, helping me with a couple of procedures, and allowing me to use their ozone cleaner on a regular basis. Kit Carson was very helpful in his assistance drawing the glass and mica structures. I would like to thank all of my friends who have made my time here very enjoyable: Andy Demaio, Rob Lowe, Cam Thomson, Fran and Matt Walsh, Stef Asher, Liz and Frank Hill, Laura Draucker, Anne Ruffing, and Paul Wissmann. Of course, I must thank Major White for always keeping me company and providing great conversation in the afternoons and evenings here at IPST.

My family have provided me with unconditional support and advice which have made my completion of this work possible. I thank my parents for their support and seemingly endless editing help. My wife, Erin, has helped me extensively with my lab work, data analysis, and maintaining sanity. Without her, I would undoubtably still be at work completing this project.

Thank you all for all of your help and friendship.

TABLE OF CONTENTS

LIST OF TABLES

LIST OF FIGURES

SUMMARY

The use of polymers as flocculating additives is a common practice in many manufacturing environments. However, exactly how these polymers interact with surfaces is relatively unknown. One specific topic which is thought to be very important to flocculation is an adsorbed polymer's conformation. Substantial amounts of previous work, mainly using simulations, have been performed to elucidate the theory surrounding adsorbed polymer conformations. Yet, there is little experimental work which directly verifies current theory. In order to optimize the use of polymer flocculants in industrial applications, a better understanding of an adsorbed polymer's conformation on a surface beyond theoretical simulations is necessary. This work looks specifically at site blocking, which has a broad impact on flocculation, adsorption, and surface modification, and investigated its effects on the resulting adsorbed polymer conformation.

Experimental methods which would allow direct determination of adsorbed polymer conformational details and be comparable with previous experimental results were first determined or developed. Characterization of an adsorbed polymer's conformation was then evaluated using dynamic light scattering, a currently accepted experimental technique to examine this. This commonly used technique was performed to allow the comparison of this works results with past literature. Next, a new technique using atomic force microscopy was developed, building on previous experimental techniques, to allow the direct determination of an adsorbed polymer's loop lengths. This method also was able to quantify changes in the length of adsorbed polymer tails. Finally, mesoscopic simulation was attempted using dissipative particle dynamics.

In order to determine more information about an adsorbed polymer's conformation, three different environmental factors were analyzed: an adsorbed polymer on a surface in water, an adsorbed polymer on a surface in aqueous solutions of varying ionic strength, and an adsorbed polymer on a surface functionalized with site blocking additives. This work investigated these scenarios using a low charge density high molecular weight cationic polyacrylamide. Three different substrates, for polymer adsorption were analyzed: mica, anionic latex, and glass.

It was determined that, similar to previous studies, the adsorbed polymer layer thickness in water is relatively small even for high molecular weight polymers, on the order of tens of nanometers. The loop length distribution of a single polymer, experimentally verified for the first time, revealed a broad span of loop lengths as high as $1.5\mu m$. However, the bulk of the distribution was found between 40 and $260nm$.

For the first time, previous theoretical predictions regarding the salt effect on adsorbed polymer conformation were confirmed experimentally. It was determined that the adsorbed polymer layer thickness expanded with increasing ionic strength of the solvent. Using atomic force microscopy, it was determined that the adsorbed polymer loop lengths and tail lengths increased with increasing ionic strength, supporting the results found using dynamic light scattering.

The effect of the addition of site blocking additives on a single polymer's conformation was investigated for the first time. It was determined that the addition of site blocking additives caused strikingly similar results as the addition of salt to the medium. The changes in adsorbed polymer loop lengths was found to be inconsistent and minimal. However, the changes in an adsorbed polymer's free tail length was found to increase with increasing site blocking additive levels. These results were obtained using either PDADMAC or cationic nanosilica as site blocking additives.

CHAPTER I

INTRODUCTION

Polymers, adsorbed on surfaces, are used in numerous applications for many different purposes including: colloid stabilization, flocculation, lubrication, adhesion, electrical properties, and other surface modifications[89, 133]. Although the effects of these processes, such as the effects of dispersants, have been observed throughout history, it was not until 1974 that these attributes were formally related to the adsorption of polymers on surfaces[156]. Due to the wide use of polymer modified surfaces in many industries, it is important to understand the interactions between polymers and surfaces and the interactions of polymer modified surfaces. With a better understanding of these interactions, the properties and use of polymer modified surfaces can be optimized and extended. This work will concentrate on how polymer modified surfaces can assist or hinder flocculation. However, the information discussed can easily be applied to other surface and colloid phenomena.

This thesis aims to provide a better understanding of adsorbed polymer conformation. This directly affects how well an adsorbed polymer can flocculate particles in a suspension. This project also investigated two factors that are commonly encountered in many industrial settings. These where how electrolytes in solution will affect adsorbed polymer conformation and the effect of site blocking additives on adsorbed polymer conformation. Chapter II reviews the literature on aspects of flocculation, polymer conformation and its measurement, previous studies on the salt effect, and the currently available literature on site blocking. Chapter III outlines the objectives of this research project. Next, Chapter IV outlines the experimental techniques used to complete this research. Following this the results of this project

will be discussed. Chapter V reports the findings on adsorbed polymer conformation. Chapter VI presents the effects of electrolyte in solution on an adsorbed polymers conformation. Chapter VII, for the first time, reports on the effects of site blocking additives on adsorbed polymer conformation. Chapters VIII and IX will discuss the results of the computational modeling and the overall summary, conclusions, and recommendations from this research project.

CHAPTER II

LITERATURE REVIEW

Chapter I introduced the use of polymers for modifying surfaces. This literature review will summarize the conformation of polymers as they adsorb on surfaces and how the conformation will affect the flocculation properties of the polymer modified surface. First, a brief review of flocculation, from a papermaking perspective, will be discussed. Next, background information on polymer adsorption and movement on surfaces will be addressed. Following this, the characteristic structures of adsorbed polymer conformations, theoretical understanding of these conformations, and the different available methods, experimental and theoretical, to determine adsorbed polymer conformation will be reviewed. The final two sections of this literature review will investigate the effect of salts, or electrolytes, and site blocking additives on adsorbed polymer conformations.

2.1 Flocculation

Flocculation refers to the aggregation of small particles into a larger "floc" or agglomerate. Polymer induced flocculation is a commonly used technique in many industries such as water treatment, oil recovery, mining, papermaking, and food processing. In this phenomena, polymers adsorbing on surfaces can help bring small particles together using a variety of different mechanisms. How these mechanisms work is dependent on the type of interactions between the polymer, the surface, and the medium. These interactions can include electrostatic interaction, hydrogen bonding, hydrophobic interactions, covalent bonding, and van der Waals' forces[21]. Polymer adsorption on a surface can be due to more than one of these interactions.

Many manufacturing environments, such as the wet end of a paper machine, contain charged components which can either attract or repulse each other. In papermaking these include: fibers, fines, chemical additive, and fillers. In these manufacturing environments, charged polymers, or polyelectrolytes, can be used to modify the particles in the system allowing flocculation to occur. In these systems, polymer molecular weight, conformation, and charge density can all affect the mechanism through which flocculation occurs[178, 98].

Modern papermaking furnishes are combinations of many different components, one of which is fillers. Many furnishes contain different fillers added to improve the optical and printing properties of the sheet. Most of these fillers have particle sizes ranging from $100nm$ to $10\mu m$[178]. In order to retain these fillers, as the furnish is dewatered on the wire, different polymer based retention aids are used. These polymer based retention aids attach or entrap fillers, in flocs or individually, onto fibers in the furnish. The mechanisms these retention aids use include charge neutralization, patch flocculation, bridging, and multicomponent flocculation[178, 98].

Most of the papermaking furnish components have an anionic charge. This charge results in electrostatic repulsion as these components approach each other. Charge neutralization works to reduce the net charges of the components as close to neutral as possible[237, 98, 178]. This allows van der Waals forces to agglomerate the particles. Cationic polymers with a high charge density and low molecular weight are usually used for this retention mechanism due to their ability to decrease the charge of the components while not extending beyond the electric double layer[178]. This mechanism of flocculation is very weak because van der Waals forces are not as strong as the forces involved in some of the mechanisms described below. This means that the flocs will not be very resistant to shear forces and will redisperse. However, after dispersion they should reflocculate due to the van der Waals forces. Van de Ven has proposed that charge neutralization is not the actual cause of flocculation[267]. He

contends some particles' charges are reversed, causing them to be attracted to each other electrostatically[267].

Patch flocculation is another polymer flocculation method which is used in papermaking, illustrated in Figure 1. In this mechanism, patches of cationic polymer are adsorbed on the surfaces of papermaking components, which allows those regions to become attracted towards other particles while not completely neutralizing the component's charges. It has been shown that the patches on the surface should cover 50% or less of the surface area[86]. Polymers with a molecular weight around 10^5 to $10^6 g/mol$ and a high cationic charge density are generally used[178]. As with charge neutralization flocculation, patch flocculation will redisperse if exposed to shear. However, as before, the particles should quickly and easily reflocculate[178, 98].

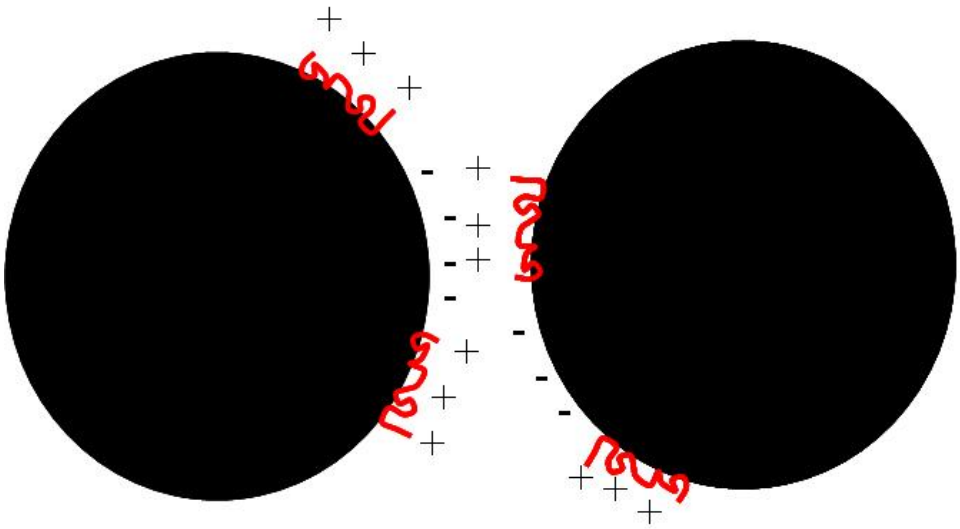

Figure 1: The formation of oppositely charge patches on a particles surface allows electrostatic interactions to floc the particles together.

The third method of flocculation that will be discussed is bridging, illustrated in Figure 2. In this mechanism, polymers with a molecular weight around, or greater, than $10^6 g/mol$ are adsorbed on the particle surface forming loops, tails, and trains, as shown in Figure 4. These loops and tails are then able to adsorb onto other particles causing flocculation. Unlike the charge neutralization and patch mechanisms, the

bridging mechanism is very dependent on the conformation of the polymer on the particles surface. The further into the solution the polymer extends, the greater chance it has of adsorbing on other particles. Because of this, polymers with a low charge density are used. A polymer with a high charge density will try to adsorb in many places to bring the charged groups to the surface, which is electrostatically favorable, but also leaves the polymer relatively flat on the surface. The bridging mechanism also creates flocs which are stronger and more resistant to shear than the previous mechanisms. However, if the shear forces become too great it will break the polymer causing reflocculation to occur using the the patch flocculation mechanism[178, 98].

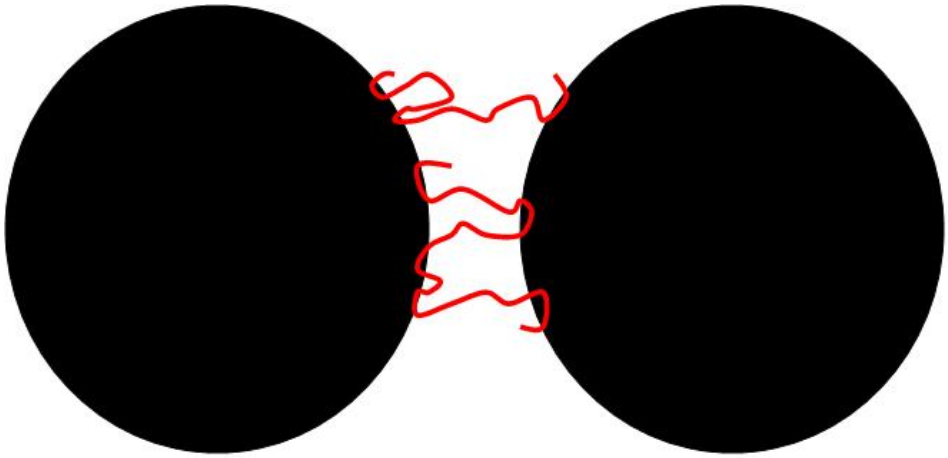

Figure 2: The formation of polymer linkages or bridges allows particles to floc together.

The final polymer flocculation mechanism that will be discussed, multicomponent flocculation, actually includes four different flocculation mechanisms: dual polymer flocculation, microparticle flocculation, network flocculation, and site blocking flocculation[178]. The multicomponent flocculation mechanisms actually work by combining parts of the previous mechanisms discussed to make the polymer more effective in industrial settings.

Dual polymer flocculation makes use of both the patch and bridging flocculation mechanisms. It is primarily used where shear forces will damage the polymer used

in bridging flocculation. First, a cationic low molecular weight polymer is added to flocculate anionic components in a suspension, this uses the patch flocculation mechanism. Following this the suspension is exposed to shear somewhere in the manufacturing process. These shear forces separate the tightly held patch flocs. Immediately following this a high molecular weight low charge density anionic polymer is added. This polymer can bridge between the cationic patches of the other polymer on the surface resulting in a more loosely held floc.

Another multicomponent flocculation mechanism is microparticle flocculation. In this mechanism, a high molecular weight low charge density polymer is added to a suspension. This results in flocculation using the bridging mechanism. As with the dual polymer mechanism, this mechanism works well when the suspension to be flocculated will be exposed to shear forces. Next, the bridged flocs are exposed to shear forces which redisperse the components of the suspension. Following this, anionic microparticles are added to the suspension. These particles attach to the cationic polymer fragments on the components of the suspension allowing the formation of a tightly held resilient floc[257].

The third multicomponent flocculation mechanism is network flocculation. The manner in which this mechanism works has yet to be fully validated[255]. It is known that, in most of the currently used network flocculation systems, hydrogen bonding is the main mechanism for polymer adsorption[178]. This attribute allows network flocculation to be used in suspensions with high amounts of electrolytes or contaminants, which would interfere with electrostatic interactions[178]. Network flocculation starts with the additions of small particles such as phenolic resins or montmorillonite clays which adsorb on the components of a suspension[178]. These components then form colloidal polymer complexes, following the addition of a polymer, which grow in size until they are able to bridge with larger components in the suspension[178].

The final multicomponent flocculation mechanism to be discussed is site blocking,

or enhanced bridging flocculation. This mechanism is the focus of this work. A description of site blocking and its mechanism of flocculation will be discussed in a following section.

2.2 Polymer Adsorption

2.2.1 Background

In order for polymers to modify surfaces, they must adsorb or connect to the surface. The method behind this adsorption is dependent on the polymer, surfaces, and the surrounding medium. The different methods in which a polymer can adsorb are generally grouped into two large mechanisms: chemisorption and physisorption. Chemisorption refers to the formation of chemical bond between the polymer and a surface such as covalent bonding[89, 191]. Physisorption refers to methods which are held more weakly than chemisorbed molecules. Examples of these methods include: hydrogen bonding, hydrophobic interactions, van der Waals forces, and electrostatic interactions[89, 191, 96]. Although hydrogen bonding is considered a chemical bond, its strength is significantly smaller than that of covalent and ionic bonds. This causes it to be placed in the physisorption category. Hydrophobic interactions, in most cases, use a polymer's preferential attraction to certain groups on a surface in lieu of the solvent medium to allow adsorption. Van der Waals force induced adsorption applies to systems in which the attractive portion, or minimum in the Lennard-Jones potential, is just enough close to a surface, to hold a polymer in place against the action of thermal and hydrodynamic forces. Electrostatic interactions, which are the focus for much of this work, involve the pairing of cationic and anionic groups between a surface and a polymer to satisfy electroneutrality. This is the same method used by hydrogen bonding. However, hydrogen bonding is much weaker than most electrostatic interactions. It is possible for adsorbed polymers on a surface to be attached by different mechanisms. Cationic polyacrylamide adsorbing on an anionic

surface can adsorb by both hydrogen bonding and electrostatic interactions. Which of these mechanisms is the most prevalent depends on many factors including the medium, polymer, and surface.

The strength of a polymer attachment to a surface is not the only difference between physisorption and chemisorption. O'Shaughnessy and Vavylonis have reported that physisorption occurs much more rapidly than chemisorption due to the large activation barrier which must be overcome to form a chemical bond[192, 190, 189, 188, 59].

Both of these broad mechanisms are used in industry to adsorb polymers on different surfaces. However, it is important to realize that adsorbed polymers are not required to stay adsorbed on a surface regardless of the adsorption mechanism. It is always possible for the energy of the polymer molecule to exceed that of the attachment to the surface causing the polymer to desorb[39]. While the mechanism of adsorption does not prohibit desorption it is important to note that desorption rates in chemisorbed polymers are usually very small and in most cases are ignored[192]. In this regard, the energy of attraction between the individual monomer units and a surface are of extreme importance to polymer adsorption and the stability of the adsorbed polymers[270, 271, 48]. The interactions of the specific monomer which will adsorb and the surface are extremely important to the adsorption stability of a polymer on a surface, but the size of the monomer units in the polymer chain also can affect the adsorption energy[271]. Polymers with less bulky side groups tend to have stronger adsorption energies and have a higher stability when adsorbed on a surface[271].

Another important factor, in the ability of a polymer to desorb from a surface is the molecular weight, or length of the polymer. With higher molecular weights, a polymer is more likely to have multiple attachment points to a surface. This decreases the chances of complete desorption from the surface[281]. As individual attachment points desorb from a surface others will be forming. The maximum number of adsorption

points increases with increasing polymer molecular weight.

Cosgrove found that, overall, the rate of polymer desorption is much lower than the rate of polymer adsorption[56]. This is most likely due to the fact that adsorbed polymers in many cases have multiple attachment points and the results of Wang *et al.* are illustrated[281]. However, for polymer adsorption only one attachment point must be made.

The factors influencing polymer desorption above deal primarily with the properties of the surface and polymer. However, the medium in which the polymer and surface are immersed, also plays an important role in the adsorption and desorption of a polymer on a surface. Factors such as mechanical and thermal energy will increase the rate at which polymers desorb from a surface[39, 281]. However, other species present in the medium will also affect the rate of polymer desorption. The effects of electrolytes have been extensively studied and found to have very significant effects on polymer adsorption and desorption[202, 245, 244]. This topic will be investigated more thoroughly in a later section. Just as with electrolytes, other molecules and polymers present in the medium can also directly affect the adsorption and desorption of polymers from a surface[270, 271, 89].

2.2.2 Movement

Adsorbed polymers on surfaces retain a dynamic character as they move towards a low energy conformation on the surface. This is done by rearrangement, or movement, on the surface to achieve the lowest energy state possible. Both polymer adsorption and desorption, regardless of the mechanism of attachment, are affected by the movement or relaxation of a polymer on a surface. A large amount of work has been performed both experimentally and theoretically to show this behavior[200, 201, 38, 2, 280, 291, 298, 8, 193, 194, 195, 1, 274, 273, 199, 87, 236, 47, 51, 50, 202, 192, 196, 284, 222, 4, 3]. Figure 3 illustrates this movement.

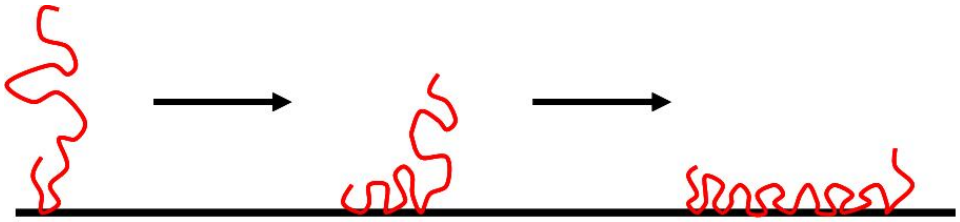

Figure 3: The progression of polymer spreading on an attractive surface over time.

Van Eijk *et al.* have described the movement of a polymer on a surface as a function of transport to the surface and spreading on the surface[274]. Initially, for high molecular weight polyelectrolytes, an adsorbed polymer will occupy a coiled conformation on a charged surface. After a period of time on a uniform surface the polymer will spread out to occupy a more flat conformation which will minimize the energy state the polymer occupies. The rate at which this occurs is dependent on the degree of surface coverage by the polymer and the charge density of both the polymer and the surface[3, 48]. If the polymer surface coverage is high, the ability of the polymer to spread out will be hindered by other polymers blocking possible adsorption sites.

If the polymer adsorption is governed by electrostatics, then the charge densities of the surface and polymer play critical roles. When both the surface and the polymer have high charge densities and opposite charges, it is energetically favorable for the polymer to adsorb at as many points as possible. This causes a much quicker spreading of the polymer on a surface. The presence of unadsorbed polymer in the solvent phase can also affect the rate of polymer spreading on a surface[196]. Oulanti *et al.* found that the presence of unadsorbed polymers accelerates the spreading of polymers already adsorbed[196]. The degree of polydispersity of a polymer sample will also affect its spreading rate as higher molecular weight polymers will displace low molecular weight polymers given time[202, 49, 50].

Another factor in the rate and ability of a polymer to spread or move about on a surface is the flexibility of the polymer chain[236]. Large bulky side groups can make a

polymer less flexible and less able to attach to a surface. This will inhibit the ability of the chain to flatten out. Previously, the effect of polymer concentration in the solution on spreading on a surface was described. The properties of the entire system can also play a role in the rate of spreading. At low temperatures, the energy available to each polymer molecule is diminished. This results in a much slower rate of spreading or relaxation[298, 38]. Chakraborty and Adriani have shown, via simulations, that polymer spreading rates exhibit a non-Arrhenius temperature dependence[38].

The times necessary for polymer spreading to reach an equilibrium vary depending on the polymer, surface, and medium. These have been reported as short as $25 seconds$ to as long as several hours[3, 222]. These times are for polyelectrolytes adsorbing on oppositely charged surfaces by electrostatic interactions. As was mentioned in the previous section the time and energy necessary for a chemisorbed polymer is much greater[2].

2.3 Adsorbed Polymer Conformation

In the previous section, the adsorption of polymers on surfaces was explained as a method to lower the energy state of the polymer. The movement of a polymer on a surface was an extension of this idea. However, no details were given as to what the polymer's structure on the surface is after it has adsorbed. As in the previous section, the energetics of the system will dictate what an adsorbed polymers structure is. Past researchers have described the structural features of an adsorbed polymer as loops, trains, and tails, an idea first proposed by Jenkel and Rumbach in 1951[126]. Figure 4 illustrates these structural features.

In the previous discussion of polymer adsorption on surfaces, the effects of many different conditions were described. These factors all play important roles in the adsorbed conformation of a polymer on a surface. Past researchers have described the conformation of polymers on surfaces using three different characteristic structures:

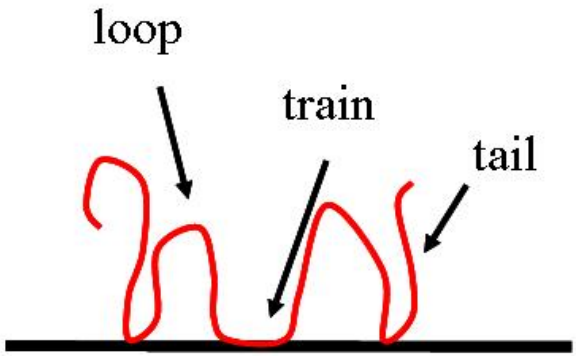

Figure 4: The characteristic structural components of an adsorbed polymer.

"pancake", "mushroom", and "brush"[248]. These structures are illustrated in Figure 5.

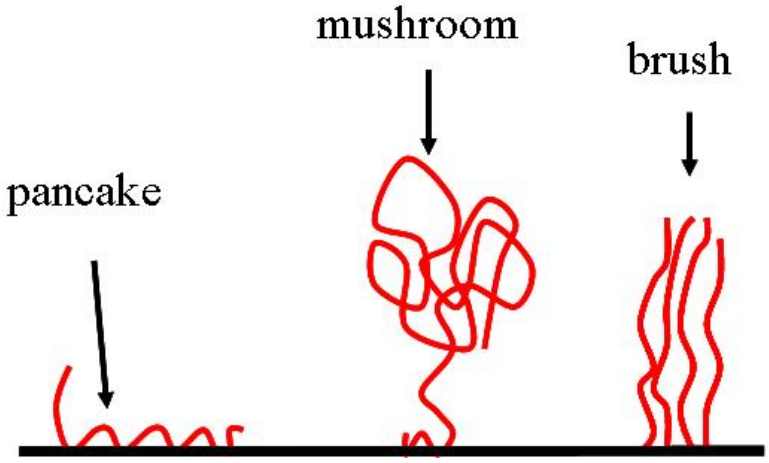

Figure 5: The three generalized characteristic structures of an adsorbed polymer. The brush structure shown is the result of multiple polymers.

Polymer affinity for a surface is one of the conditions which will greatly affect an adsorbed polymers conformation. This effect is directly connected to the distribution of groups in a polymer backbone capable of adsorbing on a surface. If it is not energetically favorable for a polymer to adsorb on a surface, or for most of the polymer to adsorb, there will only be a few attachment points on the surface. This will result in very long loops and tails with short train regions. The distributions of the monomeric units, which favorably adsorb, will also affect this. For example, if all the monomeric units which favor adsorption are on one end of the polymer,

there will be a train followed by a tail. The length of these features is directly dependent on the amount of each monomeric unit in the polymer chain. Similar to this condition, the charge density of polyelectrolytes and surfaces will directly affect the resulting polymer conformation and structure. If the polymer and surface have opposite charges and high charge densities, it is likely that the resulting structure would be a "pancake" due to the ability of the polymer to minimize its energy state by adsorbing on the surface. If the charge density of the polymer is lower, a structure with larger loops and tails would be expected. The size of the monomeric units in the polymer backbone will also affect the structure of an adsorbed polymer. Bulky side groups on the polymer backbone can make multiple adsorption points less likely resulting in large loops and tails, or conformational structures which appear to have a single attachment and a straight chain.

The concentration of polymers adsorbed on a surface will also affect the conformational structure of adsorbed polymers. As the concentration of polymers on a surface increases, competition for available adsorption sites increases. Combined with this, steric hindrance and electrostatic hindrance, in the case of polyelectrolytes, will prohibit the polymers from getting too close to each other. This will move structure from a "pancake" at low concentrations, to a "mushroom" at higher concentrations as hindrance pushes the polymer away from the surface, and finally to a "brush" where the surface is nearly saturated by adsorbed polymers and the hindrance between them causing an upright relatively straight conformation.

The molecular weight of a polymer will also affect the structure of its adsorbed conformation. Cohen Stuart *et al.* showed a relationship between the molecular weight of a polymer and its adsorbed conformation[52]. As the molecular weight of the polymer increases it is less likely that the polymer will reside in a "pancake" conformation. This is due to not only the steric constraints from the chain, but also due to reducing the polymer's entropy by tightly adsorbing it to a surface. Cohen

Stuart *et al.* were also able to relate the adsorbed polymer structure to the radius of gyration for a free polymer in dilute solution as a function of the molecular weight of the polymer[52]. They found that for low molecular weight polymers the adsorbed polymer structure had a thickness less than its radius of gyration. However, as the molecular weight of the polymer increased the adsorbed polymer structure thickness was found to be similar to twice the radius of gyration.

The properties of the surrounding environment will also affect the adsorbed polymer structure. Previously, it was mentioned that temperature will affect polymer adsorption, desorption, and movement on a surface. As the temperature of the surrounding environment of an adsorbed polymer increases, the structure of the polymer will move more from a "pancake" conformation towards an extended "mushroom" or "brush" conformation[41]. This is due to the increased energy in the polymer, which allows it to move around and extend more than a less energetic polymer. Chibowski *et al.* also found a adsorbed structure dependence on pH[41]. They found that for polyacrylic acid adsorbed on zirconium oxide, increasing the pH caused an extension of the adsorbed polymer conformation[41]. They attributed this to the increased dissociation of carboxylic acid groups on the polymer chain leading to a negatively charged chain[41]. This, coupled with the increasing negative charge of the zirconium oxide surface, as the pH increased, resulted in electrostatic repulsion causing the chain to extend away from the surface[41].

Another property of the surrounding medium is the concentration of electrolytes in solution. The effects of electrolytes has been extensively studied and found to have very significant effects on adsorbed polymer conformation[202, 245, 244]. This topic will be investigated more thoroughly in a later section. The effects of other polymers and electrolytes can cause changes in adsorbed polymer conformation depending on the specific interactions[270, 271, 89].

2.3.1 Theoretical Models

Not all information necessary to completely understand why a polymer adopts a particular conformation can be obtained experimentally. To assist in the understanding of polymer adsorption, movement, and conformation on a surface, several different theoretical models have been developed. Fleer *et al.* divided these models into two different groups: models which track chain conformation statistics, and those which model the concentration profile of a polymer on a surface[89].

Those models which track a polymer chain's conformation based on conformation statistics can be divided into models which use an exact enumeration technique, the Monte Carlo method, self-consistent mean field theory, or models which explicitly account for loops, tails, and trains[89]. By following the random walk procedure, the exact enumeration technique calculates every possible conformation a polymer can have on a surface without occupying the same space. Many researchers have used this method to gain insight into adsorbed conformation and how this may affect other properties[171, 55, 246, 282, 140, 138, 139, 265]. Using this technique, the location where a polymer is attached to a surface and its resulting conformation can be determined[265]. In most exact enumeration models, the effects of the solvent is not accounted for[89]. However, Lax discovered that this oversight can cause considerable conformational changes in the resulting structures[138]. This problem aside, the main reason exact enumeration is not used very often for polymer conformation studies is due to its high computational cost[89]. The longest polymer chains modeled were only 24 units long and this required a large amount of processing time[89].

The second modeling technique is the Monte Carlo method. This method starts with an initial conformation of a polymer, on or off the surface, and randomly moves the chain. After this movement, the energy of the chain is calculated and if it increases beyond a reasonable amount the conformation is discarded and the original

conformation is used again. Using this method, the number of steps and conformations evaluated is significantly reduced lowering the computational expense of the model[89]. This method has been used to not only predict possible adsorbed polymer conformations, but also to investigate the conformation of polymer chains in solutions[45, 129, 213, 238, 210, 101, 42]. Although faster than the exact enumeration technique, the Monte Carlo method does not, however, solve the problem of accommodating large polymers with a reasonable amount of computation time[89]. It also is calculated on a time scale of picoseconds to nanoseconds, making its applicability to actual systems difficult[89].

The self-consistent mean field lattice method reduces the number of calculations of the previous two methods. This is done by dividing up the space a polymer can occupy into a lattice. Using just this division of space, many early researchers were able to cut significant amounts of time from the simulations of small molecules and oligomers[23, 160, 9, 89]. However, in order to model larger polymers further steps needed to be taken. Many researchers have confronted this task and come up with reasonable approach to reduce the computational time[81, 223, 82]. To save time, the polymer only remembers where it was in the previous step. This allows a polymer to fold back on itself and occupy the same lattice site every two steps. These researchers also biased the lattice so polymers near an attractive surface had weighted surface layers[89]. These two enhancements accelerate the process by constraining the polymer slightly. In the previously mentioned studies, a polymer was not allowed to interact with itself or other polymers, only the surface[89]. It should also be noted, this case is not applicable for systems such as polyelectrolytes. Scheutjens and Fleer extended these models to account for interacting chains[232, 233]. In these models the weighting of interactions did not only occur relative to the surface, they extended in all directions allowing interactions with other molecules to be accounted for[89]. This method has been widely used to theoretically model adsorbed interacting polymer's

conformations[84, 249, 143, 69, 131, 152, 292, 137, 165, 289, 70, 299].

The final type of conformational models which will be discussed are those which consider a polymer, not as individual monomers or chemical groups, but rather a group of trains, tails, and loops. The adsorption of trains on a surface is governed by the energetics of the system, while the loops and tails are governed entirely by entropic arguments[89]. After a modeled polymer is adsorbed on a surface, the conformation is obtained by looking at the number of possible conformations of the polymer with the given number of attachments and units in loops and tails. From this an energetically favorable conformation can be found. During the calculation of possible conformations, this model starts at an attachment point and then uses random walk statistics, all equally viable, to determine the possible end points of a loop, tail, or entire chain[89]. When using random walk statistics, some constraints must be put on the system to prevent the polymer from moving through, or adsorbing in, a surface. These constraints, or "forbidden walks", are calculated using the methods of Hesselink[116].

The next group of models are those which deal with the concentration profile of a polymer on a surface and disregard actual chain conformations. These modeling techniques can be divided into three main approaches: lattice models, the Cahn-Hillard method, and scaling theory[89]. Although these models are affected by the actual chain conformation, it is impossible to accurately show the conformation through these techniques[89].

The lattice model, in its most basic form, works by evaluating the entropy and energy of mixing of chains around a surface[89]. This governs the structure of a polymer on a surface through the competition between the energetic costs of contacts between polymer units and the conformational entropy developed by avoiding this contacts[114]. In the lattice model, the volume near a surface is divided into lattice sections. This allows the calculation of the concentration profile of a polymer at

set distances from the surface. These models begin by filling the lattice sites with either polymer, surface, or solvent components[115]. As the free energy of mixing is calculated and evaluated, for different conformations, the concentration profile of the polymer at distances from the wall can be calculated[283]. This concentration profile is the end result of this modeling technique. It can then be related to other polymer characteristics such as the Flory-Huggins χ parameter[283].

Use of the Cahn-Hillard modeling technique to determine concentration profiles is similar to the lattice method, however, the free energy is calculated differently, using a square gradient approach[33]. These calculations relate the square of the concentration gradient to the sum of the free energy and the gradient of the free energy. A clear explanation of this can be found in Fleer *et al.*'s book[89]. This method was first applied polymer coated surfaces by Klein and Pincus[130]. However, this method did not account for the tails of adsorbed polymers making the validity of the results questionable[72, 234]. In their work, Scheutjens *et al.* found that unless the tails of adsorbed polymers are ignored the relationship of the free energy to a square of the concentration gradient is not valid[234]. Other researchers have, however, found that for specific cases this technique can be used to model the concentration gradient of adsorbed polymers[29, 89].

The final theoretically modeling technique which will be discussed is that of scaling theory. Scaling theory was introduced by De Gennes as a method to model the decrease in adsorbed polymer conformation moving away from a surface. In the scaling approach the assumption that the tails are not important is not taken, however, large loops and tails extending far into solution may be scaled out by the models[72]. The scaling technique starts similar to that of the Cahn-Hillard technique by relating the concentration profile to the free energy of the system. It does not, however, follow the square gradient relationship.

Many simplifications are made by scaling, including the removal of all numerical

values which do not change the shape of the concentration profile are removed[89]. De Gennes' scaling theory has been adopted and used by many researchers to not only investigate adsorbed polymer concentration profiles but also to relate them to adsorbed polymer conformations[11, 10, 241, 108]. A more in depth review of de Gennes scaling methods can be found in his text and publications in Macromolecules[71, 72, 73].

2.4 Methods of Measurement

In order to understand adsorbed polymer conformations and the factors affecting them, it is necessary to be able to experimentally verify what the conformations actually look like. Portions of the following section were reproduced with permission from Macromolecules[30], copyright 2007 American Chemical Society. There have been many different experimental techniques used in past research to determine the adsorbed conformation of a polymer on a surface. These methods include Brewster angle reflectivity, total internal reflectance fluorescence, dynamic light scattering, surface force analysis with a force-balance apparatus, nuclear magnetic resonance, transmission electron microscopy, neutron reflectivity, small-angle neutron scattering, and atomic force microscopy[248, 57, 59, 60, 15, 16, 177, 175, 176]. Brewster angle reflectivity, total internal reflectance fluorescence, dynamic light scattering, and surface force analysis with a force-balance apparatus all provide information on the thickness of an adsorbed polymer layer. Nuclear magnetic resonance, transmission electron microscopy, neutron reflectivity, small-angle neutron scattering, and atomic force microscopy all provide more specific information as to the actual conformation of an adsorbed polymer.

Brewster angle reflectivity, or ellipsometry, is an optical test where light passes through different materials with different increasing refractive indices[248, 89].At the Brewster angle the sample will emit zero-plane-polarized reflected light. If another material of a different density is adsorbed on a surface, the Brewster angle will

change. This technique has been used to determine the thickness of adsorbed polymer layers[231, 297, 183, 230, 229, 251, 250, 209, 211, 252]. One limitation of this approach is that one must assume a constant density in an adsorbed polymer layer. This assumption is necessary in order to have a constant refractive index in the polymer layer. However, this is not necessarily true leading to errors in the calculated adsorbed layer thickness.

Total internal reflectance fluorescence is another technique which provides information about the thickness and conformation of an adsorbed polymer layer. In this technique, light is internally reflected through a waveguide. When this waveguide is coated with polymers containing fluorophores, the evanescent field excites the fluorophores in close proximity to the surface[248]. Thus, from the fluorescence intensity, a surface concentration of adsorbed polymer and thickness can be determined. This method has not been popularly adopted by many researchers, but has been used for this purpose at times[231, 95]. One disadvantage of this technique is that the polymer used must contain fluorophores in order for measurements to be made. In most cases, this is not applicable. Also, problems will arise with labeling polymers with fluorophores, generally somewhat bulky groups, due to altering the structure of the polymer chain, thus altering the resulting conformation.

Another experimental technique used to gain information on the thickness of adsorbed polymer layers and their conformation is dynamic light scattering. This technique was used in the experimental work for this project and will be discussed in more depth in the experimental section. Briefly, dynamic light scattering is performed by monitoring the fluctuations in scattered light focused through a solution of particles in a solvent. These particles move around through Brownian motion and their rate of diffusion can be found through the changes in scattered light intensity. Using the Stokes-Einstein equation, Equation 5, this diffusion rate can be related to a particle's hydrodynamic diameter[43]. To determine the thickness of an adsorbed polymer

layer, polymer is added to the solution of particles. As the polymers adsorb on the particles their rate of diffusion will slow down which can then be related to a larger hydrodynamic diameter. The difference of these two diameters divided by two is the adsorbed layer thickness. This technique has been used by many researchers to gain information on adsorbed polymer conformations, flocculation rates, and adsorbed layer thicknesses[267, 179, 169, 185, 276, 286, 119, 167, 296, 207, 128, 75, 268, 105, 136, 66].

One problem with all of the experimental techniques discussed to this point is the issue of how small polymer particles scatter light. With dynamic light scattering, it is generally assumed that the hydrodynamic radius relates to the outermost points of the polymer layer. This is assumed following the work of Nelson and Cosgrove, who reported that the tail region of an adsorbed polymer has the largest effect on the hydrodynamic diameter in dynamic light scattering[179]. However, this is not a uniform layer and the scattered light and may be affected by the large amount of void volumes in the adsorbed polymer layer. Also, the diffusion rate is calculated assuming spherical geometry. The porosity and structure of the adsorbed polymer layer can result in different flow characteristics altering the reported hydrodynamic diameter[198].

Dynamic light scattering hydrodynamic diameters are also subject to changes in polymer conformation due to the concentration of polymer on a particle surface. It is assumed that the polymer layer on a particle is uniform in dynamic light scattering, however, this is not the case. In order to have the most uniform polymer layer, the structure of the adsorbed polymers must be that of a dense "brush". To do this the adsorbed polymer conformation has already been altered. In the cases of polymers of a "mushroom" or "pancake" structure it is difficult to describe the polymer layer as uniform.

The final experimental method to measure a polymers adsorbed layer thickness is surface force analysis using a force-balance apparatus. A force-balance apparatus

contains two surfaces which can be brought together mechanically. As these surfaces are brought together or moved past each other the force between the surfaces is measured using variable stiffness force-measuring springs[248]. These experiments can be run in both aqueous and vapor environments. The resolution for this apparatus is $0.1nm$ and is sensitive to forces as small as $10^{-8}N$[123]. Taunton *et al.* have adsorbed polymers on the surfaces used in this apparatus and measured the distance at which they first begin to feel the other surface[263, 262, 261, 26, 63]. Using this method, the adsorbed polymer layer thickness can be determined.

Similar to the use of polymer concentration profiles, in polymer adsorption theory, to determine adsorbed polymer conformation, the use of adsorbed polymer layer thickness can not give actual polymer conformation data. This adsorbed layer thickness in most experimental techniques is representative of the outermost adsorbed polymer distances. However, what that polymer's conformation is like within this layer is unknown. Figure 6 illustrates two scenarios where the adsorbed polymer layer thickness would be identical, but the actual conformations are far from this.

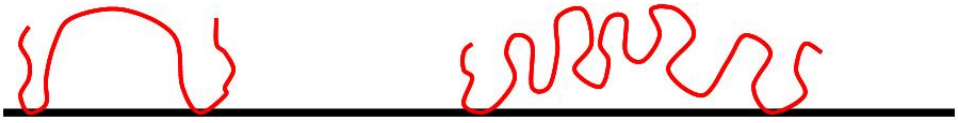

Figure 6: Illustration of how adsorbed layer thickness can misread actual conformation. Both of these conformations would give the same adsorbed layer thickness.

Most experimental techniques assume a conformation similar to the diagram on the left of Figure 6. However, if this is not the case, important information about the system and the adsorbed polymer's conformation is being overlooked. In order to get around this problem, other experimental techniques have been developed which give more detailed information regarding an adsorbed polymer's conformation. These techniques include: nuclear magnetic resonance, transmission electron microscopy, neutron reflectivity, small-angle neutron scattering, and atomic force microscopy.

Nuclear magnetic resonance, NMR, spectroscopy has been developed as a powerful

tool for determining the fraction of a polymer which is adsorbed on a surface[89]. In high resolution NMR of multiphase systems, many of the filters which the signal runs through will only allow mobile, or liquid like, components to be detected[89]. In this system, when polymers adsorb on a surface part of their signal becomes invisible because it is bound to a solid phase. By comparing this new signal with that of a well characterized control system, the amount of bound polymer can be quantified[89]. This has been applied to adsorbed polymers by different groups of researchers[172, 79].

Using NMR there are two other experimental techniques which can be used to determine adsorbed polymer bound fractions: pulsed NMR studies, and solvent relaxation[89]. Both of these techniques have been explored extensively by Cosgrove and fellow researchers[15, 16, 58, 64, 65, 57, 269, 60, 61, 168, 180, 90, 91]. In each, the decay, or relaxation, of the spin of the system is analyzed. In solvent relaxation, only the that of the mobile solvent phase is considered. In the pulsed NMR technique, the decay of the solvent and solid states must be deconvoluted and analyzed[89]. These NMR techniques provide a quantitative amount of polymer bound fractions. However, it is impossible to determine how many polymers are being analyzed and if the entire polymer is being analyzed.

The use of transmission electron microscopy to elucidate adsorbed polymer conformation was recently developed by Nanko *et al.*[177, 175, 176]. Most polymers are not conductive, which makes imaging them with electron microscopy nontrivial[272]. To get around this problem, Nanko labeled the polymers with gold nanoparticles[177]. This allows the researcher to locate the nanoparticles and therefore get an idea of where the polymer could be. This method has a couple significant barriers towards its use: the sample must be dry and run under vacuum, and the polymer must be labeled with gold nanoparticles. The dry state required Nanko *et al.* to remove water with paper towels prior to placing the sample in a transmission electron microscope. As the water is drawn away it will move the adsorbed polymer in the direction of the

flow. Nanko *et al.* interpreted this to mean the polymers always stick out in nearly straight lines. However, this is not supported by any other experiments or current theory on adsorbed polymer conformation. The second requirement of labeling the polymer with gold nanoparticles will greatly affect the polymer conformation. The gold particles can be considered bulky side groups which will cause great steric hindrance and also interact with both the substrate and the solvent phase. Therefore, this technique has not been widely adopted.

The next experimental techniques, neutron reflectivity and small-angle neutron scattering, are able to give density profiles of polymers adsorbed on a surface in the direction perpendicular to the surface. This technique can be used to gain very specific information about an adsorbed polymer's conformation. Similar to light scattering, small-angle neutron scattering detects the intensity of scattered neutrons to image objects. With respect to polymers adsorbed on a surface, neutron reflection is used[117, 217, 93, 100, 181, 63, 62, 57, 80]. Most of these studies are done by either labeling the polymer with hydrogen isotopes, such as deuterium, or performing the experiments in heavy water[117]. Unlike other methods of labeling polymers, this should add no additional size to the polymer or restrict its movements in any way. These techniques, however, are very sensitive to the amount of liquid the neutrons must travel through and the reflection that can occur from the solid surface which the polymer adsorbs on[117]. It is also impossible to determine how many polymers are being visualized and if the complete polymer is being visualized. All that being said, the most formidable barrier is the relatively inaccessibility of this equipment to most researchers.

2.4.1 Atomic Force Microscopy

The last experimental method which will be discussed is the use of atomic force microscopy, AFM, to determine adsorbed polymer conformation. There are two AFM

techniques which have been used to determine information about an adsorbed polymers conformation: tapping mode AFM, and force "pulling" experiments[135, 108].

Tapping mode AFM is a commonly used technique to image surfaces and features on a very small scale. Kumaki and Hashimoto looked to use this technique to image single polymer molecules adsorbed on a mica substrate[134]. To do this a clean mica surface was functionalized using a Langmuir-Blodgett trough with a monolayer of polymer. This was allowed to dry and was then imaged with an AFM tip. The authors reported that the polymers did not coalesce during drying or transfer to the substrate, and they published images which appear to be single polymers adsorbed on a mica surface[134]. Recently, Roiter *et al.* have also used the tapping method to image individual polymer molecules on mica surfaces[226, 224, 225, 170]. Roiter *et al.* imaged polymer molecules in water not air, removing the effects of capillary action on the coalescence of polymers on the surface. Using this method Roiter *et al.* were able to simplify the polymer preparation procedure by simply injecting a polymer solution onto the mica sheet in water[226, 224, 225, 170].

Although imaging with tapping mode AFM is a very precise technique, its use to image polymers on surfaces still requires much verification. From the work of Kumaki and Hashimoto, the drying of a polymer on a surface will have dramatic effects on its conformation[135, 134]. The capillary forces which are present during drying could easily pull physisorbed polymers together making verification of a single polymer difficult. If the polymers were covalently attached at all points to the substrate it is possible that this technique could work.

Another problem with this technique is that once dried the adsorbed polymer must lay flat on the surface, again due to capillary forces. This means that all information on loops and tails or adsorbed polymer layer thickness are lost. The work of Roiter *et al.* avoided the problem of capillary forces by performing all experiments *in situ*[226, 224, 225, 170]. However, *in situ* polymers, which are physisorbed

to surfaces, will constantly be in motion and adsorption points will change as the adsorption/desorption process occurs. With tapping mode imaging, the tip will hit the surface which allows the polymer to be pushed and pulled around the surface by the AFM tip. This will change the adsorbed conformation of the polymer which is being imaged. There is also the possibility that the polymer will physisorb to the tip and be moved around. Similar to the Kumaki method, this method also is unable to reveal information on the number of attachments, the length of loops or tails.

Unlike imaging polymers with tapping mode AFM, force "pulling" experiments, or force spectroscopy, do not raster a tip across a surface preventing the tip from dragging polymers around on the surface while being imaged. In this technique, an AFM tip is pulled from a surface, or polymer, and the force-distance curve is evaluated to determine a number of different properties. This technique was initially used on polymers by Gaub *et al.*[221, 294]. In force spectroscopy, an AFM tip is brought into contact with a surface and the lever is deflected. The tip is then retracted from the surface and the deflection of the lever is monitored. From the change in deflection of the tip as it is pulled from the surface, the interaction force and the elasticity of the molecule or bond can be calculated based on the spring constant of the cantilever. This technique has been used to evaluate the adsorption force and interaction forces of many polymer systems[294, 142, 278, 67, 287, 239, 5, 46, 125, 295, 288, 32, 293, 54, 150, 253, 37, 149, 240, 102, 107, 187, 151, 221, 203, 92, 141, 141, 147].

Another technique using force spectroscopy is the analysis of adsorbed polymer loop lengths using AFM. In this technique, the distance between quick deflections of the lever, representing the desorption of polymer attachments, is measured giving the straight chain length of the polymer loop. This method has been used by many researchers to gain information about adsorbed polymer conformations[240, 241, 5, 6, 24, 53, 107, 108, 109, 146, 148, 220, 36, 184, 215, 121, 40, 145, 144]. However, the experimental techniques used in many cases make the interpretation of the data difficult

or impossible without significant assumptions. AFM "pulling" experiments are used to determine polymer loop lengths by observing the deflections of the cantilever as it is pulled away from the surface. Figure 7 shows a typical polymer desorption event and how it may reflect the adsorbed polymer's conformation. As the tip is pulled up from the surface, moving right in Figure 7, the polymer chain stretches out. When a desorption point is approached, the straight polymer chain now begins to deflect the cantilever until enough force is applied to cleave this attachment. At this point, a sudden decrease in deflection is seen.

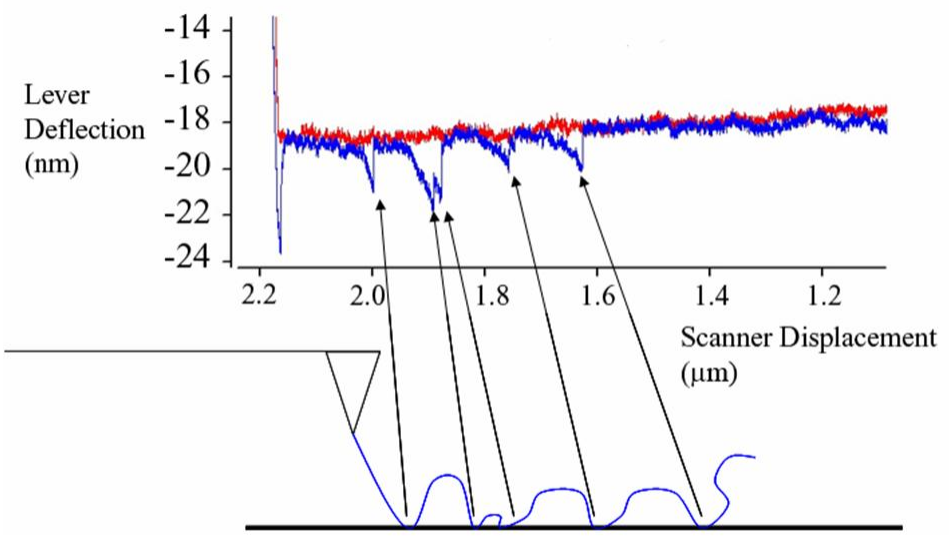

Figure 7: Illustration of how force curves can be used to obtain information on an adsorbed polymers conformation. Reproduced with permission from Macromolecules[30]. Copyright 2007 American Chemical Society.

In an AFM "pulling" experiment, the polymer can be attached to both the tip and substrate by either physisorption or chemisorption. Thus, there are three different scenarios in a "pulling" experiment: physisorption on both the tip and the surface, physisorption on one surface and chemisorption on the other, and chemisorption on both the tip and the surface. When polymers chemisorb to both surfaces, the force

profile tracks cleavage of a covalent bond[97]. Many of the currently used techniques involve bringing a clean tip or a tip laden with physisorbed polymers to a surface that may or may not contain physisorbed polymers[40, 145, 144, 240, 241]. Figure 8 shows some of the many different possible scenarios of a "pulling" experiment like this.

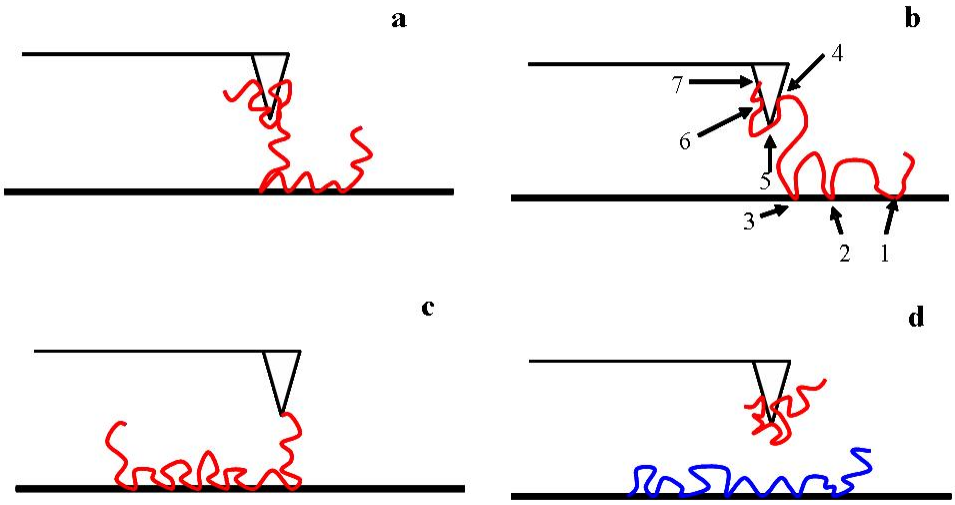

Figure 8: Possible polymer "pulling" scenarios with past AFM techniques used. (a) Polymer is bonded to the tip and surface in multiple places, each equally available for desorption. (b) Polymer bonded to tip and surface showing all points which could desorb during an AFM pull. (c) Polymer bonded by a terminal end on the cantilever. (d) Multiple polymers interacting as tip approaches and is retracted from the surface. Reproduced with permission from Macromolecules[30]. Copyright 2007 American Chemical Society.

Schemes a-c in Figure 8 illustrate possible scenarios of a single polymer being pulled from a surface. In the experiments done by Senden *et al.* and Levy *et al.*, a polymer can adsorb and desorb in multiple places on the tip and the surface[40, 145, 144, 240, 241]. Only in Figure 8c can a true measurement of the polymer loop lengths, from one end of the chain to the other, be measured, and this depends on the attachment to the tip not detaching. In Figure 8b, the desorption events do not have to occur in any particular order. If the desorption events followed the pattern 3, 4, 2, 5, 6, and then 7, not all events would be counted, and the distance between

attachment points, describing a polymer on a single surface, would be incorrectly accounted for, due to the order of desorption. Figure 8d, which is very likely in previous experiments, allows the results to be significantly complicated by measuring the desorption events of multiple polymers on the same curve. In this case, it is very likely that large loop lengths would be screened out by detachments of different polymers. With these complications, it is impossible to determine the loop length distribution of a single polymer. Figure 9 gives a detailed look at three possible scenarios of a polymer pull. It illustrates where the polymer could possibly adsorb in a physisorption-dominated experiment.

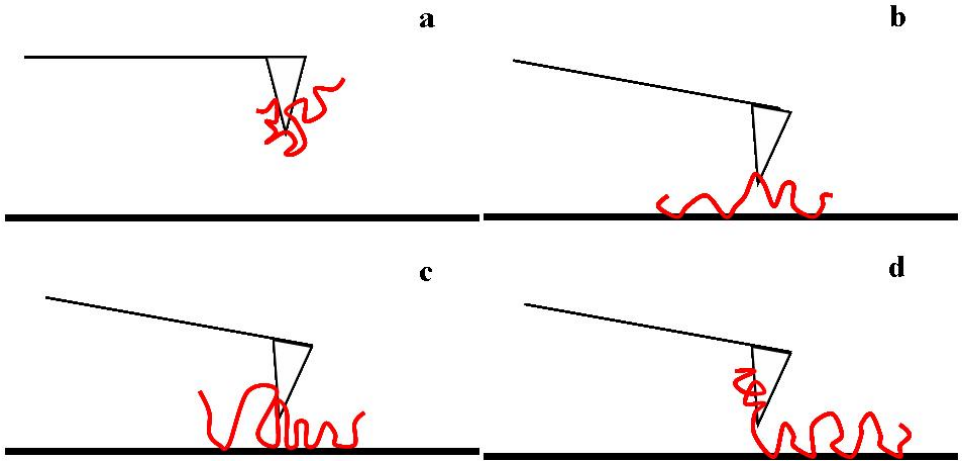

Figure 9: Possible scenarios for one physisorbed polymer. (a) Initial conformation on AFM tip. (b) Polymer adsorbs in two directions from the tip. (c) Polymer adsorption points alternate between the tip and the surface. (d) Polymer has multiple adsorption points to the tip and multiple points on the surface without alternation. Reproduced with permission from Macromolecules[30]. Copyright 2007 American Chemical Society.

As shown in Figure 9, the initial conformation, shown in scheme a, can change to that of schemes b-d due to different adsorption and desorption possibilities. In Figure 9b, if the polymer does not desorb from the tip initially, it will yield small loop lengths due to the desorption of attachments on alternating sides of the cantilever tip. In Figure 9c, the loop lengths could be altered by alternating desorption from the surface and the tip. Figure 9d shows another case where desorption from the surface and the

tip are equally likely for a physisorbed polymer.

The examples in Figures 8 and 9 were complicated by the fact that a polymer can both adsorb and desorb from the tip and surface. This problem was improved with the "pulling" method developed by Haschke *et al.*[107, 108, 109]. Haschke ensured that each polymer could only adsorb on one terminal end, as seen in Figure 8c[107, 108, 109]. To do this, a gold AFM tip was used, and one terminal end of the polymer to be used contained a thiol group. This thiol linkage is a strong covalent bond which should be stable relative to the force necessary to remove the physisorbed attachments on the surface. In addition to this, it was found that polyacrylamide does not readily hydrogen bond to gold surfaces, making only one attachment point on the surface for each polymer[107, 108, 109]. This method made large improvements to the use of AFM to determine adsorbed polymer conformation. However, these researchers were unable to control the number of macromolecules adsorbed on the tip. In the work done by Haschke *et al.*, different concentrations of thiol-terminated polymers were tested at different "soak" times to show the effect of multiple polymers on a tip[107, 108, 109]. It was reasoned that at a very low concentration and adsorption time it could be assumed that only one polymer adsorbed on the tip[107, 108, 109]. While this increases the odds of a single chain being measured, it does not guarantee it. Any cluster or agglomeration of the polymer in solution would still result in multiple chains being attached without any way to tell. This issue is of particular importance because polyacrylamide, the polymer used in many studies, does tend to agglomerate[112]. Without knowing the number of polymers on the tip, interpretation of the force curve desorption events to obtain loop lengths becomes nontrivial.

Previous literature has used the force necessary to pull a polymer attachment point from a surface to make reference as to the type of bonding responsible for the attachment[107, 108, 109, 40, 145, 144, 240, 241]. Although this seems to be a straightforward deduction, there is at least one complication which has, for the

most part, been disregarded. This is the geometry and spacing between the polymer attachment and the tip. Figure 10 illustrates how the force measured to pull a polymer from a surface is dependent on the position of the polymer on the surface.

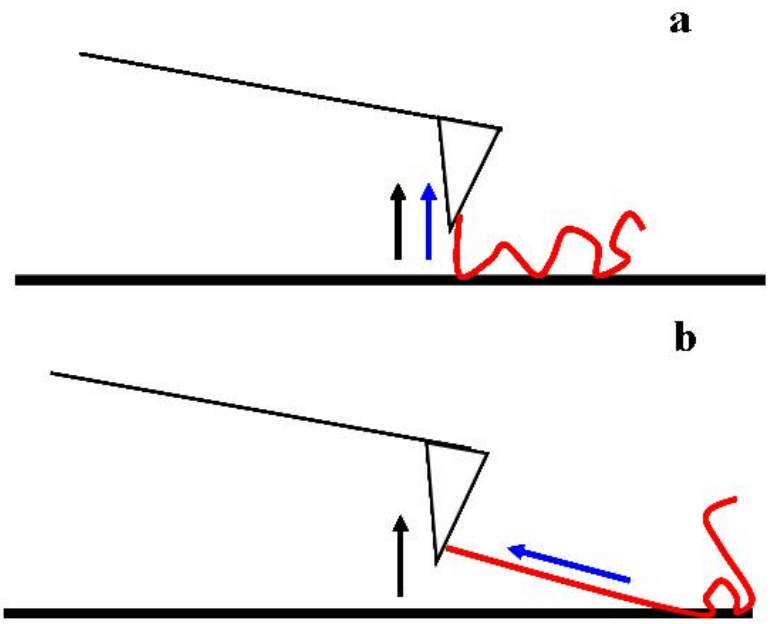

Figure 10: Geometric considerations for polymer force interpretation. (a) Force to remove polymer attachment can be related to the adsorption strength. (b) Force to remove polymer attachment, found by changes in cantilever deflection, is less than that required to remove the attachment due to the angle of the pull. Reproduced with permission from Macromolecules[30]. Copyright 2007 American Chemical Society.

If the polymer only laid directly under the tip, the geometry of the pull would not affect the resulting force. However, with a polymer all the attachment points will not lie directly under the tip. Because some polymer attachment points could lay micrometers from the tip on the surface, the geometry of the "pulling" experiment will directly affect the force to remove the attachment. Thus, as the polymer attachment point lies at greater distances from the tip, the forces to detach the polymer, detected by tip deflection, will decrease. This makes references to the force to detach the polymer questionable.

2.5 Salt Effect

The effects of electrolytes, or salts, on adsorbed polymers have been a study of great interest over the past decades[89, 245, 244, 279, 118, 35, 90, 83, 84, 277, 227, 28, 68, 155, 159, 111, 216, 18, 78, 254, 243, 229, 242, 107, 109]. Much of this interest is due to the presence of salts in most industrial applications where polymers are used. Salts can affect the adsorbed conformation and adsorption amounts of polyelectrolytes and nonionic polymers[89]. According to Shubin and Linse, this can be done in three different ways: screening of electrostatic attractions between the polymer and surface and electrostatic repulsion between similarly charged groups, competition between electrolyte ions and polymers for space near the charged surface, and competition for adsorption sites between the electrolyte and the polymer[245]. It is expected that the effects of electrolytes would be the most pronounced on polyelectrolytes due to the screening effects they have on interactions between polyelectrolytes[122]. Fleer *et al.* outlined four possible scenarios for the salt effect on polymer adsorption: charged polymer/uncharged surface, uncharged polymer/charged surface, similarly charged polymer and surface, and oppositely charged polymer and surface[89]. For uncharged polymers and charged surfaces, the salt effect is expected to be weak[89]. For charged polymers and uncharged surfaces and similarly charged polymers and surfaces, the addition of salt is expected to increase the amount of polymer adsorbed[89]. In the final case of a charged polymer and an oppositely charged surface, the addition of salt is expected to decrease the amount of polymer adsorbed unless the polymer has non-electrostatic adsorptive properties[89]. This section of the literature review will investigate previous work dealing with the salt effect on nonionic polymers, the salt effect on ionic polymers, and the salt effect on adsorbed polymer conformation.

Flood *et al.* investigated the effects of electrolytes on adsorbed layers of a nonionic polymer, polyethylene oxide[90]. They found that the adsorption amount increased and the adsorbed polymer layer thickness, found using dynamic light scattering, also

increased with increasing salt concentrations[90]. Fleer *et al.* predicted that the salt effect on nonionic polymers adsorbing on charged substrates would be very weak[89]. However, Flood *et al.*'s results seem contrary. Flood *et al.* explained the increased adsorption and increased adsorbed polymer layer thickness to a decrease in solubility of the polymer in the salt solutions[90]. The more salt present the more the polymer will want to adsorb. The final result, of interest, from this study was that monovalent salts did not have a noticeable effect on the proportion of trains in the adsorbed polymer conformation[90]. However, with increasing valency competition for adsorption sites became noticeable[90]. Karlstrom *et al.* recorded the same decrease in polymer solubility at increasing salt concentrations[127]. Avranas and Iliou have also observed similar effects of salts on different nonionic polymers[12].

Electrolytes in solution have the ability to affect polyelectrolytes in different ways depending on the polymer's properties. As was mentioned previously, electrolytes have the ability to screen electrostatic interactions and also compete for electrostatic adsorption sites. If a polyelectrolyte has a high charge density, there will be a large amount of repulsion between charged groups of the polymer. This will cause the polymer to spread out and take up a large area. When this polymer adsorbs on a surface, only a few polymers will be able to adsorb in a small area due to the electrostatic repulsion. However, when salt is added to the solution these electrostatic forces are screened allowing the polymers to move closer to one another and the adsorbed amount on the surface will actually increase[245].

The competition for adsorption sites is not as important, in this situation, as the multiple charged sites on the polymer allow most groups on the polymer backbone to adsorb. Van de Steeg *et al.* showed, through simulations, that salt ions are also able to displace highly charged polymers[266]. This illustration of the opposite case points to the effect slight differences in experimental settings can have on the results. For the case of low charge density polymers, adsorption to a surface is based on the interaction

of a few charged groups with the oppositely charged surface. Here the competition for adsorption sites can interfere with polymer adsorption resulting in decreased adsorption with increasing salt concentration[245]. Much of this effect has been shown through different modeling techniques. Dobrynin *et al.* used scaling theory to predict the effect of salt concentration on adsorbed amount of different polyelectrolytes[83]. Hoda and Kumar used Brownian dynamics, which is an intermediate coarse grained simulation technique[118]. Carrillo and Dobrynin used molecular dynamics simulations to analyze this situation[35]. Scheutjens and Fleer's self-consistent mean field theory was used by Shubin and Linse[245].

Much of the work done, modeling and experimental, on the salt effect on adsorbed polyelectrolytes has been focused on the adsorption amount. Very little work has been done to investigate the salt effect on the actual adsorbed polymer conformation. Most of the work that has been done deals with adsorbed polymer layer thicknesses which, as stated earlier, can not be used to reveal the details of an adsorbed polymer's conformation[279, 259, 166]. Both Wang and Audebert and Meadows *et al.* found that as the salt concentration was increased, the hydrodynamic thickness decreased[279, 166]. However, Takahashi and Shubin and Linse found that the opposite was true and the adsorbed layer thickness actually increased with increasing salt concentration[259, 245]. Both of these scenarios can be reasonably explained with the current understanding of these processes. For the case of Wang and Audebert and Meadows *et al.*, the increase in salt concentration screens out the electrostatic attraction of the polymer to the surface and the repulsion between the charged groups on the polymer. Both groups attributed the smaller thickness to the loops and tails being able to move much closer to each other in the electrolyte screened system[279, 166]. Takahasi and Shubin counter that as competition for surface adsorption sites increases the polymer will extend away from the surface[259, 245]. The only experimental work

which has been done and gives a direct measurement of parts of an adsorbed polymer's conformation was done by Flood *et al.*[90, 91]. This work showed the effect of salt concentration on the train portion of adsorbed polymers. However, this was done on nonionic polymers[90, 91].

In 1995, Shubin and Linse looked to experimentally and theoretically model the conformation of an adsorbed polyelectrolyte on a surface and evaluate the effect of electrolytes on the resulting conformations. As was mentioned previously, they found, using ellipsometry, that with increasing electrolyte concentration the adsorbed layer thickness increased. After performing self-consistent mean field theory modeling, they proposed, for the first time, that the increase in layer thickness was due to larger loops and tails[245]. The larger loops were explained to be due to the competition with electrolyte ions for surface adsorption cites, resulting in fewer adsorption site meaning larger loops and tails[245]. Over the past 12 years this work has been cited 77 times, according to SciFinder Scholar. No researcher, to date, has been able to verify, experimentally, the effect of electrolytes on adsorbed polyelectrolyte conformation.

2.6 Site Blocking

Site blocking flocculation, or enhanced bridging flocculation, uses additives which occupy possible polymer adsorption sites causing the polymer to have fewer attachments to the surface which is thought to result in longer loops and tails[178, 153, 251, 275, 174, 21, 19, 186, 20, 164, 173]. The critical component of this system is the ability of the blocking additive to adsorb on the possible particle surface sites to which the polymer flocculant can adsorb. This in turn, decreases the surface area to which the polymer flocculant can adsorb. In order for this to happen, it is important to know what properties the polymer flocculant has and how it bonds to a particle's surface. Behl *et al.* noted that polymers can adsorb to a surface through chemical bonding, hydrogen bonding, hydrophobic interactions, electrostatic interactions, and van der

Waals forces[21]. To block adsorption sites for a polymer, which adsorbs through electrostatic interactions, putting similarly charged particles or polymers, site blocking additives, on the surface prior to addition of the retention polymer would limit the possible sites where it could adsorb. The similarly charged site blocking additives will adsorb on the same vacant sites which would available for the retention polymer. In addition to limiting the possible sites for retention polymer adsorption, the similarly charged site blocking additives will create an electrostatic repulsion with the retention polymer. This will prohibit the retention polymer from approaching the site blocking additives too closely. This is illustrated in Figure 11.

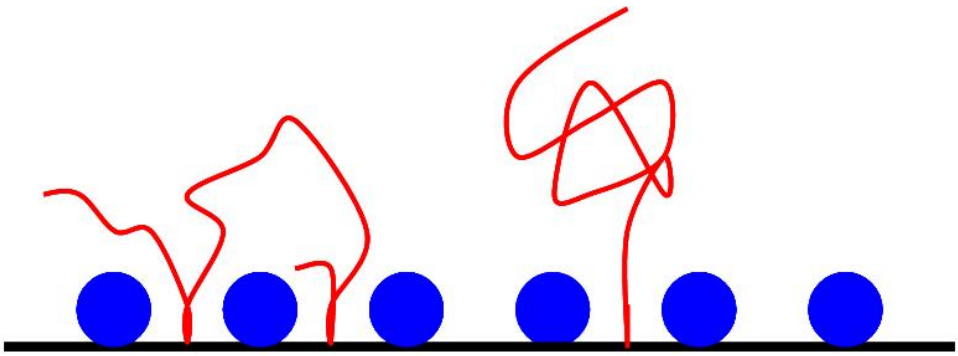

Figure 11: Illustration of the site blocking mechanism's effect on adsorbed polymer conformation.

A site blocking agent will, in most cases, have similar properties as the polymer used for flocculation. It is important for it to block adsorption sites, but it must not be able to flocculate particles without the retention polymer[19]. If the site blocking agents were able to flocculate the particles in the system, it would create a competition between the desired bridging mechanism and either a less favorable bridging mechanism, patch mechanism, or charge neutralization mechanism. If the patch and charge neutralization mechanisms dominate the flocculation, flocs, weaker than the those formed in the bridging mechanism, are formed. By having similar properties to the retention polymer, a site blocking additive will, in certain desirable cases, have a high energy barrier towards association with the polymer flocculant.

The electrostatics case illustrates this point well, as like charges repel each other.

Critical to the site blocking mechanism, is how much of the site blocking agent should be added to get the desired effects. If too much of the site blocking agent is added, the polymer flocculant will not be able to adsorb and aid in flocculation. If too little is added, the polymer flocculant will spread out on the particle surfaces giving a more flat "pancake" structure which is less favorable for flocculation. Behl *et al.* used the expression, in Equation 1, to describe the maximum collision efficiency of two particles as a way of explaining how site blocking additives affected flocculation[21].

$$\overline{E}_{max} = \frac{1}{2}(\Phi - \overline{\Phi}\overline{\theta})^2 \tag{1}$$

In Equation 1, Φ is the fraction of available sites for polymer adsorption, $\overline{\Phi}$ is the fraction of available sites for site blocking agent adsorption, and $\overline{\theta}$ is the fractional coverage of the site blocking agent on the surface. From this equation, one might postulate that site blocking surface coverage at 50% would give the greatest flocculation, however, this is not the case for all systems[21]. It is important to remember that this equation does not allow the site blocking additive to flocculate the particles[256]. Swerin *et al.* developed an expression to describe the collision efficiency for this more complicated system, shown in Equation 2.

$$E = 2\theta(1-\tau)(1-\theta-\phi) + 2\theta^2\tau(1-\tau) + a[1 - e^{b\theta/(1-\phi)}] \tag{2}$$

In Equation 2, θ is the surface coverage of the polymer flocculant, ϕ is the fractional coverage of the site blocking additive, and τ, for the case of microparticle flocculation systems, is the fractional coverage of microparticles over preadsorbed polymer. Both of these equations use the total available area for flocculation and the polymer surface interaction to estimate the most favorable collision efficiencies.

Another important factor in the site blocking mechanism is the size of the site blocking agent used. Behl *et al.* found that if the same polymer was used as the site

blocking agent and the retention polymer, the molecular weight of the site blocking agent was important[21]. If the site blocking polymer had a high enough molecular weight, it could prevent the adsorption of the retention polymer because of the area it occupies due to its conformation on the surface. Ono and Deng found similar results using different sized cationic microparticles in site blocking experiments[186]. Figure 12 shows that if the site blocking agent is too large, the polymer will not extend much beyond it, thereby decreasing, or possibly eliminating, its collision efficiency.

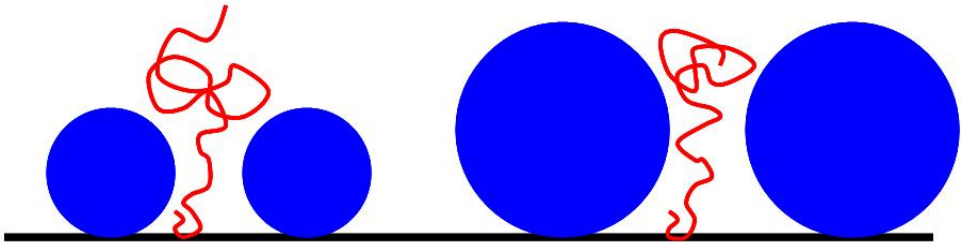

Figure 12: Effect of the size of blocking agents used in site blocking.

Although both polymers and small particles can be used as site blocking agents, Ono and Deng found that there were five advantages for using microparticles over water-soluble polymers in papermaking systems: (1)microparticles shapes will be constant on a particles surface; (2) the length of the polymer bridge can be controlled by the microparticle size; (3) the cationic demand in the pulp furnish can be reduced; (4) cationic microparticles do not penetrate into fiber pores; (5) and the strong bonding force of the microparticles with the furnish will prevent them from being accumulated in the white water[186].

CHAPTER III

THESIS OBJECTIVES

The goal of this research was to provide a better understanding of the conformation of an adsorbed polymer and some of the conditions which affect it. To do this, both experimental methods and computer simulation were used to directly determine the increase in the adsorbed polymer layer thickness.

The first experimental method used was dynamic light scattering. The second experimental method, developed for this research, directly measured the length of an adsorbed polymer's loops and inferred changes in tail lengths using atomic force microscopy. Computer simulation of this system was performed using dissipative particle dynamics which uses the equations of motion to model the movement of a chain of beads representing a polymer. Using these methods, this research investigated the effects of cationic polymeric and inorganic site blocking systems on cationic polyacrylamide. Work was also completed to gain insight into the effect of inorganic salts on adsorbed polymer conformation.

The specific objectives of this thesis are to determine and clarify explanations concerning:

1. Develop AFM technique to analyze a single polymer molecule
2. Adsorbed polymer conformation
3. Salt effect on adsorbed polymer conformation
4. Site blocking effect on adsorbed polymer conformation

CHAPTER IV

EXPERIMENTAL METHODS AND PROCEDURES

4.1 Experimental Overview

The many different experimental and modeling techniques discussed in the literature review were considered for use in completing this work. Based on availability, accuracy, and ability to compare results with previous work dynamic light scattering, atomic force microscopy, and course grained simulation using dissipative particle dynamics were selected to use in this investigation. The polymer chosen was cationic polyacrylamide, a common choice in previous studies. In this work, the cationic groups in the copolymer were (3-(methacrylamido) propyl)trimethylammonium chloride (MAPTAC). This polymer is shown in Figure 13. The substrates selected for polymer adsorption were mica, glass, and anionic latex spheres.

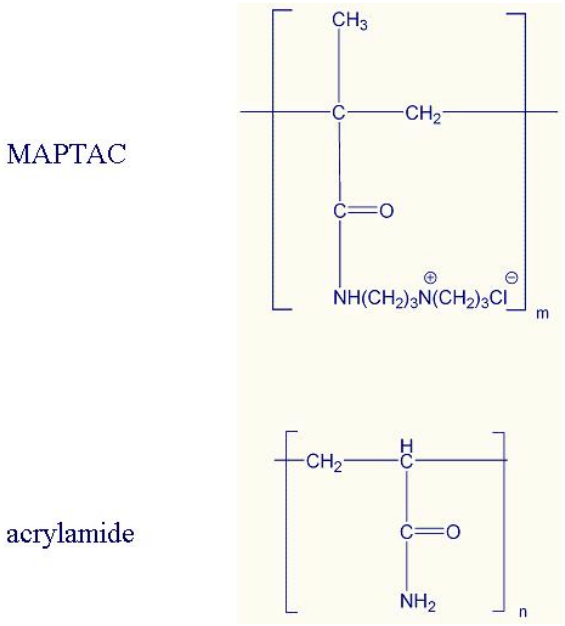

Figure 13: The structures of the MAPTAC and acrylamide units in the polymer used.

4.2 Dynamic Light Scattering

4.2.1 Dynamic Light Scattering Background Information

Dynamic light scattering(DLS) is a commonly used technique to find the particle size of small particles[43]. DLS measures the changes in scattered light intensity from a sample as its particles move around by Brownian motion. From these changes in intensity, the self diffusion coefficient can be found by Equations 3 and 4[169].

$$g^{(2)}(\tau) = \frac{\langle I(\tau)I(0)\rangle}{\langle I(0)\rangle^2} = 1 + c[g^{(1)}(\tau)]^2 \tag{3}$$

$$g^{(1)}(\tau) = exp(-D_0 q^2 \tau) \tag{4}$$

In the above equations, I is the intensity, τ is the time difference between measurements, c is an instrument constant, D_0 is the self diffusion coefficient, q is the magnitude of the scattering wave vector, $g^{(1)}(\tau)$ is the normalized electric field correlation function, and $g^{(2)}(\tau)$ is the intensity autocorrelation function. Using this diffusion coefficient, the Stokes-Einstein equation, Equation 5 , can be used to find the hydrodynamic radius of the particle, assuming a spherical geometry[169].

$$R_H = \frac{k_b T}{6\pi\eta D_0} \tag{5}$$

In the Stokes-Einstein equation, k_b is Boltzmann's constant, T is the temperature, η is the fluids viscosity, and D_0 is the self diffusion coefficient. It is important to note, with regard to the experimental method used, that the self diffusion coefficient is calculated assuming infinite dilution. In accordance with past publications, the thickness from DLS was considered to be that of the average outermost points.

4.2.2 Dynamic Light Scattering Materials

For this study, anionic latex spheres, as supplied by Interfacial Dynamics Corporation, were used as an adsorption site for the cationic polyacrylamide polymers. These

particles have mean diameter of $0.24\mu m$ with a standard deviation of $0.010\mu m$ as determined by transmission electron microscopy. The anionic charge content, from conductometric titration, and surface charge density are $3.8\mu Eq/g$ and $1.5\mu C/cm^2$ respectively. The polymer, a polyacrylamide/(3-(methacrylamido)propyl)trimethylammonium chloride (MAPTAC) copolymer, was made by SNF. This polymer has a molecular weight and polydispersity similar to that made by Ciba Specialty Chemicals, which was used for the atomic force microscopy, AFM, testing in this work. The SNF copolymer contained 15 weight% MAPTAC groups. Gel permeation chromatography, GPC, testing here at Georgia Tech gave the SNF polymer a number average molecular weight of $86{,}554 g/mol$. The number average molecular weight of the Ciba Specialty Chemicals polymer, done by GPC at Ciba, was $1{,}040{,}000 g/mol$. Testing of the Ciba polymer here at Georgia Tech gave a number average molecular weight of $192{,}788 g/mol$. The differences in these values are most likely due to the use of a polyethylene oxide calibration standard here at Georgia Tech and the practice of filtering the polymer solution prior to testing. The polyethylene oxide standard does not contain charged groups as the polymer used for this research does, which can alter the values reported. Filtering the polymer solution can pull out higher molecular weight polymers reducing the values found using GPC. The molecular weight of the SNF polymer used for light scattering, although smaller, is of a similar order of magnitude to that used for the AFM portion of this work.

Sodium chloride was used to evaluate the salt effect on adsorbed polymer conformation. To evaluate the effect of site blocking, two different blocking additives were used: poly-diallyldimethylammonium chloride, PDADMAC, and cationic nanosilica particles. A low molecular weight, $100{,}000 g/mol$ - $200{,}000 g/mol$, PDADMAC, from Aldrich Chemicals, was used as a polymeric site blocking additive. Ludox-CL, $12nm$ cationic nanosilica particles, obtained from Sigma-Aldrich, were used as a non-polymeric blocking additive.

4.2.3 Dynamic Light Scattering Methods

DLS measurements were performed on a Brookhaven Instruments BI-200SM Goniometer with a 632.3nm helium neon laser. The detector was positioned at an angle of 90° from the laser to minimize the effects of noise as much as possible. It was determined that using a latex sphere concentration of 5.4726x10^7*particles/mL*, in a 10mL sample, gave noticeable polymer layer thickness increases with the least possibility of flocculation. The lowest concentration of particles which gave a high enough signal was chosen to ensure this. All data sets obtained began with 5 measurements of the latex spheres without the addition of any blocking additives or polymer to get the average size of the particles. The measurements were run for a duration of 5 minutes and the CONTIN, non-negatively constrained least squares: regularized, data analysis values are recorded. For experiments in which only the adsorbed polymer layer is desired, a set amount of cationic polyacrylamide was added to the vial and immediately put back in the goniometer. Five measurements of 5 minutes each were performed. For the analysis of the effects of site blocking, the site blocking additive was added to the vial and allowed to sit for 30 seconds. Following this, the set amount of cationic polyacrylamide was added to the vial and measurements were started.

All polymer layer thickness measurements were obtained by subtracting the average latex sphere diameter from the hydrodynamic diameter after treatment. The reported overall average thickness increase was the average of all thickness changes for that data set. The cleaning of the glass vials used for DLS was a simple soap washing followed by 10 warm tap water rinses. After this, an extensive set of 10 Barnstead deionized water rinses and a 4 minute soak in fresh Barnstead deionized water was performed.

The amount of the SNF cationic polyacrylamide polymer to be added was determined by checking the change in hydrodynamic diameter against the amount of polymer added. Figure 14, below, shows this plot.

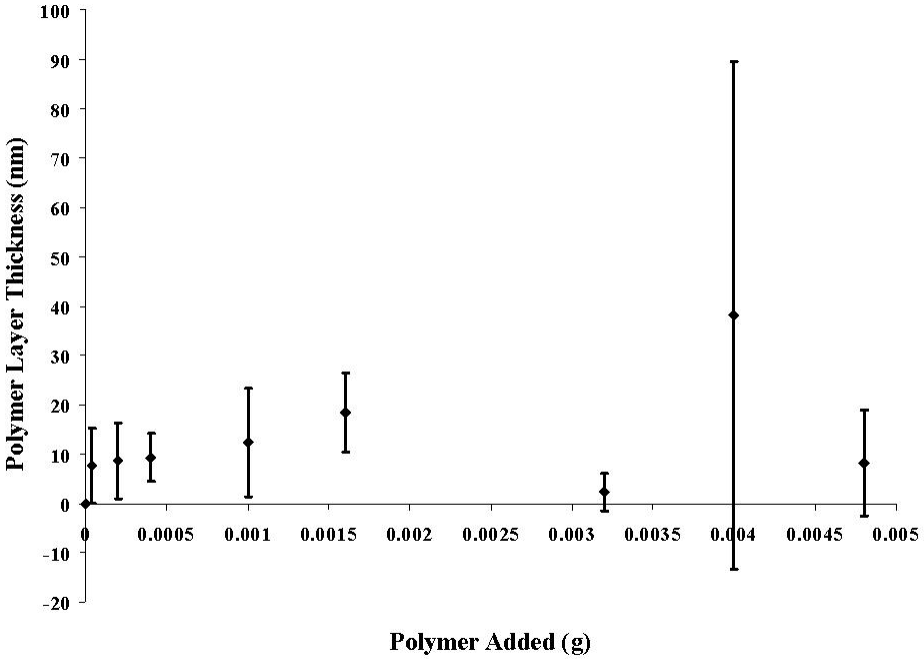

Figure 14: Effect of amount of cationic polyacrylamide added on adsorbed layer thickness using DLS.

Using Figure 14, it was decided that $0.0004g$ would be added to each vial. This value was chosen because it used the least amount of polymer while obtaining a layer thickness increase greater than the standard deviation of the individual test. It is desirable to add the least amount of polymer to each system to avoid flocculating the individual spheres. If too much polymer is added the chance that the adsorbed polymer's conformation will be pushed into a different regime, such as a brush, is increased.

The amount of different site blocking additives added was determined using a similar plot to Figure 14. The first site blocking additive tested was PDADMAC. As described previously, a given amount of PDADMAC was added to the vial with latex spheres, allowed to sit for 30 seconds, and then $0.0004g$ of the SNF polymer was added and testing began. Figure 15 shows the increase in adsorbed polymer layer relative to the amount of PDADMAC added. It is important to note that the

addition of PDADMAC, as reported in previous work, does not increase the particle size of the latex spheres by a detectable amount[251]. 1.75x10^{-9}g of PDADMAC was chosen to be the ideal amount to add for site blocking because of its larger increase in adsorbed polymer layer thickness.

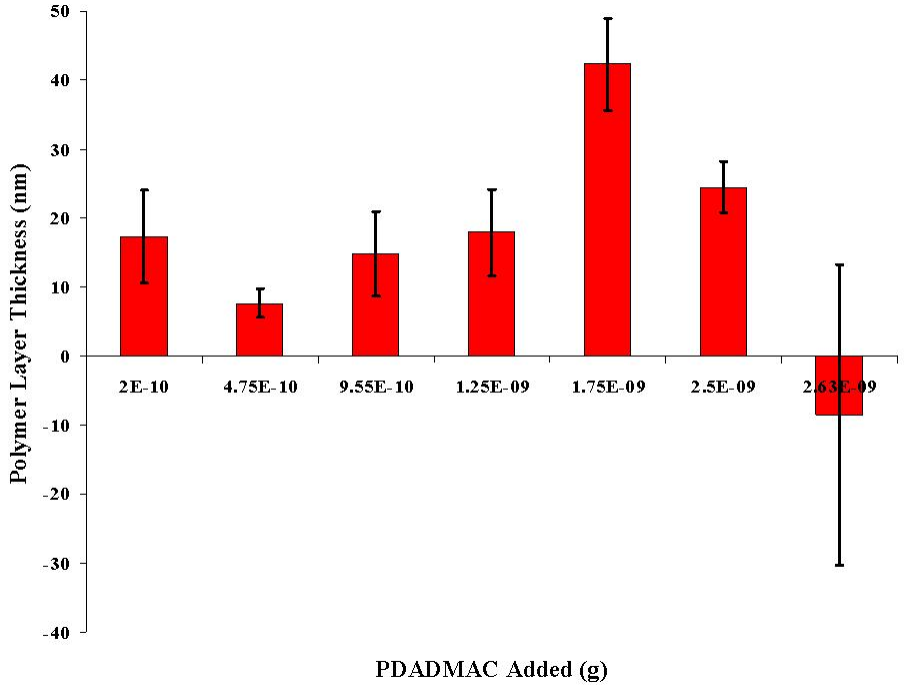

Figure 15: Effect of amount of PDADMAC added on adsorbed cationic polyacrylamide layer thickness using DLS.

The same procedure above was performed using cationic nanosilica as a site blocking additive. Figure 16 shows the effect of the amount of cationic nanosilica added as a site blocking additive on the adsorbed polymer layer thickness. Although 1.8x10^{-9}g of cationic nanosilica gave the largest increase in adsorbed polymer layer thickness, the sudden drop in thickness at 1.2x10^{-9}g of nanosilica directed the focus for this research to the amount of 9.168x10^{-10}g of cationic nanosilica to be used as a site blocking additive.

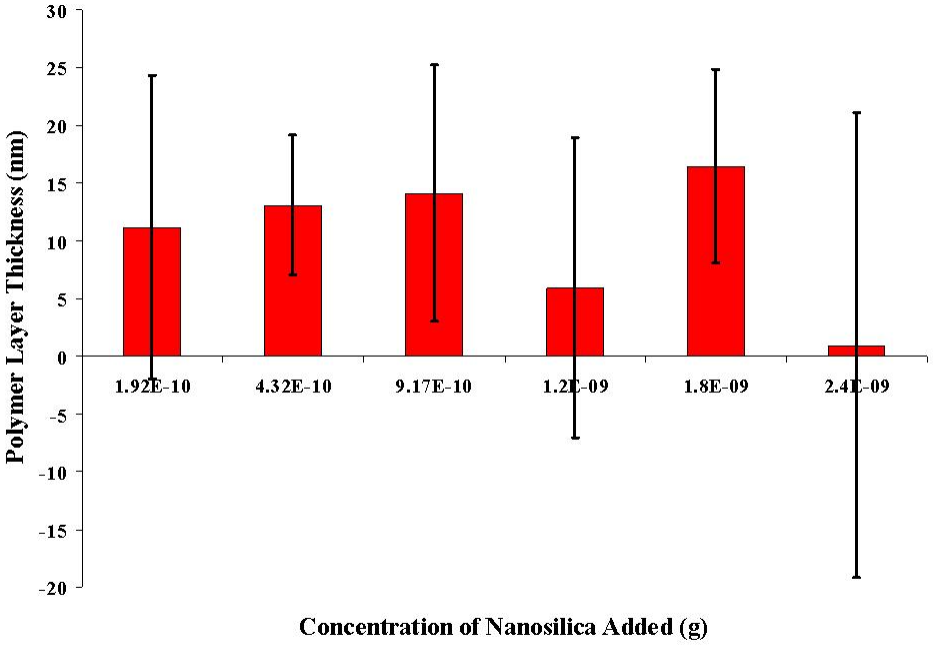

Figure 16: Effect of amount of cationic nanosilica added on adsorbed cationic polyacrylamide layer thickness using DLS.

4.3 Atomic Force Microscopy

4.3.1 Atomic Force Microscopy Background Information

The second experimental technique that was used to determine adsorbed polymer conformation was atomic force microscopy(AFM). Portions of the following sections were reproduced with permission from Macromolecules[30], copyright 2007 American Chemical Society. Many different groups have recently used AFM to determine properties or conformations of polymers adsorbed on surfaces. Some of these groups have used a tapping method where an AFM probe tip is tapped along a surface and if it hits objects on the surface it deflects to determine where polymers are[134]. Other groups have used a method of generating force curves to determine the conformation or other properties of adsorbed polymers[121, 108, 109, 240, 241, 144, 145]. This basic technique is illustrated in Figure 7. For this work polymer pulling generated force curves were used to determine adsorbed polymer conformation.

To date, published methods which have used force curves to determine adsorbed polymer conformations, have employed different techniques. Senden *et al.* used mica surfaces as a substrate and then allowed polymers to hydrogen bond to the AFM tip by treating it with cold water plasma to put hydroxyl groups on the surface and then adding the polymer[241]. The tip was then brought to the mica surface and given time to allow the polymer to adsorb, presumably through hydrogen bonding[241]. As the tip was again retracted it would deflect as it had to break any adsorbed points from the surface. The distance between these deflections is the distance of the polymer chain in between adsorption points. This study, however, did not account for the location in which the polymer was detaching or how many polymers were being viewed in each measurement. It would not be possible to tell if the polymer was desorbing from the tip or the mica surface. This would not allow an accurate picture of the conformation. A second possible problem is that it is unknown how many polymers are on the tip or are being measured. Multiple polymers could cancel out deflections or give extra deflections that aren't from an individual polymer. Therefore making interpretation impossible.

To resolve these issues, the methods used by Haschke *et al.* will be modified and used[109, 108]. Haschke used polymer chains which had a single thiol group on a terminal end. They used gold coated AFM tips allowing the polymer to covalently bond to the tip using thiol chemistry. Because the force to break a covalent bond is much greater than that to break hydrogen bonds or electrostatic interactions, the deflections of the cantilever that Haschke *et al.* measured had to be caused by the polymer detaching from the surface. In order to solve the problem of having multiple polymers on the tip, Haschke adjusted the concentration and time each tip was exposed to a polymer solution. This was iterated to the point at which if any less polymer or time would produce no desorption events[108]. However, this does not necessarily guarantee that only one polymer is present.

For this research, modified cantilever tips were used to not only help ensure only one polymer was bonded to the tip, but also to specify the location of this polymer. These tips had all of the gold removed from the area near the apex of the tip except for a $70nm$ circle, shown in Figures 17 and 18.

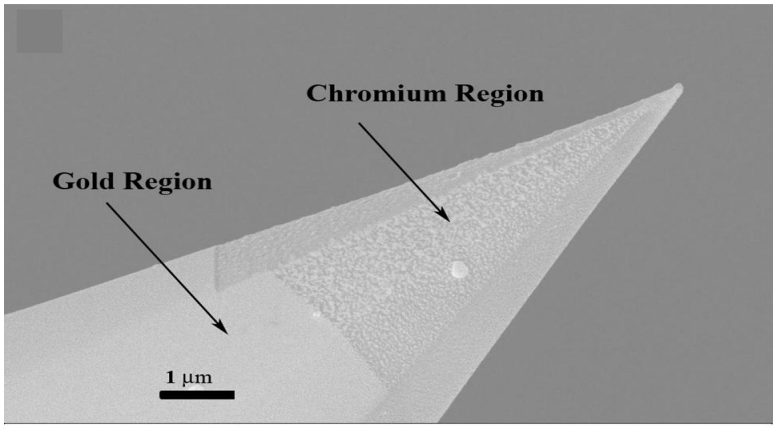

Figure 17: Large SEM image of modified AFM tip showing the milled region. Reproduced with permission from Macromolecules[30]. Copyright 2007 American Chemical Society.

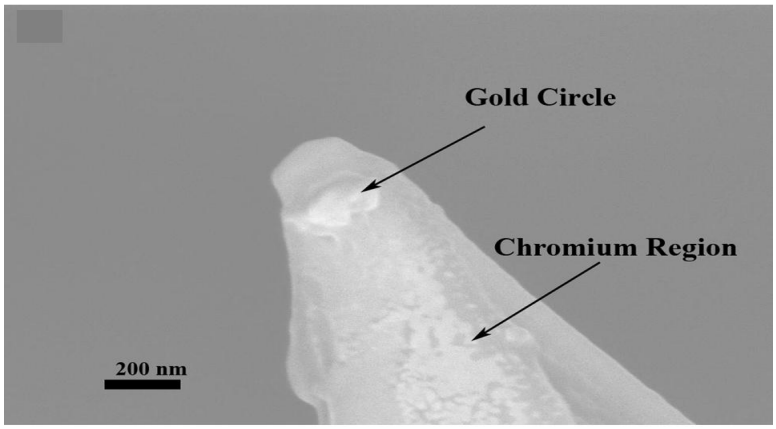

Figure 18: A closer SEM image of the apex of a modified AFM tip showing the $70nm$ gold circle. Reproduced with permission from Macromolecules[30]. Copyright 2007 American Chemical Society.

4.3.2 Atomic Force Microscopy Materials

For this research, two different anionic substrates, mica and glass, were used. The mica used, V-1 grade $15mm$x$15mm$ squares, was obtained from SPI Supplies. The glass used, micro cover glasses, $18mm$x$18mm$ squares, was obtained from VWR. The glass surfaces were first cleaned with soap and water followed by extensive rinsing with Barnstead deionized water. Each of these substrates was affixed to a small petri dish using Loctite Quick Set Epoxy and were used only once then discarded. In the case of mica, a fresh surface could be exposed by placing tape on the top surface and removing it, leaving a freshly cleaved surface. Figure 19 shows the structure of a sheet of mica.

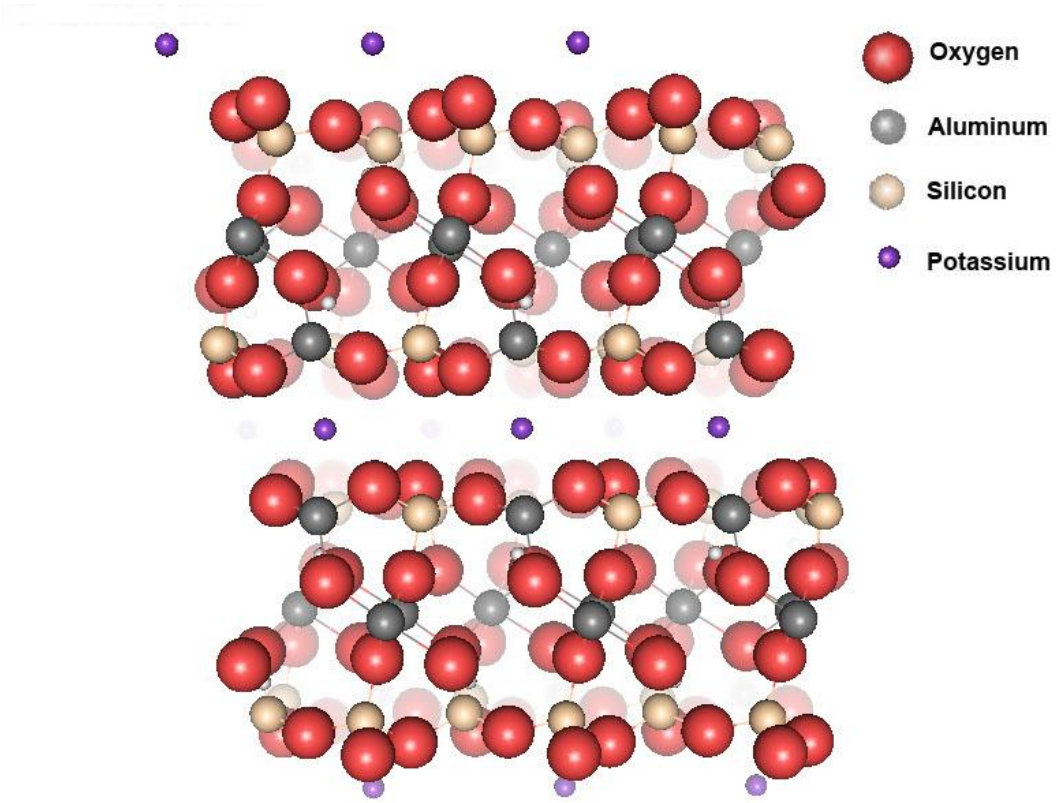

Figure 19: An image of the crystal structure of the muscovite mica used for this research.

When cleaved this structure will divide along the plane of potassium molecules.

It is assumed that this cleaving will leave 50% of the potassium ions on one side and 50% on the side not being used. This is illustrated in Figure 20.

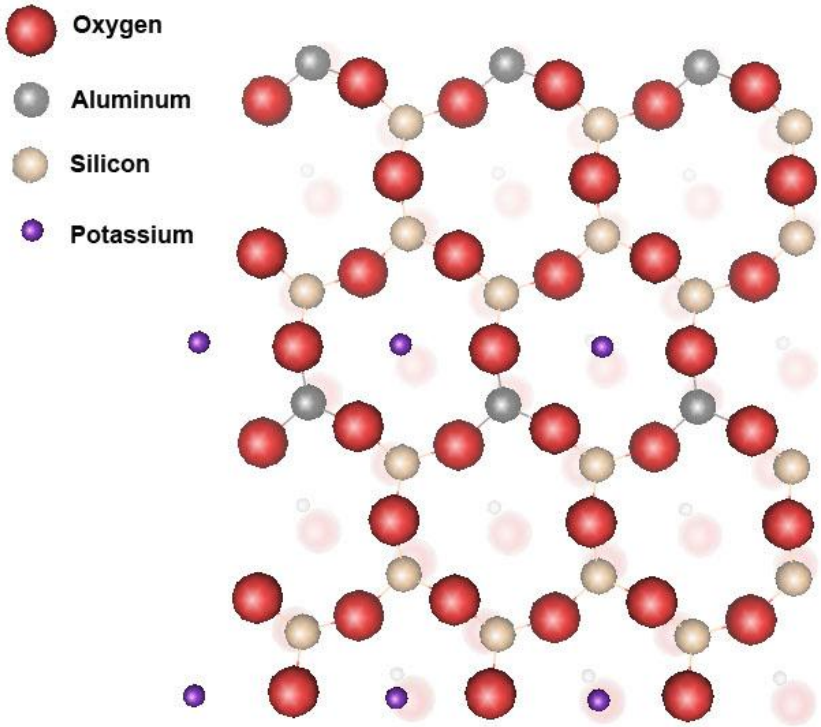

Figure 20: A representation of the atoms that make up a cleaved muscovite mica interface.

Along with this, Pashley found that when a cleaved surface is placed in water about 1% of these potassium molecules will dissociate leaving about 1% of the surface area with an anionic charge[197]. It is unclear if this means only 1% has an anionic charge or 51% has an anionic charge. However, it is very likely that 50 - 51% of the potassium sites could be available for polymer adsorption. This is due to the equal probability that potassium ions in the cleavage plane could adhere to either surface.

A cationic high molecular weight copolymer of acrylamide and MAPTAC with one terminal SCH_2COOH group was synthesized by Ciba Specialty Chemicals. This polymer was functionalized with a terminal thiol group by using thiolglycollic acid

as a chain transfer agent that left a single thiolglycollic acid group at one end of the polymer. The molecular weight as given by Ciba was 1.04x10$^6 g/mol$ (determined by GPC), and the R_g was found to be $151.3nm$ (determined by static light scattering) at the tip functionalization conditions.

MikroMasch CSC17/Cr-Au AFM cantilevers were modified, by MicroMasch, using focused ion beam milling. The spring constants for these levers was between $0.05N/m$ and $0.3N/m$. Focused ion beam milling of the gold surface of these cantilevers was done to remove the gold layer except for a $70nm$ circle about $40nm$ from the apex of the leading edge of the tip. This left a small gold circle on an exposed chromium sublayer. The gold coating was removed about $6\mu m$ up the tip surface to ensure any polymer adsorbed on the top of the cantilever tip can't influence the results. A modified tip is shown in Figures 17 and 18.

4.3.3 Atomic Force Microscopy Methods

Polymer-modified AFM tips were prepared for testing by first soaking them in a 9.074x10$^{-6} g/mol$ solution of polymer in water for 1 minute. The tips were then rinsed in Barnstead deionized water and mounted for testing. It was then lowered down to the surface at a rate of $2\mu m/s$ until the deflection of the lever was $10nm$. At this point, the tip was allowed to dwell on the surface for 5 minutes and then was retracted. To ensure clean and accurate force plots, the data acquisition rate used was $50kHz$. All retractions were extended the full range of the z piezo to ensure complete polymer desorption from the surface. For site blocking experiments, the blocking additive was added to the bubble of water on the surface being tested. It was allowed to sit for approximately 5 minutes as the tip was again lowered to the surface. After this, testing began again. Following testing the cantilevers were cleaned using an ultraviolet ozone cleaner, UVO-Cleaner Model No. 42, from Jelight Company, Inc. for 50 minutes. When not in use, the cantilevers were stored in a sealed plastic bag

to avoid contamination of the tip surfaces.

4.3.3.1 Verification of Methodology

In Figures 17 and 18, it is shown that the gold layer, except for the $70nm$ gold circle, was removed leaving only the chromium sublayer. The composition of the AFM tip surface was confirmed, by the Advanced Materials Processing and Analysis Center at the University of Central Florida, using scanning Auger microscopy. Figures 21, 22, and 23 show an area near the apex of the tip. It is important to note that no gold regions can be seen, not even the $70nm$ gold circle, due to the poor resolution of scanning Auger microscopy. But, it does show that no more than a small portion of the surface is gold.

The silicon map was performed to confirm that no silicon regions of the tip had been exposed. If this occurred it would be possible for the polymer used to adsorb to these regions via hydrogen bonding. There are regions of excited silicon Auger electrons which were detected. However, these same regions also show excited chromium Auger electrons. This is because the chromium layer was thin enough that the excited silicon Auger electrons were able to pass through the chromium layer. Although the chromium layer was thin, it was still present and confirms that the silicon layer is not exposed on the surface.

Following the verification of the surface composition of the modified tips, any interactions of the chromium regions of the modified tips with the polymer needed to be accounted for. To do this a chromium tip and a gold tip were tested following treatment in low and high concentration polymer solutions ($0g/ml$, and $6.98\text{x}10^{-4}g/ml$). Figures 24 and 25 show the force curves of both the chromium and gold tips after a treatment time of 1 minute in the high concentration polymer solution followed by rinsing in Barnstead deionized water. The tests clearly indicated that the polymer will only attach to the gold surfaces on our modified tips. This can be determined by

Figure 21: A scanning Auger map of the modified AFM tip showing the gold regions.

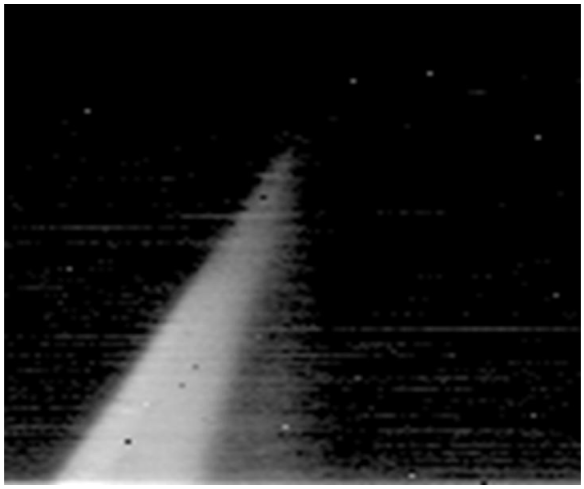

Figure 22: A scanning Auger map of the modified AFM tip showing the chromium regions.

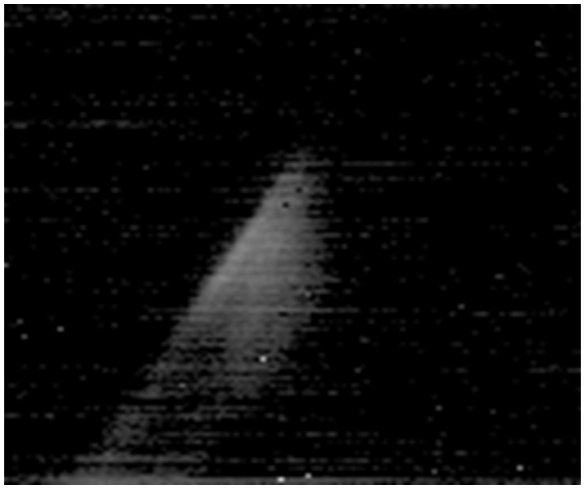

Figure 23: A scanning Auger map of the modified AFM tip showing the silicon regions.

looking at the deflections of the cantilever as it is retracted from the surface. In Figure 24 the line is straight confirming that no polymer is adsorbed between the tip and the substrate. It was also shown that physisorption of the polymer to the chromium surface of the tip was not present after rinsing in Barnstead deionized water. This verifies that the technique of exposing the chromium sublayer is an effective method to prohibit polymer adsorption.

The technique selected to ensure a single polymer for testing, leaving only a small area of gold on the tip available for polymer adsorption, is very likely to limit polymer adsorption to a single polymer. This reasoning is supported by the cationic polyacrylamide's tendency to form "mushroom" conformations when tethered by one end to a surface. This large "mushroom" will experience electrostatic repulsion between the cationic groups both within the polymer and with other polymers which may be trying to access the gold circle. This "mushroom" conformation would be expected to shield the gold circle, prohibiting any additional polymers from adsorbing. Griebel *et al.* reported the radius of gyration, R_g, for a cationic polyacrylamide of a similar molecular weight and charge density to be $95nm$[104]. The R_g of the polymer used for this research was found to be $151nm$ at the tip functionalization conditions. This

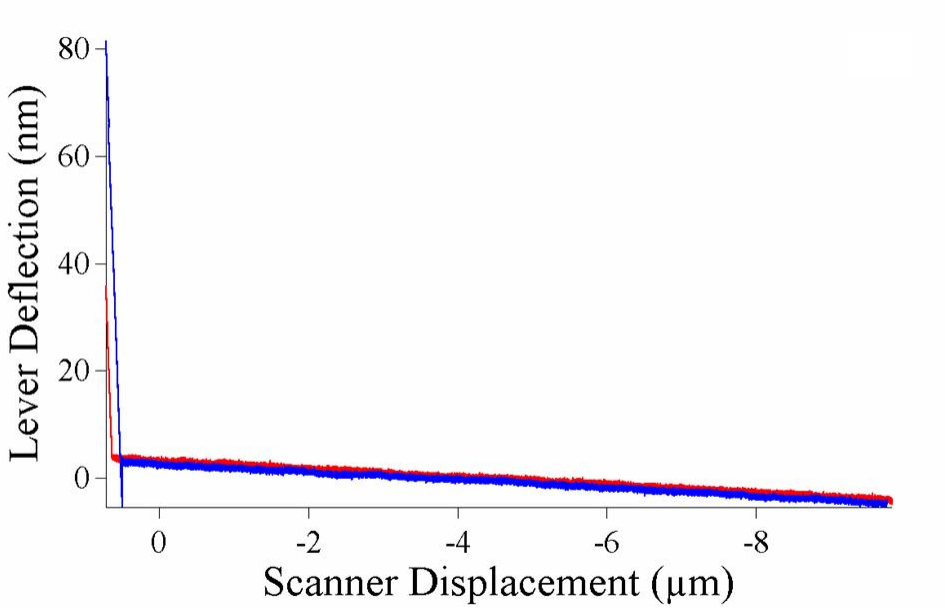

Figure 24: Force curve verification of a polymer treated chromium tip. Reproduced with permission from Macromolecules[30]. Copyright 2007 American Chemical Society.

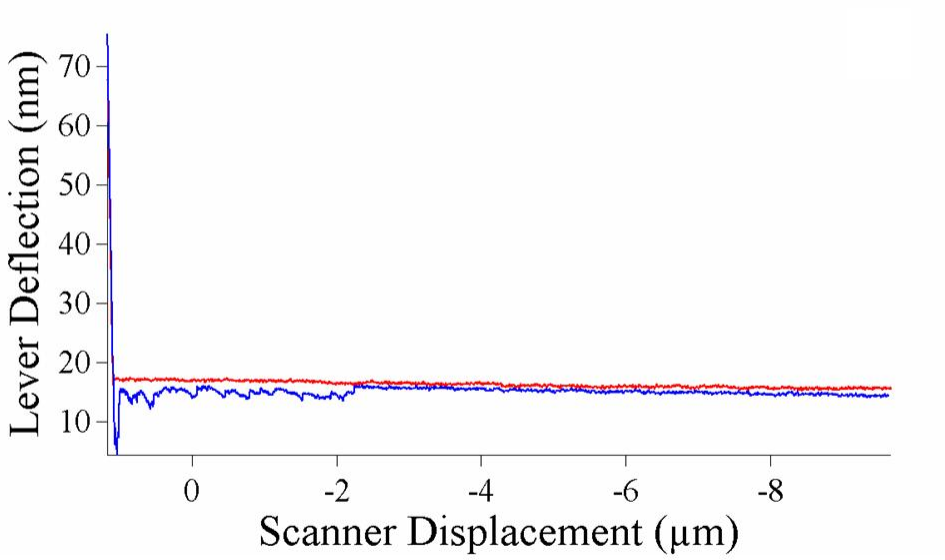

Figure 25: Force curve verification of a polymer treated gold tip. Reproduced with permission from Macromolecules[30]. Copyright 2007 American Chemical Society.

would result in a "mushroom" with a cap diameter of about $300nm$, which should easily cover the $70nm$ gold circle left on the cantilever tip, illustrated in Figure 26. This suggests that once a polymer is adsorbed on the gold circle on the tip of the cantilever, the adsorption of other polymer molecules to the gold circle is unlikely. Because the polymer does not chemically bond to the chromium surface, only one polymer molecule will adsorb on the surface by the chemical bond formed between the gold and thiol end group on the polymer.

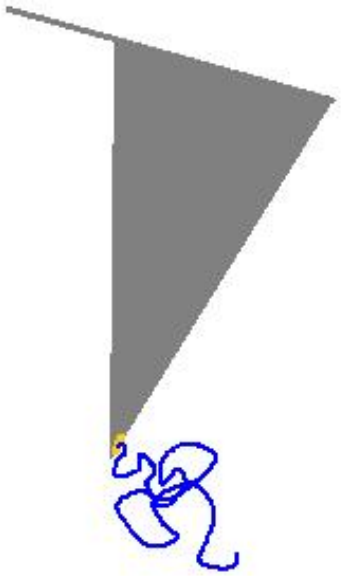

Figure 26: Illustration of how the single adsorbed polymer's "mushroom" cap covers the $70nm$ gold circle(near the apex of the tip).

This assumption was tested by exposing the AFM tip to polymer solutions of different concentrations and then looking for changes in the force curves. As can be seen in Figures 27 and 28, the extended treatment in a high concentration solutions of polymer does not significantly change the force curve. The total number of attachment points and the span in which they were found in Figure 28 were within the average deviation for those values in Figure 27. This does not conclusively prove that there is only one polymer on the tip. However, using the best methods currently available the assumption of a single polymer holds.

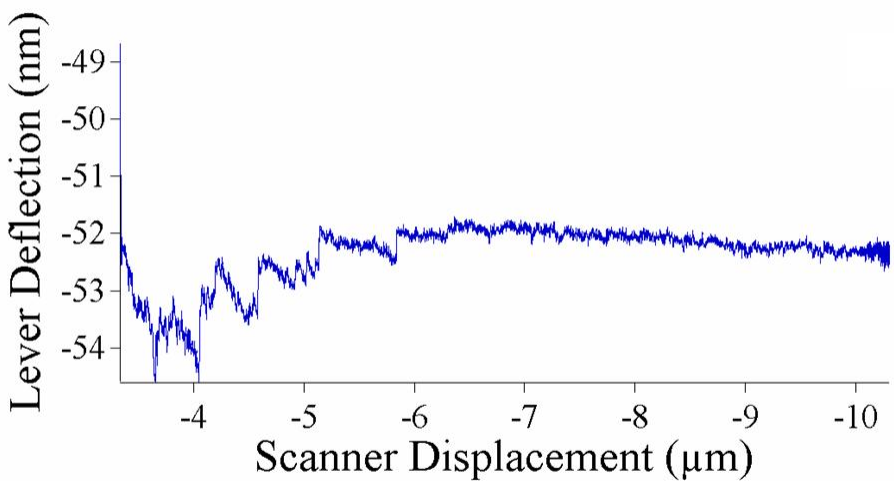

Figure 27: Force curve of cantilever tip treated for 1 minute in a $9.074\text{x}10^{-6} g/mL$ polymer solution. Reproduced with permission from Macromolecules[30]. Copyright 2007 American Chemical Society.

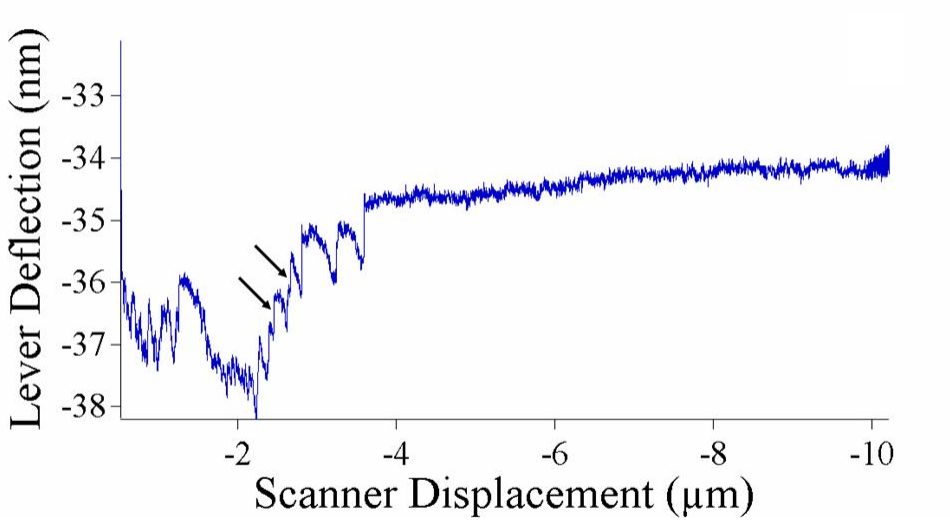

Figure 28: Force curve of cantilever tip used in Figure 27 treated for 5 additional minutes in a 6.98x10^{-4}g/mL polymer solution. Reproduced with permission from Macromolecules[30]. Copyright 2007 American Chemical Society.

4.3.3.2 Tip Retraction Rate

Past literature, using "pulling" AFM experiments to determine polymer loop lengths, has employed a wide range of cantilever retraction velocities with very little explanation for the selected velocities[108, 144]. Before this research could be started, the effect of tip retraction rate on the resulting polymer loop length distributions had to be investigated. In order to cover the span of retraction velocities used in the literature, the following rates were tested: $200nm/s$, $400nm/s$, $2\mu m/s$, $4\mu m/s$, and $10\mu m/s$. Figures 29, 30, 31, 32, and 33 show the population distribution of an adsorbed polymer put into $20nm$ bins. Bin sizes of 10, 20, 30, and $50nm$ were all tested to ensure the results were not significantly affected by the choice of bin size. A bin size of $20nm$ was selected because it gave the most detail without significantly decreasing the frequency of events in each bin. All frequencies were reported as the percentage of loops which fell in respective bins. This allowed for comparison using statistical methods without needing to account for the number of loops. The minimum number of loops used in a distribution was 74, the maximum number of loops was 517. The majority of the populations contained more than 100 loops, thereby showing statistical significance.

Unlike Hashcke *et al.*, no parts of the population on either end of the distribution have been removed leaving all data points that passed the criteria for selection described in the following sections[108]. This is an important criteria as a few very large loops, which Haschke would have discarded, can have profound effects on the interactions of the substrate this polymer is adsorbed, such as the collision efficiency in flocculation[108, 21]. The large loop lengths found in Figures 29, 30, 31, 32, and 33 may have resulted from nonuniform distribution of charged groups in the random copolymer used and also encounters with nonuniform regions of the mica surface. The shape of the polymer loop length distributions, above, are very similar to that those found by Levy and Maaloum, although the location is different[144, 145]. This

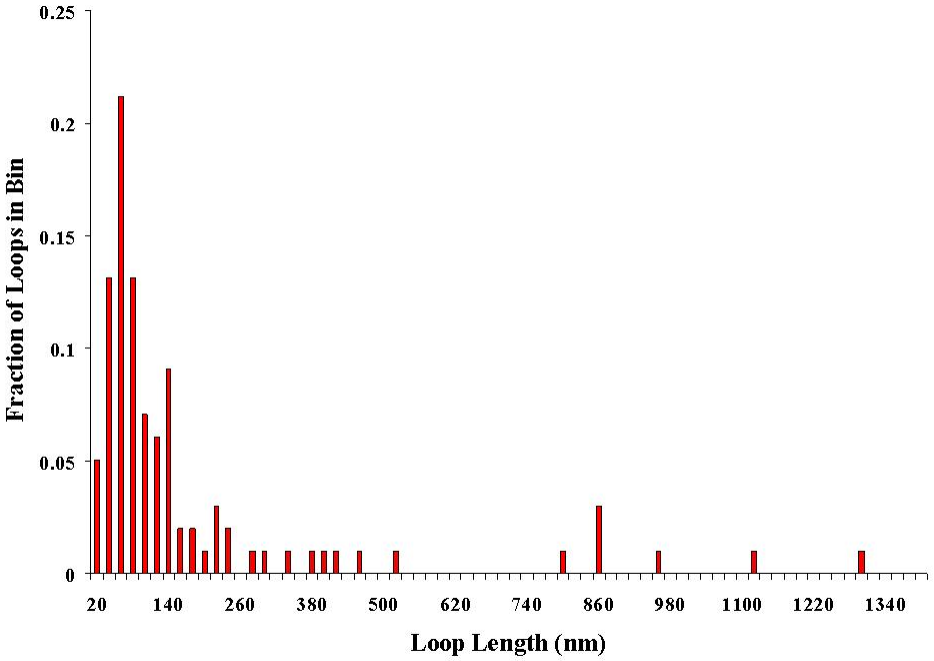

Figure 29: Adsorbed polymer loop length distribution using $200nm/s$ retraction rate on mica. Reproduced with permission from Macromolecules[30]. Copyright 2007 American Chemical Society.

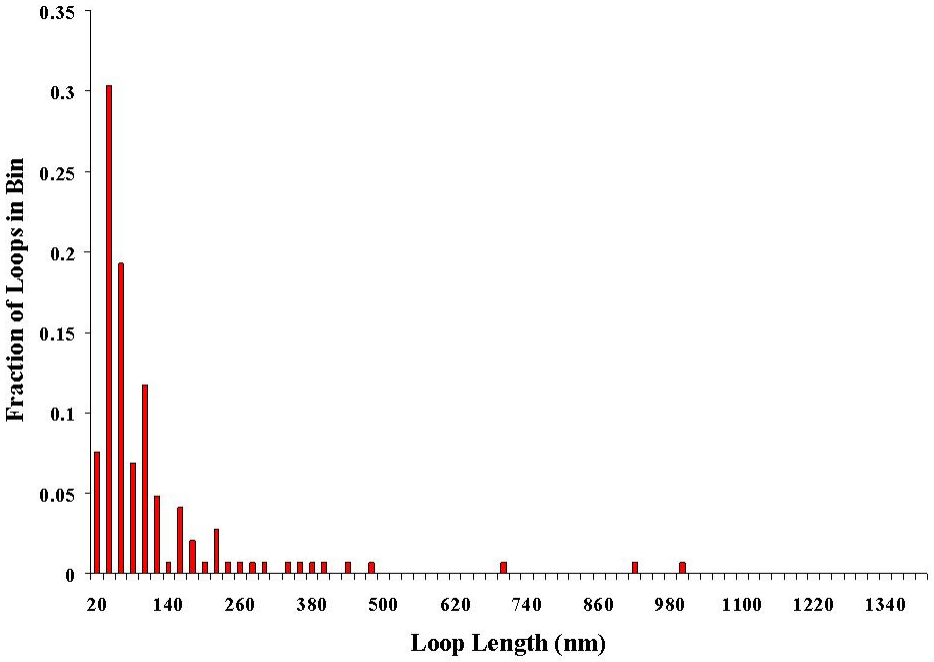

Figure 30: Adsorbed polymer loop length distribution using $500nm/s$ retraction rate on mica.

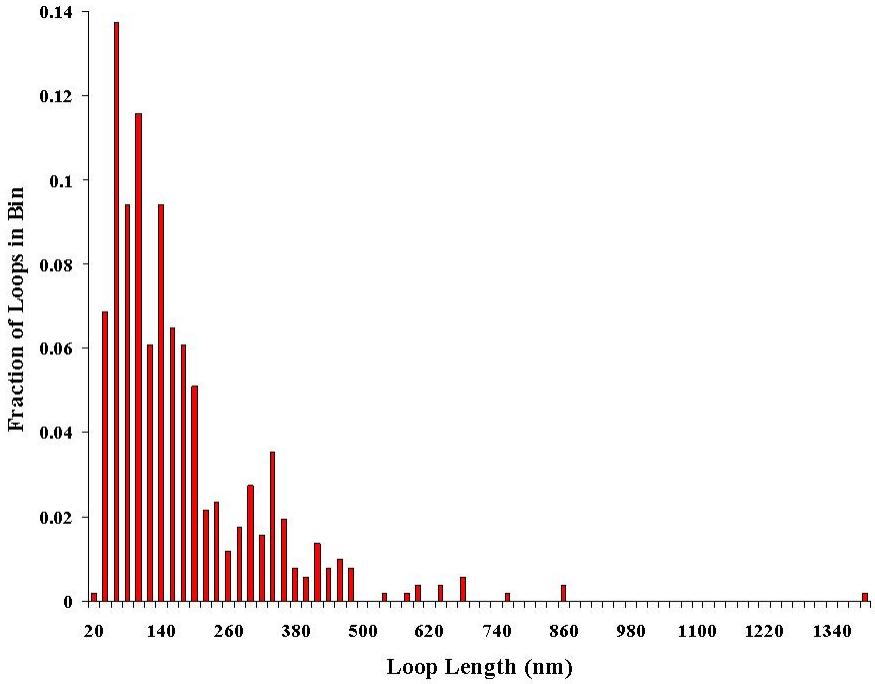

Figure 31: Adsorbed polymer loop length distribution using $2\mu m/s$ retraction rate on mica. Reproduced with permission from Macromolecules[30]. Copyright 2007 American Chemical Society.

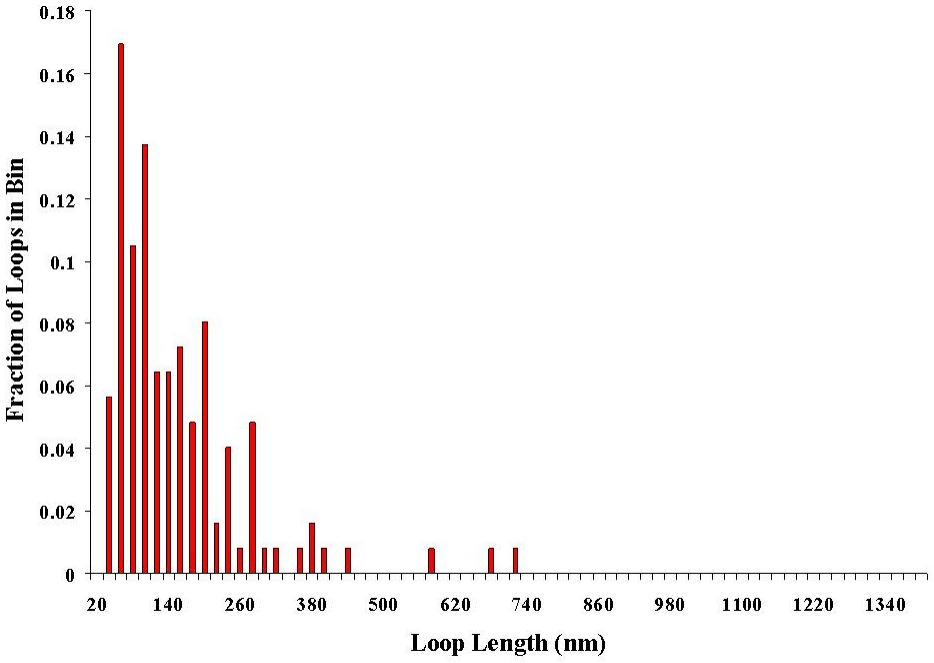

Figure 32: Adsorbed polymer loop length distribution using $4\mu m/s$ retraction rate on mica. Reproduced with permission from Macromolecules[30]. Copyright 2007 American Chemical Society.

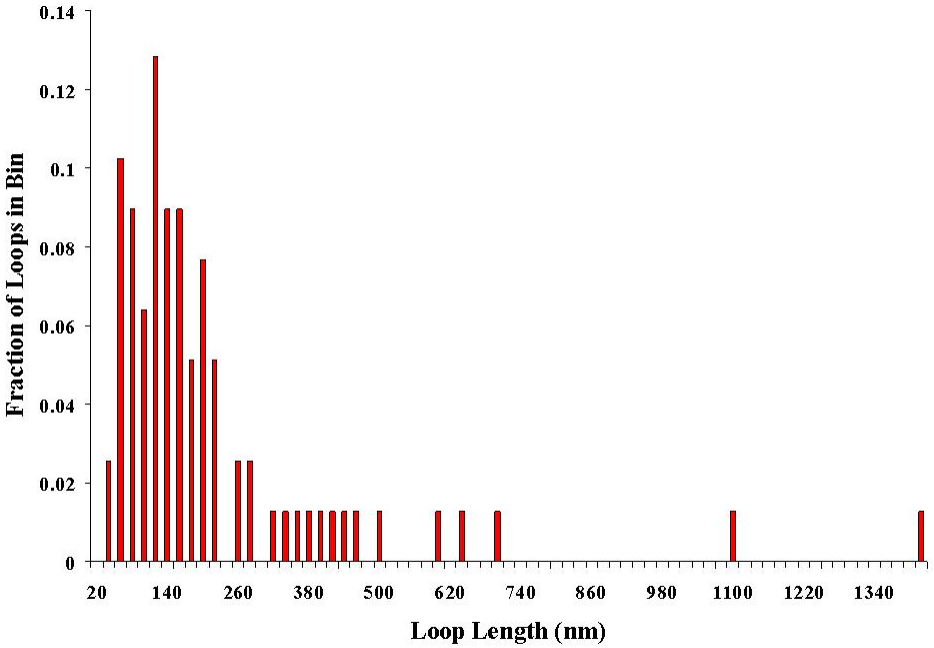

Figure 33: Adsorbed polymer loop length distribution using $10\mu m/s$ retraction rate on mica. Reproduced with permission from Macromolecules[30]. Copyright 2007 American Chemical Society.

is most likely due to the methodology used and the polymers analyzed[144, 145].

Figure 34 shows a plot of three different retraction rates on the same graph. The population distributions have the same scale and shape, but are not exactly the same. In order to compare these distributions, the chi-squared test for homogeneity was chosen. This test can be used for non-normal distributions, which this clearly is. Evaluating with a significance level of 99.9995%, it was shown that the population distributions for all retraction velocities were statistically the same. From this analysis, it has been shown that within the above testing limits the retraction rate does not have an effect on the polymer loop length distribution. This is significant in that future research may be conducted at whatever rate yields appropriate data. Following this test, the rest of the AFM work done for this research used a retraction rate of $2\mu m/s$.

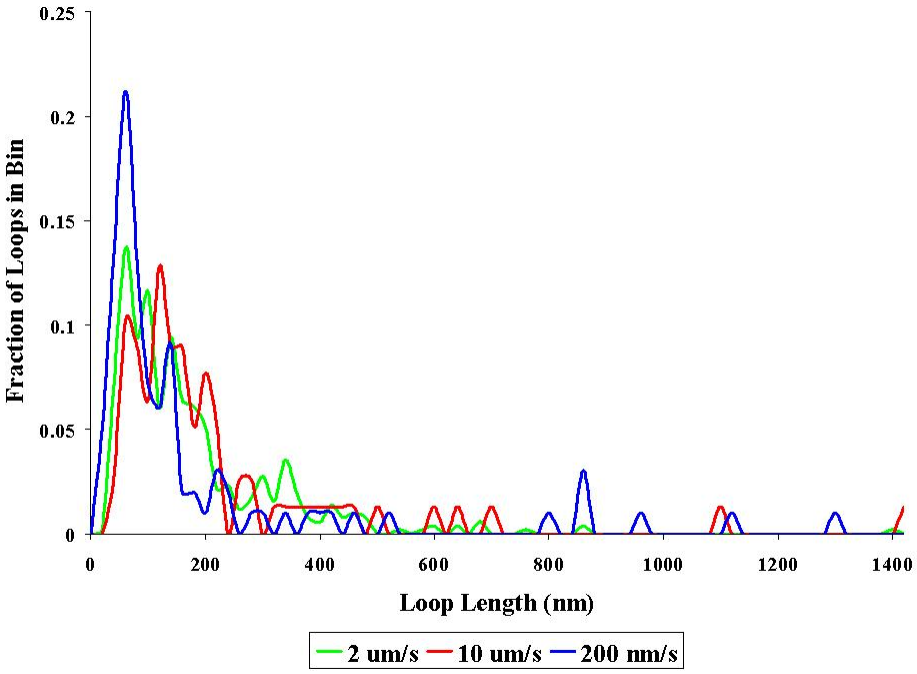

Figure 34: Effect of different retraction rates on the loop length distributions of adsorbed cationic polyacrylamide.

4.3.3.3 Data Selection

To analyze the polymer conformation and lengths of polymer loops, a method that can correctly determine the desorption points from a force curve must be developed. Much of the past work simply states that only "clear desorption events" are selected, which show a stretching of the polymer chain followed by a sharp detachment, as shown in each of the peaks selected in Figure 7. However, it is, in practice, difficult to determine the "clear desorption events". First, the minimum magnitude of the deflection necessary to make a point must be determined. Second, the number of data points required to be present to make up the stretching portion of an event should be determined. Levy and Maaloum wrote an algorithm to automatically pick out desorption events based on the magnitude of the detachment relative to the noise of the freely vibrating chain[145]. By doing this, they have set criteria to select points and limited the number of false events which could be selected. Levy and Maaloum required the deflection to be greater than the mean-squared deviation of the freely vibrating cantilever after the last desorption event[145]. For this research, this standard was taken a step further. It was required that the deflection of the lever must be greater than 3 times the average standard deviation of a freely vibrating lever and chain. This adds to the confidence that the deflections seen are not due to noise in the cantilever vibration. An investigation into the effects of the requirements on the stretching of the polymer chain relative to point selection was also performed. Table 1 shows how the selection of desorption events is altered by requiring different stretching lengths for acceptance.

Table 1 shows the effects of requirements on polymer stretching relative to desorption event selection. For this research, a minimum of 200 data points leading to a desorption event was required. This, in combination with the requirement on the magnitude of desorption events, will significantly reduce the chance of counting false desorption events. If the stretching criteria was increased to 1000 data points, events

Table 1: Effect of Polymer Stretching Criteria on Selection of Desorption Events in Figure 28. Reproduced with permission from Macromolecules[30]. Copyright 2007 American Chemical Society.

Number of Points in Stretch	**Number of Desorption Events**
50	19
100	19
200	14
500	9
1000	5

which appear to be significant, as illustrated by the arrows in Figure 28, are not counted.

4.4 Computer Simulation using Dissipative Particle Dynamics

The final method that was used in this research project is dissipative particle dynamics(DPD). DPD is a coarse grained modeling method which can be used to model large systems over long timescales. Molecular simulations, although able to yield exact results, are not capable, due to limitations of computing power, of simulating the dynamics of large molecules over large time spans. In order to model systems containing large molecules, coarse grained modeling was introduced. Coarse grained modeling doesn't account for the properties and movement of individual atoms, but groups them together and follows the group. In the case of DPD, these groups of atoms are represented by a hard sphere. These spheres are also set to only interact with each other if they are closer than a set r_c, cutoff radius[106]. The way these spheres interact with each other is governed by the Newton's Laws, shown in Equations 6 and 7, ensuring that momentum is conserved in the model.

$$\frac{\partial r_i}{\partial t} = v_i \tag{6}$$

$$m_i \frac{\partial v_i}{\partial t} = f_i \tag{7}$$

In DPD, the force term in Newton's Second Law is divided into three parts: (1)conservative force (2)dissipative force (3)random force[94]. This is shown in Equation 8.

$$f_i = \sum_{j \neq i} [f^C(r_{ij}) + f^D(r_{ij}, v_{ij}) + f^R(r_{ij})] \tag{8}$$

The components of this force are a conservative force, f^C, a dissipative force, f^D, and a random force, f^R. The conservative force corresponds to the interactions between spheres due to their affinity for each other. This can be seen in Equation 9[94].

$$f^C(r_{ij}) = a_{ij}(1 - r_{ij})\hat{r}_{ij} \tag{9}$$

In Equation 9, a_{ij} refers to the repulsive interaction parameter between two particular spheres. The next force component in DPD is the dissipative force given by Equation 10[94]. The dissipative force slows the movement in the system down, acting as a drag force.

$$f^D(r_{ij}, v_{ij}) = -\gamma \omega^D(r_{ij})(v_{ij} \cdot \hat{r}_{ij})\hat{r}_{ij} \tag{10}$$

γ is a variable which controls the strength of the drag force in the system, $\hat{r}_{ij}$ is a unit vector in the direction of r_{ij}, and ω^D relates to how the drag between spheres changes with distance from each other[94]. The final force component used in DPD is the random force. Equation 11 shows how the random force is determined[94].

$$f^R(r_{ij}) = \sigma \omega^R(r_{ij}) \xi_{ij} \hat{r}_{ij} \tag{11}$$

σ, used in the random force calculation, gives the magnitude of the random pair forces between different spheres, ξ is a random variable, and ω^R relates to the effect of

distance on the random force[94]. The random force is added to conserve momentum in the system by adding speed to the system to counteract the dissipative force. The two forces are directly related to each other through Equations 12 and 13[94].

$$\omega^D(r_{ij}) = [\omega^R(r_{ij})]^2 \tag{12}$$

$$\sigma^2 = 2k_B T\gamma \tag{13}$$

The previous group of equations can be used to find the forces acting on individual spheres in the system. In order to solve these equations simultaneously, the velocity-Verlet algorithm was used[106]. The only other parameters needed in this model to make it applicable to this project's scope were a wall, to which the polymer can adsorb, and a method to connect beads to form a polymer. Walls for use in DPD can be created using two different methods: creation of an actual wall or creation of a virtual wall[218].

First we will consider the technique of creating a physical wall composed of "frozen" beads. In this technique beads are frozen in place preventing the mobile phase of beads from moving through the wall. This technique has been popular with many researchers[218, 161, 205, 27, 99, 132]. This system also allows the mobile phase of the simulation to interact with the wall through the bead/bead interactions parameters, a_{ij}. One disadvantage of this wall technique is that it requires the parameterization of a physical wall[218]. To get around this disadvantage, the creation of virtual walls for certain systems can be helpful.

There is very little research published, which clearly discusses, using virtual walls in DPD simulations[27]. Boek *et al.* modified the boundary conditions of their system to allow it to accurately represent shear flow in their system[27]. As stated in the previous paragraph, this allows the physical interactions of the wall beads to be disregarded and modeled theoretically only. For this work, due to the size of the

system which will be modeled, the virtual wall was chosen to be the best method to model polymer adsorption on a surface. In order to create an impenetrable wall thousands of beads would be necessary. This would severely increase the computation time as the interactions between all beads in the system must be calculated each time step. Because the beads in the wall must be close enough that no other beads may pass through many of the wall beads will be within the cutoff radius for the force calculations.

In order to simulate a wall, which a polymer can adsorb on, a hypothesis for the mechanism of adsorption needed to be assumed. Because this work deals with systems of cationic polymers adsorbing on anionic substrates an assumption of electrostatics as the mechanism of adsorption is reasonable. This is not the only adsorption theory which has been used. The Langmuir equation has been used to simulate molecular adsorption on substrates[113]. However, this equation does a poor job simulating polymer adsorption[113].

For this project, the assumption of electrostatics dominated adsorption led to the use of the Poisson-Boltzmann equation, Equation 14[25].

$$\nabla^2 \frac{\nu e \psi}{k_B T} = \kappa^2 sinh \frac{\nu e \psi}{k_B T} \tag{14}$$

In Equation 14, e is the electronic charge, $k_B$is Boltzmann's constant, ν is the charge number, ψ is the surface potential, T is the temperature, and κ is the inverse Debye screening length. Because this form of the Poisson-Boltzmann equation is nonlinear it is difficult to use. The linearized Poisson-Boltzmann equation, Equation 15, is a commonly used solution to this problem[25].

$$\nabla^2 \frac{\nu e \psi}{k_B T} = \kappa^2 \frac{\nu e \psi}{k_B T} \tag{15}$$

The use of the linearized Poisson-Boltzmann equation to determine the energy between two charged surfaces has been shown in the literature[219, 122, 25]. The original

derivations of this equation for use between two infinite flat plates was performed by Gregory[103]. Since then, derivations have been extended to include interactions between similar spheres and also interactions between a sphere and a flat plate[34, 25]. In the DPD system which is being modeled, all particles are spherical beads. Because of this, the derivation by Bhattacharjee and Elimelech between a sphere and flat plate will be used. This energy derivation is shown in Equation 16.

$$E = \pi\epsilon_0\epsilon_r a \left(\frac{k_B T}{\nu e}\right)^2 (\Psi_s^2 + \Psi_p^2) \left[\frac{2\Psi_s^2\Psi_p^2}{\Psi_s^2 + \Psi_p^2} ln\left(\frac{1 + e^{-\kappa D}}{1 - e^{-\kappa D}}\right) + ln(1 - e^{-2\kappa D})\right] \quad (16)$$

Equation 16 gives an interaction energy between a sphere and a plate. In this equation a is the radius of the sphere and D is the distance between the sphere and the plate. DPD, however, requires the use of forces. To do this, the force can be calculated as the first derivative of energy with respect to distance[14]. The force obtained with the derivative of Equation 16 is used on all the beads in the system in the direction perpendicular to the wall. The surface potential of the wall is considered constant making this approach reasonable.

To use DPD to model a polymer's movement, individual spheres in the system need to be connected to form a polymer. The same methods of solving movement of the polymer apply here as well except the individual beads will be held together by a defined spring constant. This technique has been used by many researchers using dissipative particle dynamics[124, 235, 258]. For this work, Equation 17 describes the force holding the polymer beads together.

$$F = k_{polymerbond}(L - D)(\hat{r}_{ij}) \quad (17)$$

In Equation 17, $k_{polymerbond}$ is the spring constant of the bond, L is the equilibrium bond length, D is the actual bond length, and $\hat{r}_{ij}$ is the unit vector this force is applied along. Most computer simulations of polymer conformation are done using atomistic

models and small polymers[247, 157, 162, 290, 214]. Other simulations modeled polymer adsorption on surfaces and its adsorbed conformation using molecular dynamics simulations and Monte Carlo simulations[88, 204, 76, 158, 264, 274, 110, 44]. Groot and Warren simulated a polymers conformation in solution using DPD[106]. This work attempted to use this approach to model polymer adsorption on a surface under the same conditions which were evaluated in the two experimental methods of this project.

4.4.1 Dissipative Particle Dynamics Materials

All simulations for this research were carried out using Molecular Operating Environment software from the Chemical Computing Group. Because this software does not have dissipative particle dynamics code, it was necessary to develop that code. This was done by Andrew Swann and John Melnyczuk. The developed code can be found in Appendix A.

Table 2 lists the variables which can be modified in the code. In the DPD code, used for this research, all of the variables are scaled based on certain parameters of the system. This leaves them dimensionless and this approach is always used in DPD simulations[124, 235, 94, 163, 13, 258, 120]. Scaling eliminates the need to convert units in the DPD code.

The dissipative particle dynamics code developed also included the use of a periodic box to describe the system. This allows beads or polymers which pass through limits of the box to be placed back on the other side conserving their momentum and direction. This is a commonly used technique in modeling to allow the simulation of large systems without modeling the entire system[7]. The modeling done in this research, also, does not simulate the solvent phase of the systems. This was done to reduce the number of beads in the system. Interactions between the polymer and solvent can be accounted for by adjusting the a_{ii}, a_{jj}, and a_{ij} parameters. Solvent effects

Table 2: Input parameters for DPD code.

Variables	**Variable Name in DPD Code**
Total number of polymer A chains	NA
Mass of an A bead	massA
Number of beads in polymer A	NA_beads
Total number of polymer B chains	NB
Mass of a B bead	massB
Number of beads in polymer B	NB_beads
X dimension of box	edgex
Y dimension of box	edgey
Z dimension of box	edgez
σ	sigma
$k_B T$	kbT
a_{ii} parameter	aii
a_{ij} parameter	aij
a_{jj} parameter	ajj
Cutoff radius	rc
Total simulation time	sim_length
Time step	dt
Number of time steps between save points	sample_time
Value of the bond spring constant between beads	bond_spring
Equilibrium bond length	blength
Radius of a bead	bead_radius
Inverse Debye length	kappa
Lennard Jones energy of attraction	energy_attraction
Lennard Jones collision diameter	collision_diameter
ν_{sphere}	nu_s
ν_{wall}	nu_p
ψ_{sphere}	psi_s
ψ_{wall}	psi_p

on bead movement are also accounted for, in DPD, by adjusting specific stochastic and viscous drag terms. These terms, σ, γ, ω^D, and ω^R, and their relation to one another are shown in Equations 10 - 13. The DPD code used for this work allows the stochastic and viscous drag terms to be adjusted by altering the value of σ, or Equation 18 which relates distance effects on the random force while $r_{ij}<r_c$.

$$\omega^R = 1 - \frac{r_{ij}}{r_c} \tag{18}$$

One last detail is the location of the wall that the polymers will attempt to adsorb on. It was chosen, for this work, to place this wall in the middle of box. This allows the periodic box use to continue unaltered. It also allows the investigation of two surfaces with each simulation.

4.4.2 Verification of DPD Code

The DPD code, developed by Swann and Melnyczuk, used for this work was coded here at Georgia Tech. Because of this, it was necessary to validate that the code used gives the same results as other researchers DPD code. To do this, an example of a phase separating system from Frenkel and Smit's book was used[94]. Table 3 details the values used in this test.

Table 3: Input parameters for DPD code.

Variables	**Variable Name in DPD Code**
NA	3000
massA	1
NA_beads	1
NB	3000
massB	1
NB_beads	1
edgex	10
edgey	10
edgez	20
sigma	1.5
kbT	0.45
aii	25
aij	30
ajj	25
rc	1
dt	0.03

For this DPD model, all the beads were randomly placed inside the box, checked

to ensure no bead overlaps were allowed, and the simulation was started. This is shown in Figure 35. Because no length of time was given for the simulation, the model was allowed to run for about one week. Frenkel and Smit reported a nearly complete split of the beads on opposite halves of the box[94]. The results shown in Figure 36 do not show this complete separation. However, it is apparent that phase separation has begun by the large patches of similar beads. With more simulation time complete phase separation would be expected. This simple test has verified that the code written for this work does work properly for a well known system tested by other researchers.

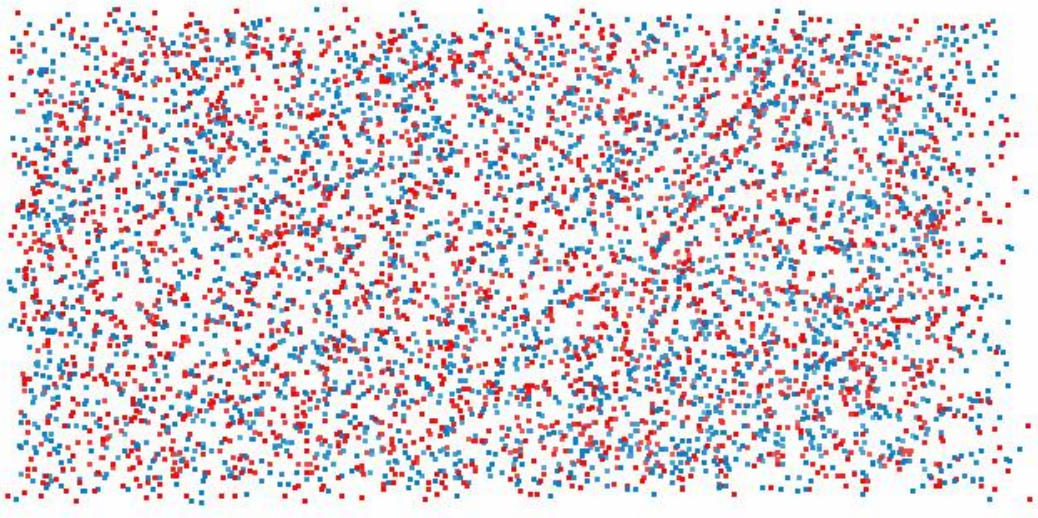

Figure 35: Beginning of Frenkel and Smit phase separation test.

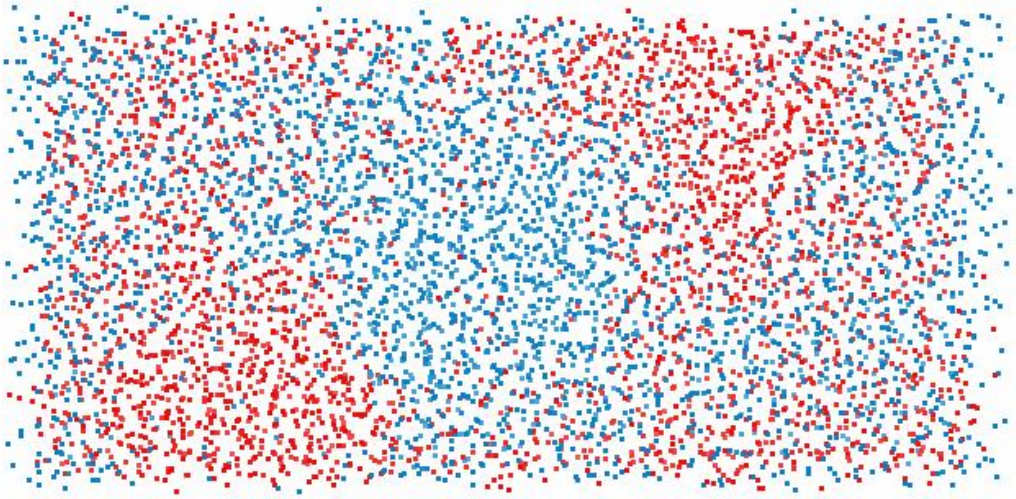

Figure 36: End of Frenkel and Smit phase separation test.

CHAPTER V

ADSORBED POLYMER CONFORMATION

5.1 Overview

In order to understand how site blocking and other factors affect adsorbed polymer conformations, an initial study of what an adsorbed polymer's conformation actually is must be performed. Using the experimental methods outlined in Chapter IV, this chapter will evaluate how the MAPTAC/acrylamide copolymer's conformation can be described.

5.2 Dynamic Light Scattering to Measure Adsorbed Polymer Conformation

Dynamic light scattering has been used extensively in the literature to determine the thickness of adsorbed polymer layers on surfaces[267, 179, 169, 185, 276, 286, 119, 167, 296, 207, 128, 75, 268, 105, 136, 66]. With the addition of a MAPTAC/acrylamide copolymer, it was expected that the hydrodynamic radius of the latex spheres, used for this research, would increase. This was shown in Figure 14. As explained in the experimental portion of this thesis, a low concentration of MAPTAC/acrylamide copolymer was chosen and added for these studies. The thickness of the adsorbed polymer layer found is illustrated in Figure 37.

Figure 37 reports an average thickness, of an adsorbed polymer layer, to be $9.45nm$. The small increase in hydrodynamic diameter, after addition of the polymer, was of the same order of magnitude as the results found by previous researchers[128]. From this average thickness, it was possible to propose possible scenarios about the adsorbed polymers conformation. For example, it is known that the polymer used for this research is around 2 to $3\mu m$ in length. From this, a $10nm$ adsorbed layer

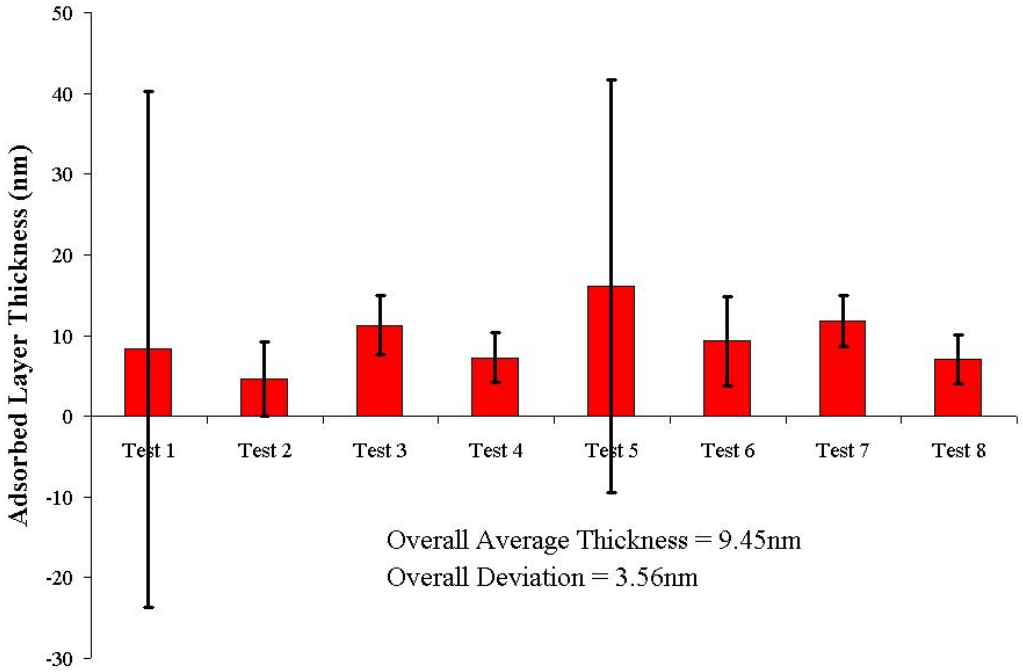

Figure 37: Dynamic light scattering layer thickness results for adsorbed MAPTAC/acrylamide copolymer on anionic latex spheres.

thickness could be explained by the polymer adopting a relatively flat conformation. Unfortunately, what this thickness actually describes is unclear.

Using the conclusions of Nelson *et al.* that the tail portion of an adsorbed polymer's conformation has the most significant effects on adsorbed polymer layer thickness, it could be presumed that the tail length's of the polymers adsorbed on the latex spheres are relatively short. If these tails are not short, then the remaining polymer on the surface is most likely adsorbed very tightly, or flat, on the surface.

The standard deviations on the adsorbed polymer layer thicknesses are large, as shown in Figure 37. For Tests 1 and 5, the standard deviation is extremely large. The high deviation for these tests was due to a couple thickness readings being either far higher or far lower than the average value. For this work, an algorithm which removes scattering noise generally associated with dust, was not used due to the inability to get an accurate description of how this dust filter worked from Brookhaven Instruments.

Because all data was allowed, it was not unreasonable to see significant deviations from the average adsorbed polymer layer thicknesses.

It is known that by keeping the polymer concentration low, the chances of the latex spheres flocculating are reduced. However, this also prevents full coverage of the sphere surface with the polymer, which can interfere with the assumptions made to describe the particle diameter in dynamic light scattering. Since dynamic light scattering is a common experimental technique to analyze adsorbed polymer conformation, the results presented in Figure 37 will be noted. Further evaluation would be required to accurately describe what is actually happening(not included in this work).

5.3 Atomic Force Microscopy to Measure Adsorbed Polymer Conformation

Using atomic force microscopy, more information was gained regarding the adsorbed conformation of cationic polyacrylamide. Portions of the following sections were reproduced with permission from Macromolecules[30], copyright 2007 American Chemical Society. Two substrates were used for the atomic force microscopy portion of this work, glass and mica.

In order to understand how a polymer can adsorb onto these surfaces, the composition of these surfaces must be known. The surface composition and structure will directly affect the geometric arrangement of an adsorbed polymer. Figure 20 illustrates the crystal structure of a cleaved sheet of mica with 50% of the potassium ions removed. Information regarding the possible adsorption sites of the MAPTAC/acrylamide copolymer is directly related to where the desorbed potassium ions are located. Figure 38 shows the structure of a cleaved sheet of mica containing all the potassium ions along the cleavage plane.

The purple balls, in Figure 38, are the potassium ions. The distance between the potassium ions is 5.189Å, found using the crystal parameters given by Radoslovich[212].

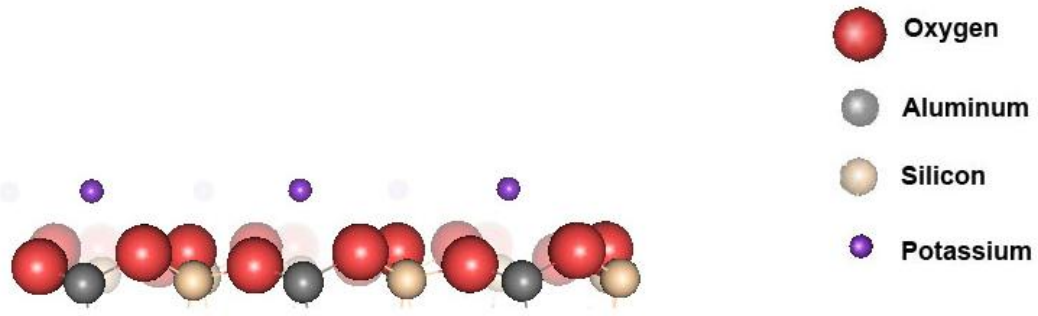

Figure 38: Surface structure of a cleaved mica surface in which all the potassium ions of the cleavage plane are attached.

Knowing this distance, and looking at the structure of mica, from Figure 20, the distance to any of the nearest potassium ions, or vacant lattice sites, from any potassium lattice site is 5.189Å. Knowing this distance, the total number of potassium ions, or possible adsorption sites, can be calculated for the $15mm$x$15mm$ mica squares used. The total number of potential potassium ions present on a cleaved, defect free, mica square is 8.36x10^{14}. If all of the potassium ions remained on the mica surface being evaluated, when 1% of the potassium ions dissociate into the water present, the number of possible adsorption sites would be 8.36x10^{12}. If 50% of the potassium ions were lost during the cleaving of the surface, the number of possible adsorption sites would be 4.18x10^{14}. If an additional 1% of these adsorption sites are gained when the surface is submerged, the total number of sites available would be 4.22x10^{14}. The previous calculated possibilities are the total number of sites to which the MAPTAC unit in the polymer backbone can possibly adsorb. Hydrogen atoms from the amide group in the acrylamide repeat units can hydrogen bond with the oxygen atoms in the vacant sites[77]. However, this hydrogen bonding will not occur in the center of the oxygen ring. It will occur over a single oxygen atom. Deng *et al.* also noted, that when polyacrylamide adsorbes on a surface via hydrogen bonding, the carbonyl oxygen minimally participates in the bonding[77]. This states that only one hydrogen atom on each acrylamide group can participate in hydrogen bonding and there will

only be one hydrogen bond formed.

With the total number of possible adsorption sites listed previously, it was possible to investigate the limiting cases in adsorbed polymer loop lengths. The minimum distance of a possible polymer loop length is 5.189Å. This distance, however, is unlikely to occur due to the distance between polymer backbone groups which could possibly adsorb. To address this, a quick simulation of a repeat unit of the acrylamide/MAPTAC copolymer was performed to determine the distance between possible adsorbing sites, shown in Figure 39.

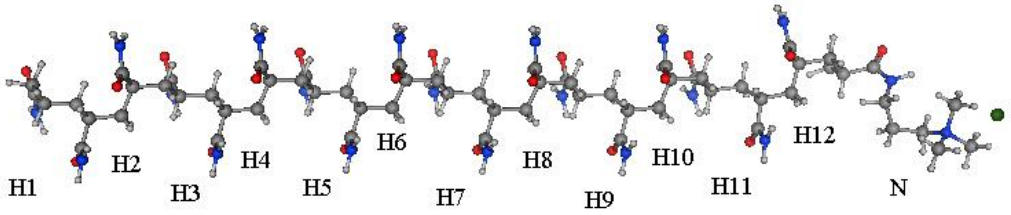

Figure 39: Repeat unit of the MAPTAC/acrylamide copolymer, containing 18 acrylamide groups and 1 MAPTAC group, used. The conformation shown was taken at a minimized energy state.

In this simulation, the energy of the system was minimized to give the most likely structure present in the polymer. However, because only one repeat unit was modeled, the system lacks the additional constraints the rest of the polymer chain would add. Therefore, the distance between the nitrogen atom, of the MAPTAC unit, and the hydrogen atoms on the amide group of the acrylamide which could possibly adsorb are given in Table 4.

In Table 4 and Figure 39, it is illustrated that if every possible hydrogen that can hydrogen bond(6 total) and the MAPTAC unit adsorbs there would be 7 adsorption points in a span of approximately 42Å. It was determined, after studying the mica crystal lattice, the minimum distance between two possible MAPTAC unit adsorption sites was 5.189Å. Combining these discoveries, if the hydrogen atoms on

Table 4: Distance, in Å, between nitrogen atom and hydrogen atoms, shown in Figure 39, capable of physisorbing on the mica surface.

	H1	**H2**	**H3**	**H4**	**H5**	**H6**	**H7**	**H8**	**H9**	**H10**	**H11**	**H12**	**N**
H1		1.73	6.35	7.92	12.71	13.34	19.26	19.85	26.08	26.56	33.02	33.34	41.95
H2	1.73		6.08	6.31	12.32	12.73	18.86	19.31	25.67	26.05	32.57	32.81	41.44
H3	6.35	6.08		1.73	6.36	7.98	12.91	13.52	19.73	20.22	26.67	27.00	35.60
H4	7.92	6.31	1.73		6.12	6.42	12.60	13.00	19.40	19.74	26.27	26.50	35.13
H5	12.71	12.32	6.36	6.12		1.73	6.55	7.21	13.38	13.87	20.31	20.65	29.24
H6	13.34	12.73	7.98	6.42	1.73		6.35	6.58	13.05	13.33	19.87	20.08	28.71
H7	19.26	18.86	12.91	12.60	6.55	6.35		1.73	6.82	7.41	13.76	14.18	22.72
H8	19.85	19.31	13.52	13.00	7.21	6.58	1.73		6.57	6.75	13.29	13.51	22.13
H9	26.08	25.67	19.73	19.40	13.38	13.05	6.82	6.57		1.73	6.96	7.56	15.95
H10	26.56	26.05	20.22	19.74	13.87	13.33	7.41	6.75	1.73		6.58	6.79	15.39
H11	33.02	32.57	26.67	26.27	20.31	19.87	13.76	13.29	6.96	6.58		1.73	9.00
H12	33.34	32.81	27.00	26.50	20.65	20.08	14.18	13.51	7.56	6.79	1.73		8.64
N	41.95	41.44	35.60	35.13	29.24	28.71	22.72	22.13	15.95	15.39	9.00	8.64	

the acrylamide groups hydrogen bonded with an oxygen atom at the empty potassium ion sites, it would be possible that all of these groups could adsorb. However, the hydrogen atoms will bond with a specific oxygen atom, in most cases increasing the distance between adsorption sites by approximately 2.6Å, or half the distance between potassium ions.

Figure 40 illustrates the typical atoms present on a glass surface similar to that used for this work. Because glass is an amorphous material, the distance between oxygen atoms, or possible adsorption sites, can not be calculated with any accuracy. However, the knowledge that each silicon atom will be surrounded by three oxygen atoms is helpful in understanding how the oxygen atoms in the surface may be arranged.

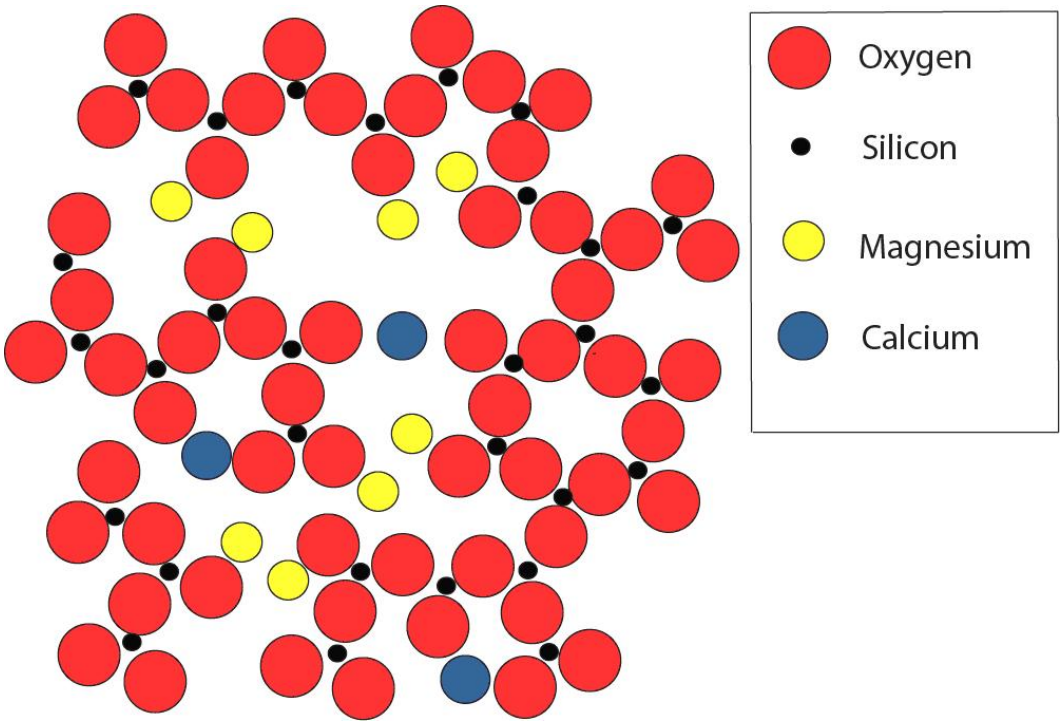

Figure 40: Approximate representation of the atoms that make up the type of glass used and their approximate ratios.

Using the AFM technique outlined in the experimental section, it would not be possible to resolve desorption events which are only separated by 42Å. This is due

to the requirements on the number of data points leading up to a desorption event relative to the sampling frequency. Coupled with this, each desorption event found could be a sum of multiple close events pulling off due to noise. This aspect, along with the angle of the pull, makes deriving information regarding the type of bonding by desorption force impossible.

From the AFM research done for this project, a loop length distribution of the MAPTAC/acrylamide copolymer on mica was compiled. This is illustrated, along with the weighted average maximum loop length, in Figure 41. In order to calculate the effect of the loops on the expected adsorbed polymer layer thickness, the weighted average maximum loop length must be divided by two. This assumes that the loop goes straight up into the solution and comes back down on the exact point it left from. This is, of course, not possible, but it gives a good approximation for relating loop length distributions to adsorbed polymer layer thicknesses. When this was performed on the data from Figure 41, the adsorbed polymer layer thickness was calculated to be $87.14nm$. It should be noted, however, that if the loops were analyzed with more emphasis on the location of the attachments, it would be possible to develop a range of lower maximum adsorbed polymer loop lengths, which may help in system analysis.

Although a method to compare AFM experimental results to those of dynamic light scattering is desirable, there is a large amount of information hidden in the AFM data which was not shown by the weighted average maximum polymer layer thickness. The distribution, shown in Figure 41, is of particular interest, as it shows direct evidence of the adsorbed polymer conformation. From this distribution it is shown that the majority of the polymer loops, for a MAPTAC/acrylamide copolymer on mica, lie between 40 to $260nm$. There were relatively few large loops present, possibly due to the five minute relaxation time allowed. Information on the length of the adsorbed polymer tail would be particularly valuable in clarifying this information.

Figure 41 also allows conclusions to be made regarding higher order polymer

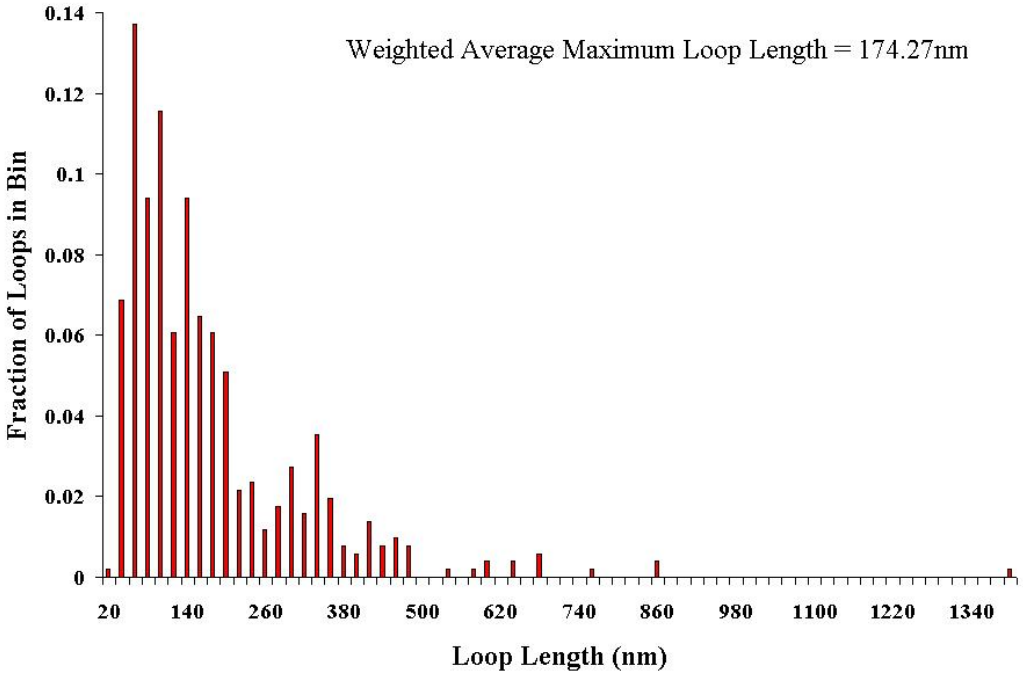

Figure 41: Loop length distribution for polymer on mica.

structures and their affect on adsorbed polymer conformation. Table 4 showed that if a polymer adsorbed flat on a surface the separation between groups would possibly allow multiple attachments at close range down the polymer chain. However, due to the inaccessibility of many of the sites, the MAPTAC/acrylamide copolymer was not allowed to adsorb tightly to the mica surface. The distance between attachment points is a function of the availability of surface sites and the constraints placed on the polymer by its higher ordered structures.

It was expected that the MAPTAC/acrylamide copolymer used for this work would adsorb more tightly to a glass surface than a mica surface. This was thought to be primarily due to the increase in the number of anionic sites present on the glass surface available for adsorption. Glass acquires a negative surface charge in water through the dissociation of silanol groups[22]. Behrens and Grier predicted that the charge density of a glass plate, at neutral pH, was between -1 and -1.2mC/m^2[22].

Figure 42, reports the adsorbed polymer loop length distribution of MAPTAC/acrylamide

copolymers from a glass surface. From this figure it was shown that the loop length distribution did not appear to be much different than that on a mica substrate. However, the number of attachments on the glass substrates were significantly larger. Although the polymers used on the glass and mica surfaces were different it is probable that the MAPTAC/acrylamide copolymer is held more tightly to the glass substrate, as shown by the number of attachments. The weighted average maximum loop length is $133.18\mu m$. This is about $50\mu m$ smaller than the mica substrate's value. The shape and range of adsorbed polymer loop lengths are similar. Much of this can be attributed to the very heterogeneous structure of the glass relative to mica.

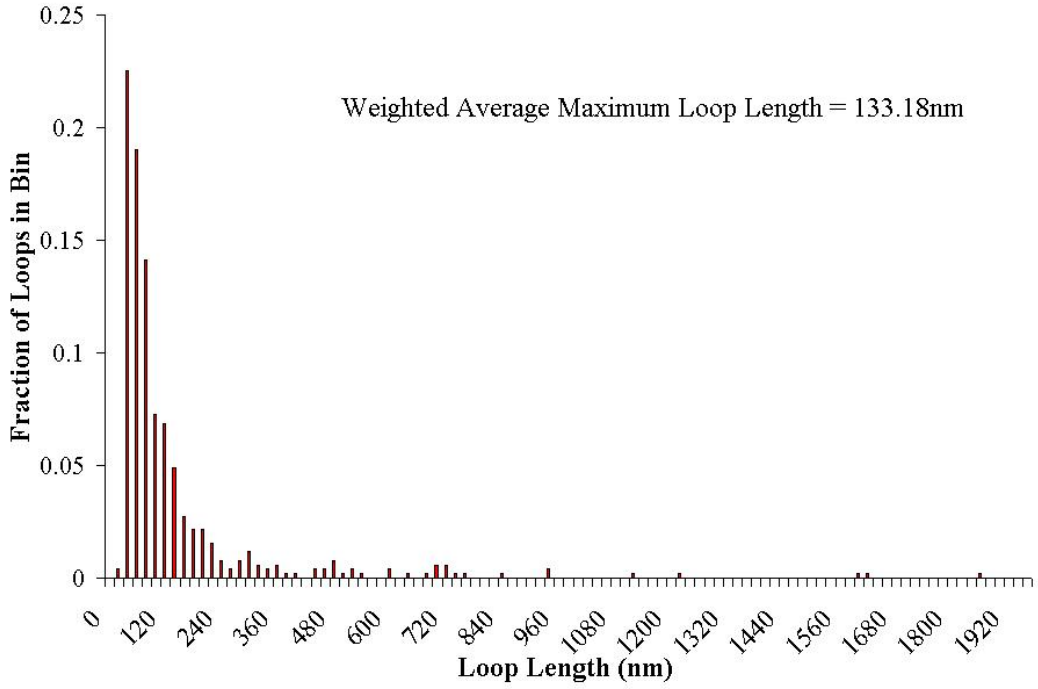

Figure 42: Loop length distribution for polymer on glass.

Although the data presented in Figure 42 appears to support current theory on changes in the substrate on adsorbed polymer conformation, some problems with the experimental methods used for this research were found. To prepare the glass coverslips as a substrate they were washed in a hot water/soap solution. Following this they were rinsed extensively to remove the surfactants from the glass surface.

However, it is possible that some of the surfactants could have remained on the glass surface following the rinsing allowing for contamination of the AFM results. A couple experiments had unexpected AFM results which would relate to a polymer being over $10\mu m$ long. It is possible that these results were due to an association of the surfactant and the cationic copolymer resulting in a multiple polymer pull. The results reported above are thought to be acceptable. However, there is no way to verify this. Therefore, the glass results will be reported and discussed but caution should be used when applying this data.

A common trend to this work and all other AFM "pulling" experiments, is shown in Figures 27 and 28. In these figures, it appeared that the majority of the polymer attachment points are present in the beginning of the pull, the left side. One possible explanation for this assumes that the method of polymer adsorption is electrostatics.

Although the MAPTAC/acrylamide copolymer used is thought to have a random distribution of MAPTAC units throughout the polymer chain, this may not be the actual situation. Tanaka found that the rate of polymerization of acrylamide is greater than that of MAPTAC[260]. This means that the acrylamide in solution will add to the growing chain faster than the MAPTAC units. In the polymerization method used to make this polymer with a terminal thiol group, the polymerization starts at the terminal end without the thiol group. As the polymer chain grows, initially, more acrylamide groups could add to the chain. However, once there is a concentration gradient in the polymerization solution then the MAPTAC units will have a higher probability of reacting with the growing chain. Finally, the thiol group will sit at the other terminal end of the polymer. This may cause more MAPTAC units to be closer to the thiol terminal end of the polymers, or the region closest to the AFM tip. If this is the case, and electrostatics dominates adsorption, it would be expected that the majority of the adsorption points would be relatively close to the AFM tip. Coupled with this the fact that the AFM tip confines a the polymer near the surface

will also cause more adsorption points to occur, as the polymer is not attracted to the tip and is forced near the surface.

5.3.1 Comparison with Theory

A considerable amount of work has been performed in the past to theoretically model adsorbed polymer conformations[233, 10, 11, 72, 71, 89]. With the development of atomic force microscopy testing techniques, researchers are now able to determine what the loop length distribution for an adsorbed polymer actually is. It has been shown that the distribution of polymer concentration at different lengths from the surface decays at different rates[74]. The central region, where most of the polymer's concentration lies, decays following a power law, but the distal region follows an exponential decay[74]. Previous work done by Senden *et al.* and Haschke *et al.* has looked to fit the obtained loop length distributions to the scaling models developed by Aubouy *et al.*[108, 241, 11, 10]. Aubouy *et al.* showed that the number of loops in a distribution with exactly n monomers scaled with $n^{-11/5}$ in the dilute regime and good solvent[11]. To compare the power law distribution of polymer loop lengths, the data were plotted on a log/log scale and the slope of the distribution was found, as shown in Figure 43.

The short-dashed trend line in Figure 43 shows that when all points in the distribution are included, the power law does not fit very well. Past researchers have discarded small and large loop lengths to fit the central region of the distribution[108]. When this is done, the slope and fit of the power law distribution fit much better. The effect of this change is illustrated in the solid trend line in Figure 43, which shows that the central region of the polymer distribution does not fall in the dilute regime with a good solvent. This has been explained by Haschke *et al.* through confinement of the polymer between the tip and the surface, resulting in a transfer to the semidilute regime which would scale to $n^{-3/2}$[108]. The data found in this work agrees with

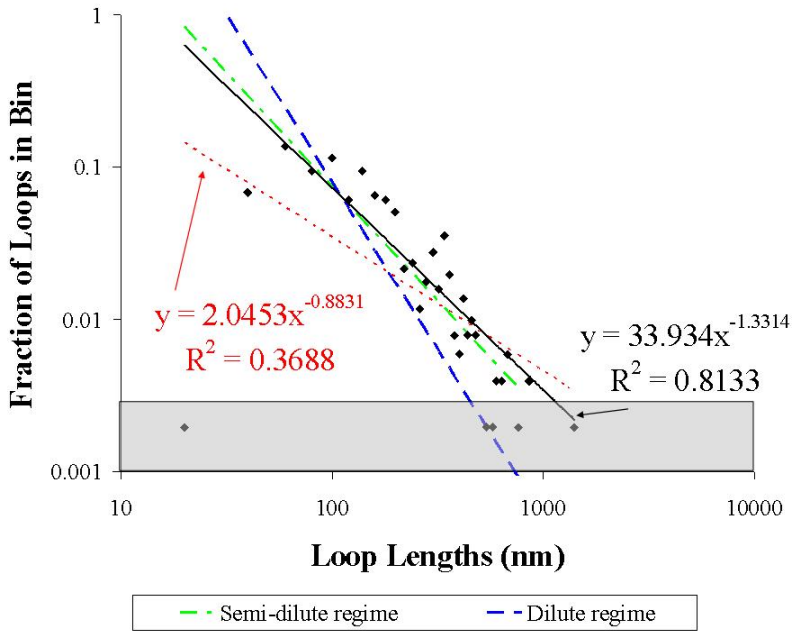

Figure 43: Loop length distribution for $2\mu m/s$ retraction rate. The short-dashed trend line includes all points while the solid trend line only includes points in the unshaded region. Reproduced with permission from Macromolecules[30]. Copyright 2007 American Chemical Society.

this explanation, within the deviation of the distributions. However, past researchers have not given adequate reasoning for discarding both the proximal and distal regions of a distribution in order to fit it to a model[108]. Also, these regions of the polymer loop length distribution, although only a small percentage of the distribution, are still valid data points and should be used to describe the overall distribution.

In order to include more data into the modeling techniques, attempts to model the distal region of an adsorbed polymer's conformation using an exponential decay was attempted. The first assumption necessary was to pick a point where the distal region of the adsorbed polymer's conformation begins. This was chosen to be loop lengths greater than $440nm$. The results of this attempted fit are shown in Figure 44.

As is shown by the R^2 value in Figure 44, this exponential decay does not fit the measured loop length distribution very well. It is important to remember that these fits are based on concentration profiles of the polymer on the surface. In the distal

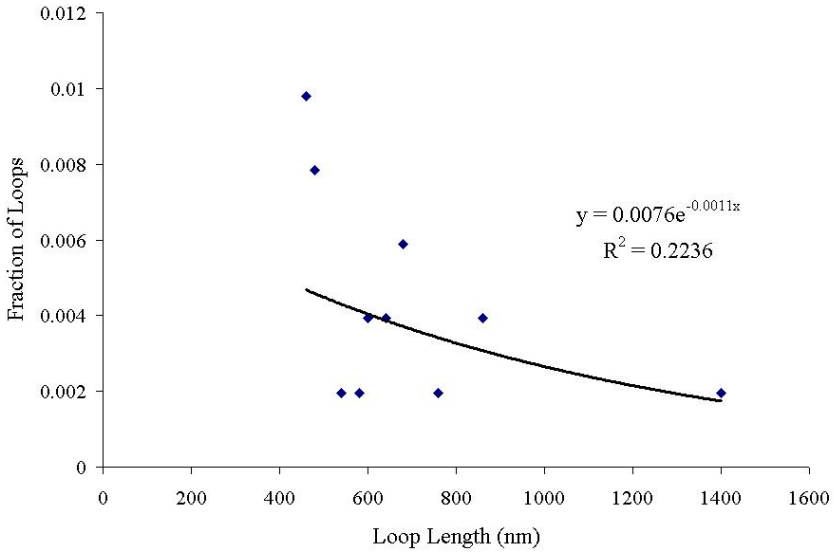

Figure 44: Loop length distribution for $2\mu m/s$ retraction rate, using loop lengths greater than $440nm$.

region it is likely the tail portion of the adsorbed polymer will play a significant role in the concentration profile. The loop length distribution, used for the fit in Figure 44, contains no information on the tail segment of the polymer.

The above discussion used DeGennes scaling theory in order to gain information on an adsorbed polymer's conformation. Scaling theory has received a large amount of attention for predicting polymer conformations[108, 241]. However, it was mentioned previously, in the literature review, that scaling theory can not be used to determine actual polymer conformations. Because it only describes the concentration profile of an adsorbed polymer at given distances from a surface. There are many possible conformations which could give the same concentration profile making the deconvolution of the theoretical predictions extremely difficult. In this work, the results fit to scaling theory are only included for comparison to previous work.

5.3.2 Movement on Surface

Following adsorption on a surface, a polymer is still capable of moving around on the surface or even desorbing. This process has been referred to, in the past, as relaxation

which occurs as the polymer finds its most energetically favorable conformation on a surface[47]. Cohen Stuart *et al.* have shown that a polymer will spread out on a surface over time[47]. This was determined by measuring the change in thickness of the adsorbed polymer layer. The approach taken to investigate this process using AFM was to monitor the number of polymer attachments to a surface over time. By doing this it was shown, for the first time using AFM, that adsorbed polymers do move around on surfaces[30, 31]. Figure 45 shows that with increasing dwell time the number of attachment points on the surface increases. Figure 45 also shows that this number appears to plateau quickly, also seen by Cohen Stuart and Tamai using streaming potential measurements[47]. This plateau occurs at about 60 to 90 seconds of dwell time on the surface. This relaxation time is the same as the values, found previously, by Cohen Stuart and Tamai[47].

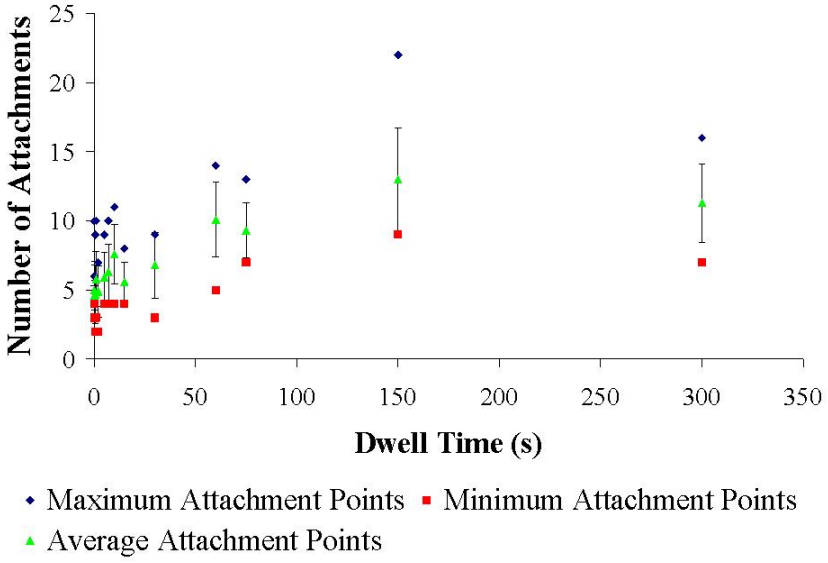

Figure 45: The effect of dwell time on the number of polymer attachment points to a mica surface. Reproduced with permission from Macromolecules[30]. Copyright 2007 American Chemical Society.

Figure 45 shows that there is a large variation in the number of attachments with the same polymer at the same dwell time. This is most likely due to the instantaneous

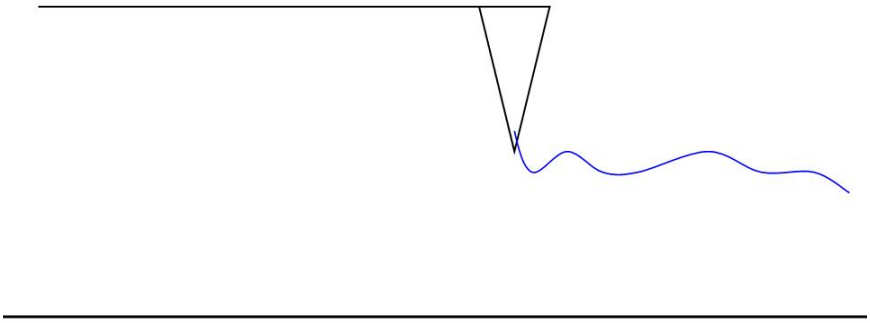

Figure 46: Example of a possible extended conformation of the polymer bonded to the AFM tip.

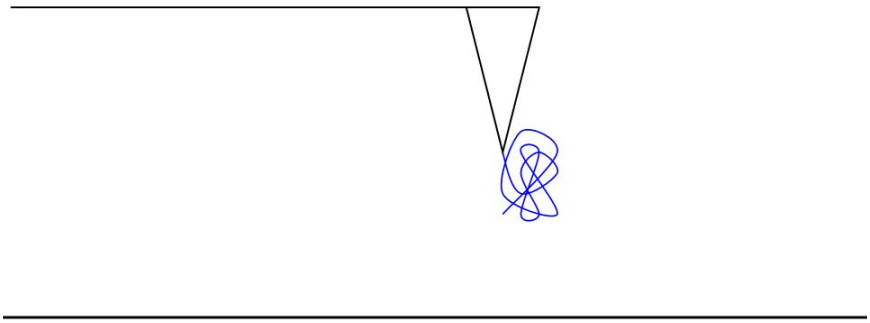

Figure 47: Example of a possible compacted ball conformation of the polymer bonded to the AFM tip.

conformation of the polymer as it is put on the surface. If the polymer lies in a loose ball, as in Figure 47, it is possible that there could be multiple attachments in a small area. However, if the polymer is extended, as in Figure 46, the likelihood of having many attachment points decreases due to the amount of polymer that will come in contact with the surface. These effects cannot be avoided due to the polymer's confined movement in solution away from the surface. However, with multiple tests it was shown that a trend was able to be detected, even with the large deviations included.

5.4 Conclusions

This work has investigated the adsorbed polymer conformation of a MAPTAC/acrylamide copolymer. The following conclusions will report the differences in the results of the two experimental techniques, the information found from AFM analysis on adsorbed polymer conformation, comparisons of this work with theory of polymer conformation, and the effects of the relaxation time a polymer has on a surface on the adsorbed polymer conformation.

In the work, performed using dynamic light scattering, it was found that the adsorbed polymer layer thickness was relatively small. When this value was compared with the computed maximum polymer layer thickness, the values differed by almost an order of magnitude. This was most likely due to the following reasons: the coverage of the latex spheres for DLS is unknown, the affinity of the polymer to the anionic latex is different towards the mica or glass surfaces, the curvature of the latex spheres, and the possible molecular weight difference of the polymers used for DLS and AFM.

The surface coverage assumptions of light scattering were discussed in Chapter II. Because we can not verify this condition, the values found using DLS carry a high potential to be different from the actual value. The affinity of the anionic latex for the MAPTAC/acrylamide copolymer is much higher than that of mica. This can be seen

in the higher charge density of the latex surface. This would cause the polymer to attempt to be attached more closely to the latex than on the lower charge density mica surface. The effects of curvature of the latex spheres could play a possible role in the adsorbed polymer conformation. If the curvature is too high, the adsorbed polymers will be forced to adsorb with fewer attachment points due to the geometry and steric constraints in the polymer. This could cause changes in the surface coverage and adsorbed layer thickness.

The final difference, from the two experimental methods, is that of the molecular weight of the polymers used. It was shown, using GPC, that the DLS polymer is about half the size of the AFM polymer. However, it was noticed that during AFM measurements there were very few "short" polymers found during testing. Most of the polymers tested had minimum chain distances of around 2 or $3\mu m$. The average calculated chain length was around $4\mu m$, based on the molecular weight. Although not proved, this work suggests that the longer polymers adsorb preferentially on the AFM tips. This, as compared with the large variety of polymer sizes in the DLS polymer, could have an effect.

The use of AFM to determine adsorbed polymer loop lengths, allowed many conformational details of an adsorbed polymer's structure to be used for characterization. This study has shown that for a high molecular weight low charge density MAPTAC/acrylamide copolymer the majority of the loops, from the loop length distribution, have lengths between 40 and $260nm$. However, it is common, although not statistically abundant, to see much larger loops in the distributions. Because of the polymer's random structure, no inference as to the effects of order in the monomeric units relative to the adsorbed polymer conformation could be drawn. It was found that there is a significant deviation in loop lengths and the number of attachment points with the same polymer. This work concludes that this was most likely due to the ability of the polymer to move freely in solution, while the resulting adsorbed

polymer conformation was taken from an instantaneous conformation in solution followed by relaxation on the surface.

The relaxation of a single polymer on a surface was, for the first time, proven using AFM. By analyzing the number of polymer attachment points it was shown that the polymer attachment points rapidly increase in number until around 60 to 90s. At this point, the changes in the number of attachments plateaus. The polymer was most likely still moving around on the surface, but due to energetic and conformational constraints, it was not expected that the number of attachments should increase.

CHAPTER VI

SALT EFFECT ON ADSORBED POLYMER CONFORMATION

6.1 Overview

The methods of dynamic light scattering and atomic force microscopy will be used to evaluate how electrolytes, or salt, in solution affects an adsorbed polymer's conformation. These experimental results were compared with those found in Chapter V to verify the conclusions made. This chapter describes many novel techniques to evaluate adsorbed polymer conformations.

6.2 Dynamic Light Scattering to Determine the Salt Effect on Adsorbed Polymer Conformation

Past literature has shown that increases in the salt concentration, in the medium surrounding an adsorbed polymer, can increase its hydrodynamic diameter[17, 285]. For this work, this effect was tested using dynamic light scattering. In Chapter V, it was shown that the average adsorbed MAPTAC/acrylamide copolymer layer thickness increase was $9.45nm$ with a standard deviation of $3.56nm$. To investigate the salt effect the same tests were performed in different NaCl solutions. The results are shown in Figures 48 and 49.

With increasing salt concentration, the adsorbed layer thickness increased to $19.35nm$, at 0.001M NaCl, and then to $43.07nm$, at 0.01M NaCl. The standard deviations of these average values show that these increases are statistically significant, when all data is averaged. However, as with the previous chapter's light scattering results, the variation between test runs was very large, as shown by the standard deviation bars in Figures 48 and 49. In addition to this variation, the hydrodynamic

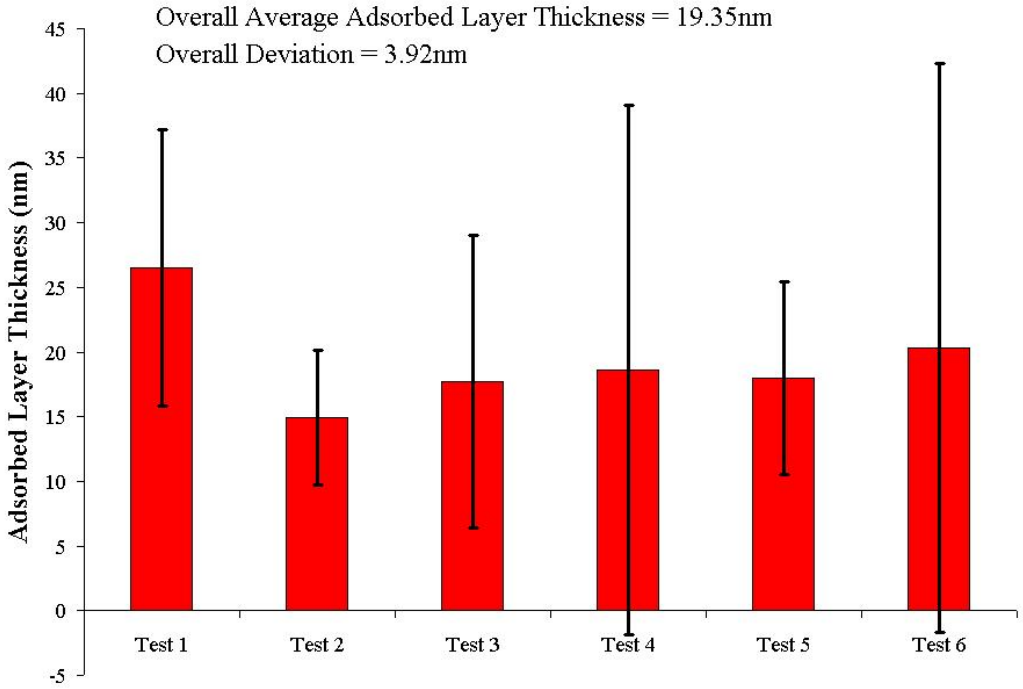

Figure 48: Dynamic light scattering adsorbed polymer layer thickness in 0.001M NaCl solution.

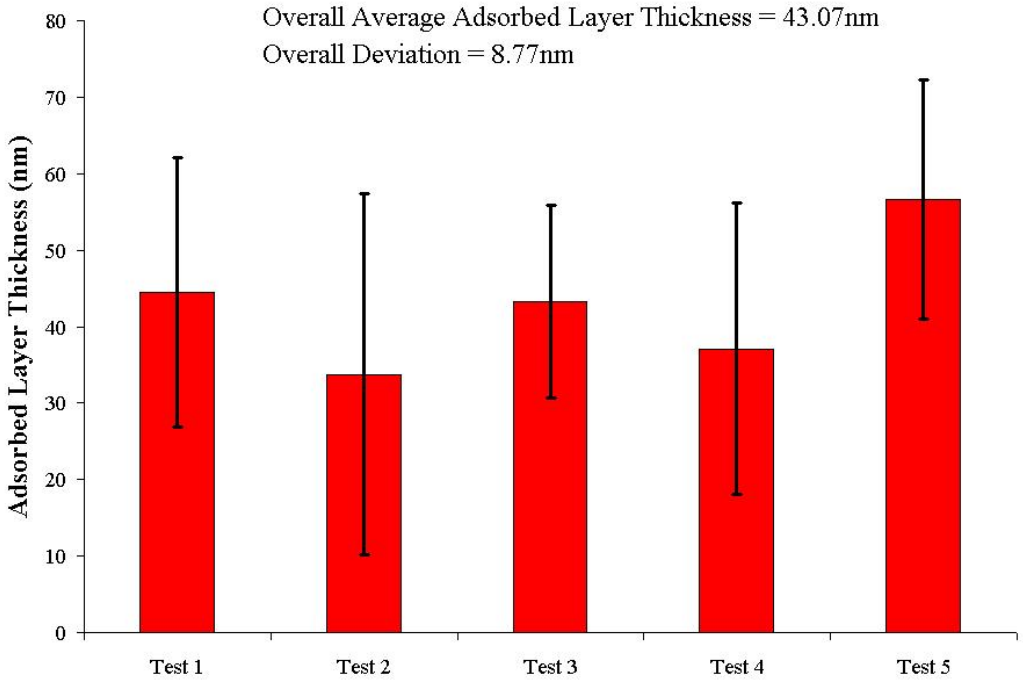

Figure 49: Dynamic light scattering adsorbed polymer layer thickness in 0.01M NaCl solution.

diameter of the anionic latex spheres in the different salt solutions was unexpected.

The light scattering results for the size of the anionic latex spheres used showed that their hydrodynamic diameter increased with increasing salt concentration. Table 5 lists the average values found from these experiments.

Table 5: Effect of NaCl concentration on the hydrodynamic diameter of anionic latex using dynamic light scattering.

	0M NaCl	**0.001M NaCl**	**0.01M NaCl**
Hydrodynamic Diameter (nm)	202.44	285.84	332.90

The increase shown in Table 5 was unexpected. Previous work has shown that the hydrodynamic diameter of latex spheres should be unaffected by increasing electrolyte concentration[208, 169]. The viscosity of the medium, in which dynamic light scattering, experiments are being performed is critical to the particles movement in solution. At first thought, the possibility that the viscosity increased with increasing salt concentration seemed reasonable. However, at these dilute regimes, viscosity changes would not be expected, as can be seen from previous work[17]. It was also expected that the electric double layer surrounding the particles would shrink as the electrolyte concentration increases. This reduces the chances that the increase in size is due to a thick layer of ions being trapped on the latex sphere slowing it down.

A conclusive answer to this problem was not determined. Therefore, because there was an additional increase in hydrodynamic diameter after polymer addition, this problem was ignored. It is not being inferred that it is not important, only that due to the time constraints in this work, it was not in feasible to continue working to resolve this problem.

6.3 Atomic Force Microscopy to Determine the Salt Effect on Adsorbed Polymer Conformation

To analyze the salt effect on adsorbed polymer conformation using AFM, four different analysis methods were performed on the AFM force curves. These include: analysis of the number of polymer attachment points, the change in adsorbed polymer tail length, the change in adsorbed polymer loop lengths, and the effect on the adsorption force of the polymer with the substrate. Table 6 lists the total number of data points analyzed for the different conditions.

Table 6: The total number of data points taken for all the different conditions during the salt effect study.

	Number of attachments	**Number of loops**
0M LiCl	292	282
0.001M LiCl	232	222
0.01M LiCl	90	80
0M NaCl	497	466
0.001M NaCl	184	155
0.01M NaCl	59	35
0M CsCl	246	231
0.001M CsCl	161	146
0.01M CsCl	40	25
0M $MgCl_2$	218	203
0.0001M $MgCl_2$	118	103
0.001M $MgCl_2$	66	52

6.3.1 Number of Polymer Attachment Points

Previously, it was mentioned that dissociated salt ions will compete with polymers for adsorption sites on a surface. Knowing this, it should be possible to limit the amount of polymer adsorption points by increasing the salt concentration of the medium. Additionally, at increasing salt concentrations the electric double layer should become smaller and more dense with counterions. It is also possible that electrostatic repulsion within the Stern layer could prohibit polymer adsorption on

the surface. After performing this control experiment(the effect of salt concentration on the number of polymer attachment points), the information obtained also helps verify that the polymer desorption events seen in the AFM force curves are not due to other, unknown, variables. Figure 50 illustrates the resulting trend of polymer desorption events with increasing NaCl concentration.

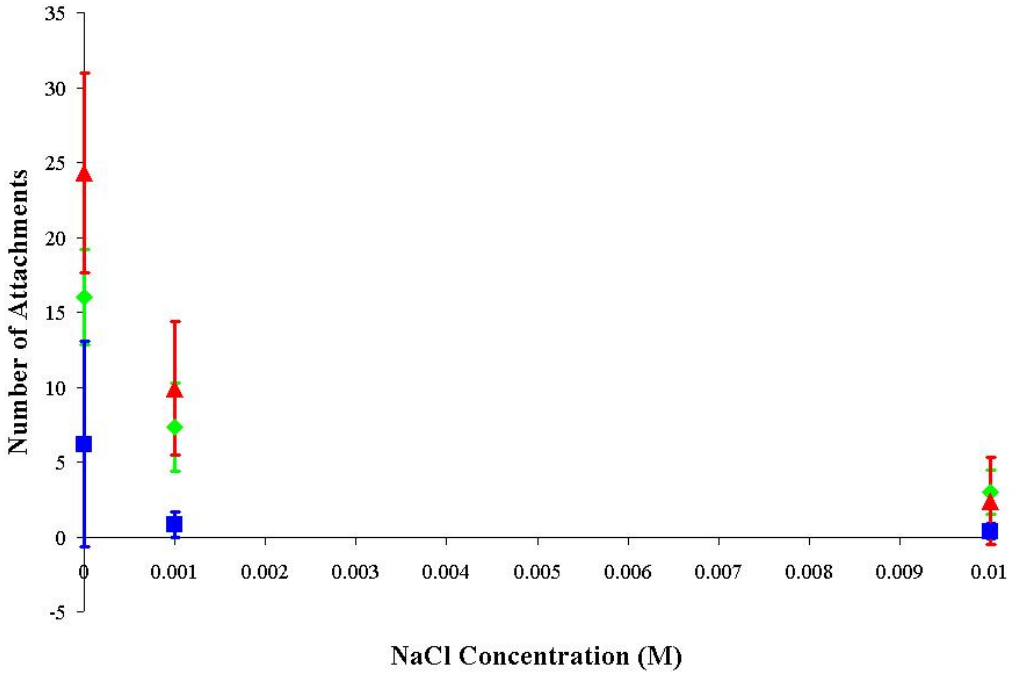

Figure 50: The effect of dissociated NaCl ions competing for adsorption points with the MAPTAC/acrylamide copolymer on a mica surface. Three different plots, each representing a different polymer, are displayed.

Figure 50 shows that as the concentration of sodium ions in the liquid phase increases, the number of polymer attachment points decreases. At salt concentrations greater than 0.01M, not shown in this figure, no desorption events are seen. As the sodium ion concentration increased, its ability to fill the vacant anionic sites, left by the potassium ions, increases. For the case of a salt concentration greater than 0.01M, this can be interpreted to mean that the sodium ions competing for the anionic oxygen sites, on the surface of the mica, have diffused into the electric double layer reducing the opportunity for the polymer to adsorb on the surface. Figure 51 illustrates how

ions are held in the electric double layer. This reduction in polymer attachment points was also predicted by van de Steeg *et al.* and Shubin and Linse[266, 245]. It is important to remember, however, that the adsorption of sodium ions on the mica surface is a process that is in equilibrium with the desorption of sodium ions. Because of this it is always possible for the MAPTAC/acrylamide copolymer to adsorb on the surface. However, as the concentration of sodium ions in solution increases, the likelihood of this decreases.

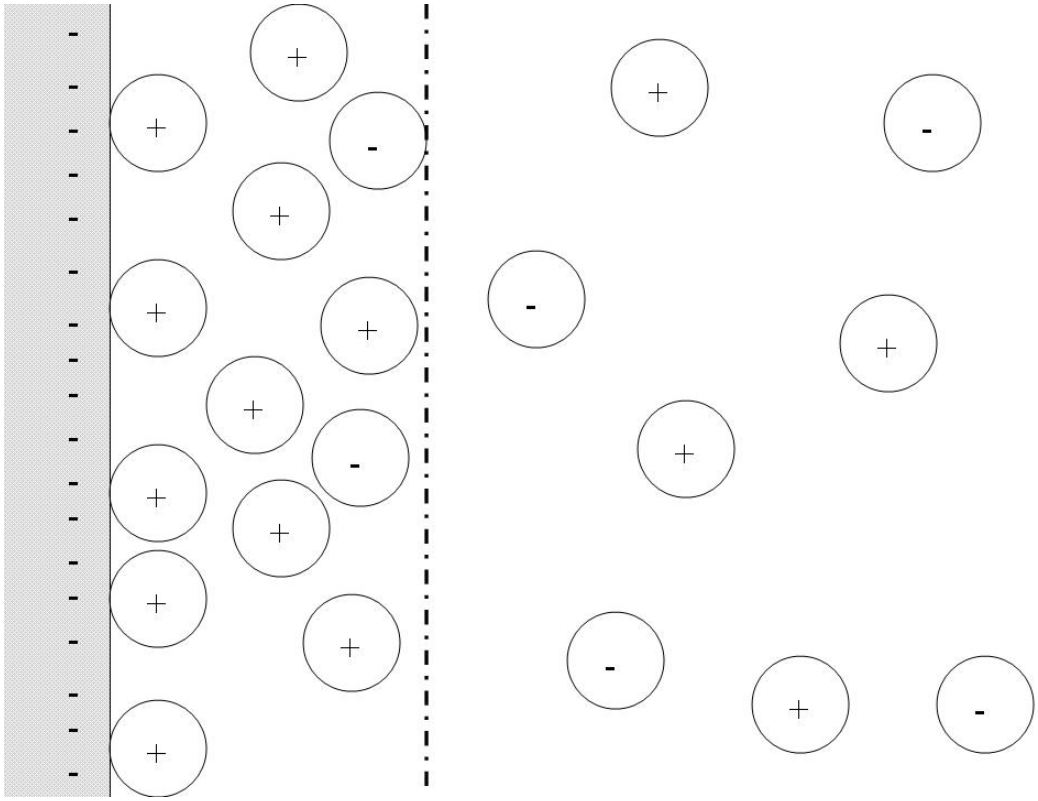

Figure 51: Diagram of the electric double layer. The region in between the surface and the dashed line is the Stern layer. The region to the right of the dashed line is the diffuse layer.

In the work of Shubin and Linse, the effects of the size and charge of the dissociated salt ions were varied[245]. Pertaining to the number of polymer attachments, this test would not be expected to show any changes unless the cationic salt ion was large enough to cover multiple sites on the surface. It is also important to remember that the anionic sites on the mica surface are constantly changing as potassium ions desorb

and adsorb. This leaves a never constant or uniform distribution of anionic sites on the surface. It also resulted in data influenced by not only the salt cation being evaluated, but also the potassium ions present on the surface and in the solution. Because of this, it is impossible to determine the effect of ion size on the number of attachments.

Although the effect of different salt ion sizes with respect to the number of attachments is not expected to change, the tests were performed anyway. Figures 50, 52, 53 illustrate the effect for each salt. For this work, three different monovalent salts were chosen to investigate the effect of ion size on adsorbed polymer conformation. These salts included LiCl, NaCl, and CsCl, listed in increasing ionic radius, shown in Table 7.

Table 7: Ionic radii of the cations used for this work according to the CRC Handbook[154].

Ion (Coordination Number)	**Radius (Å)**
Li^{+1} (6)	0.76
Na^{+1} (6)	1.02
Cs^{+1} (8)	1.74
Mg^{+2} (6)	0.72

Figure 52 illustrates the effects of a smaller ion, lithium, and Figure 53 illustrates the effects of a larger ion, cesium.

In Figures 50, 52, and 53, different polymers were used for each salt, and in the case of NaCl, three different polymers were used. This was done to ensure that changing the salt solutions on the tip did not create any possible corrosive environments which could damage the cantilevers. Because of this, the number of adsorption points can not be compared between the different salts. In all cases, an increase in salt concentration resulted in a decrease in the number of attachment points the polymer had with the surface. It is important to remember, though, that we would not expect to see an effect in the number of attachments due to ion size.

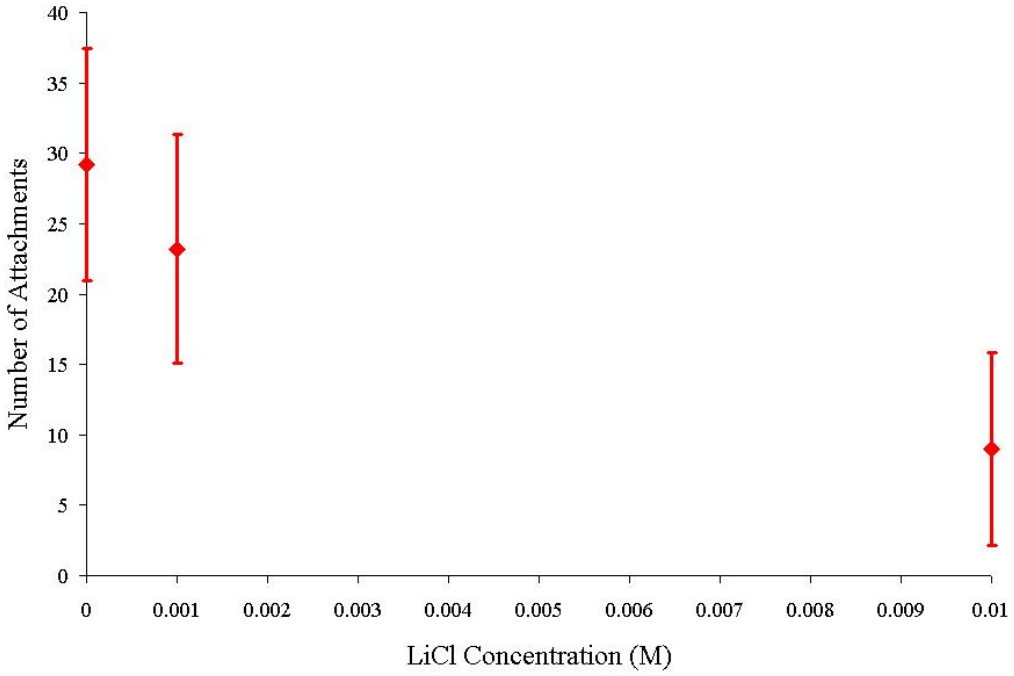

Figure 52: The effect of dissociated LiCl ions competing for adsorption points with the MAPTAC/acrylamide copolymer on a mica surface.

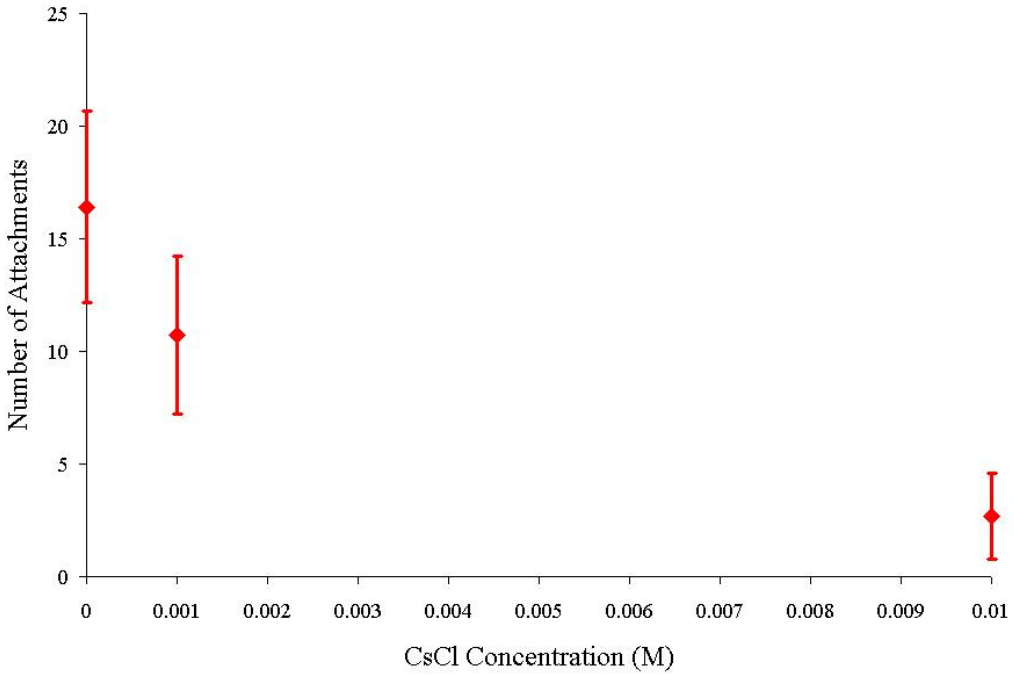

Figure 53: The effect of dissociated CsCl ions competing for adsorption points with the MAPTAC/acrylamide copolymer on a mica surface.

One property in which different ions could have a noticeable effect is the valence charge of the ions. If the dissociated salt ion is divalent or trivalent, it should be attracted to the anionic sites on the mica surface more than the monovalent groups on the polymer backbone. To test this, the same salt addition tests were performed using $MgCl_2$, a divalent salt.

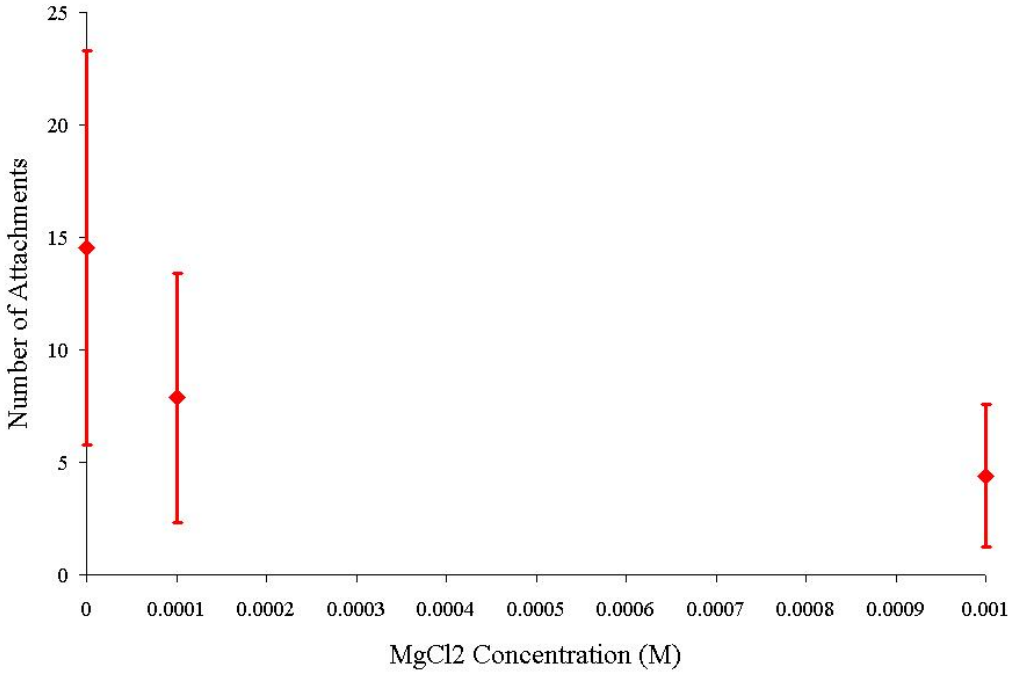

Figure 54: The effect of dissociated $MgCl_2$ ions competing for adsorption points with the MAPTAC/acrylamide copolymer on a mica surface.

Figure 54 shows that the same trend is present as with the monovalent salts. However, the concentrations are shifted lower. This is expected because the Mg^{2+} ion has a lower energy barrier of adsorption than the monovalent polymer unit. After the Mg^{2+} ion is adsorbed on the surface it still possess a positive charge. This would be repulsive towards any positively charge polymer units attempting to adsorb on the surface. For the divalent magnesium ion, no polymer adsorption points are found if the concentration of $MgCl_2$ is equal or greater than 0.01M.

6.3.2 Polymer Tail Length

The second aspect of adsorbed polymer conformation which will be analyzed, relative to salt concentration, is the change in adsorbed polymer tail length. Shubin and Linse predicted that increases in salt concentration would also increase the length of adsorbed polymer tails[245]. The work of Bauer *et al.*, under the assumption of Nelson *et al.*, supports this theory that the tail length increases with increasing salt concentration[17, 179]. However, no research, to date, has been able to infer information on the length of adsorbed polymer tails, not to mention the effect of salt concentration on this, using atomic force microscopy.

Due to the design of many AFM "pulling" experiments, there is no method to determine the exact length of the tail portion of the polymer, not attached to the tip. This research, for the first time, has shown that even without a direct measurement of a polymer's tail length, conclusive information regarding the length of the free tail portion of a polymer can be determined. Because the AFM method used for this work has been shown to most likely leave a single adsorbed polymer on an AFM tip, it is possible to investigate changes in the free tail portion of the polymer in its adsorbed conformation. The other advantage of this technique is the knowledge that only one terminal end of the polymer being analyzed is attached to the tip and the rest of the polymer is free.

By testing the same polymer on an AFM tip under different conditions on the same substrate, this research could directly measure changes in the adsorbed polymer's free tail length. Because of the aspects of this experimental technique, mentioned previously, the distance from the point where the tip is removed from the surface during retraction and the last desorption point on the AFM force curves obtained, represents the straight chain length of the polymer that is involved in all of the loops on the surface plus the constrained tail covalently bonded to the tip. Figures 55 and 56 illustrate how this could be done.

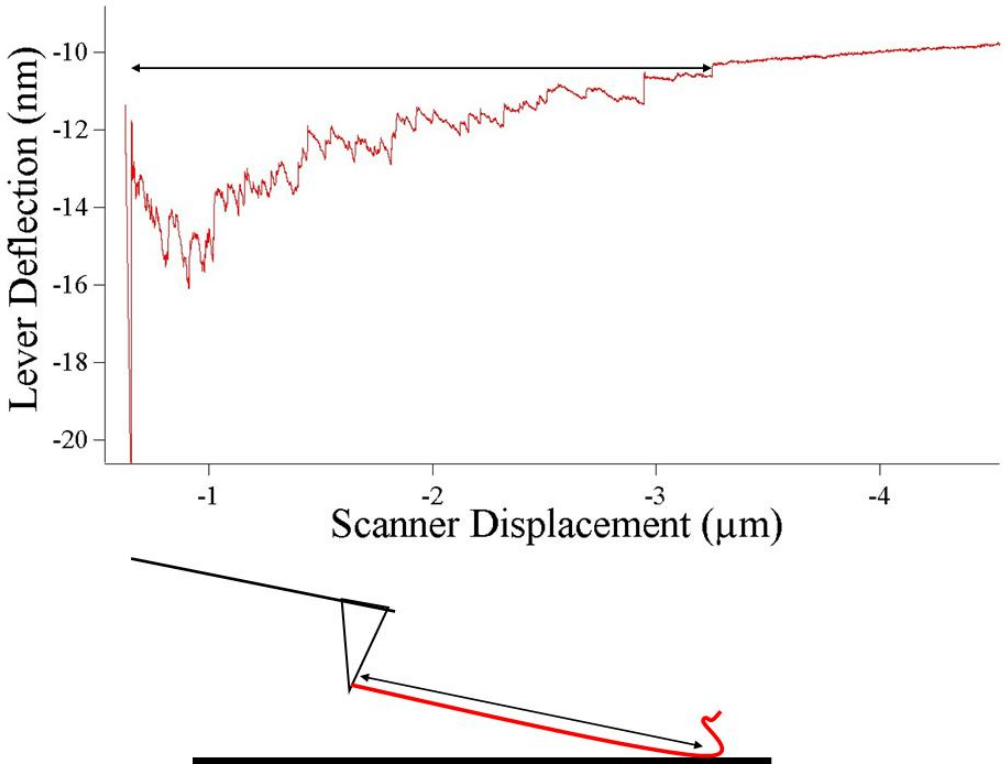

Figure 55: Schematic of how the length of a polymer chain leading up to the last adsorption point can be found. The distance to the last desorption point for this polymer, in Barnstead deionized water on mica, is $2626.4nm$.

In Figure 55, the distance from the tip to the last polymer adsorption point was found to be 2626.4nm. This shows that the polymer is at least 2626.4nm long.

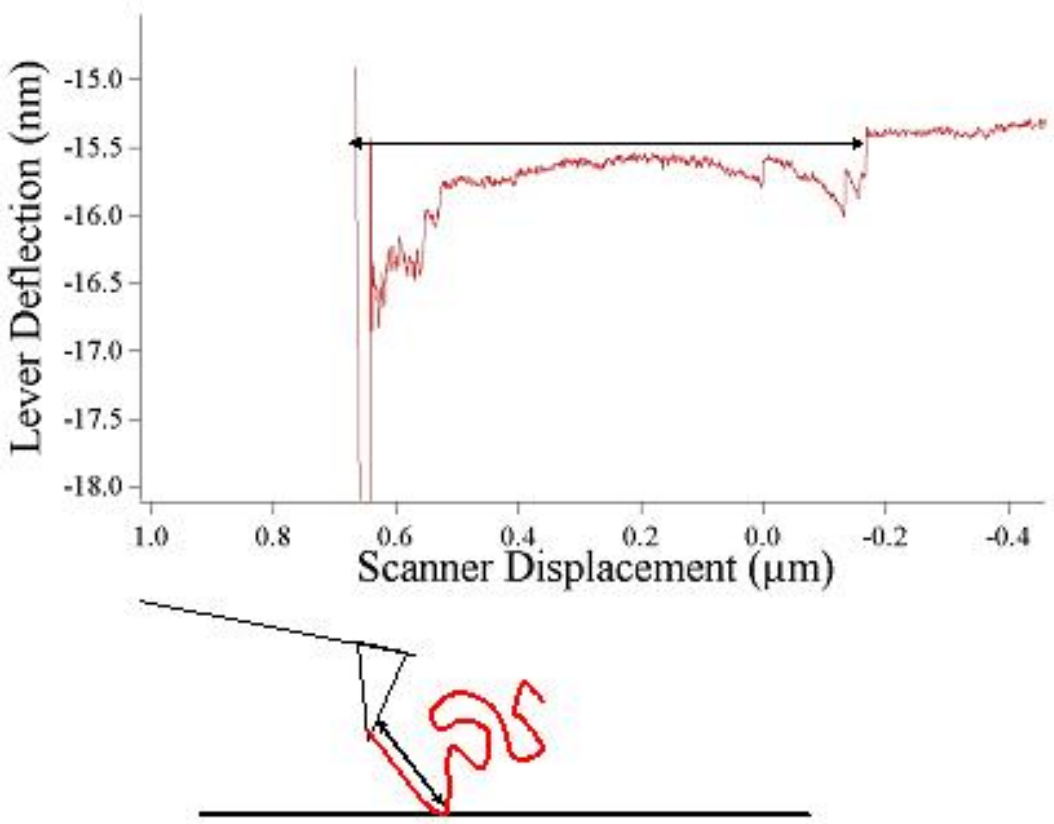

Figure 56: Schematic of the same polymer chain shown in Figure 55 in a 0.001M NaCl solution on a mica surface. Here the distance to the last desorption point is 834.66nm.

Figure 56 was obtained from the same polymer used in Figure 55. It is shown that the distance to the last adsorption point is significantly shorter at 834.66nm. The acrylamide copolymer used in this research will not quickly degrade or dissolve in water. This allows, with significant confidence, the assumption that the length of the polymer does not change between different salt conditions. With this assumption, any decreases in the length to the last adsorption point could be attributed to an increase in the length of the tail portion of the adsorbed polymer. For the specific case in Figures 55 and 56, the tail of the polymer increased 1791.74nm by increasing the salt concentration of the medium.

It is important to remember that a polymer adsorbed on a surface is moving around as it relaxes on a surface. This means that adsorbed points are gained and lost over time. This leads to a deviation in the distance to the last attachment point even when all the experimental conditions are kept constant. This is illustrated by the error bars of Figure 57.

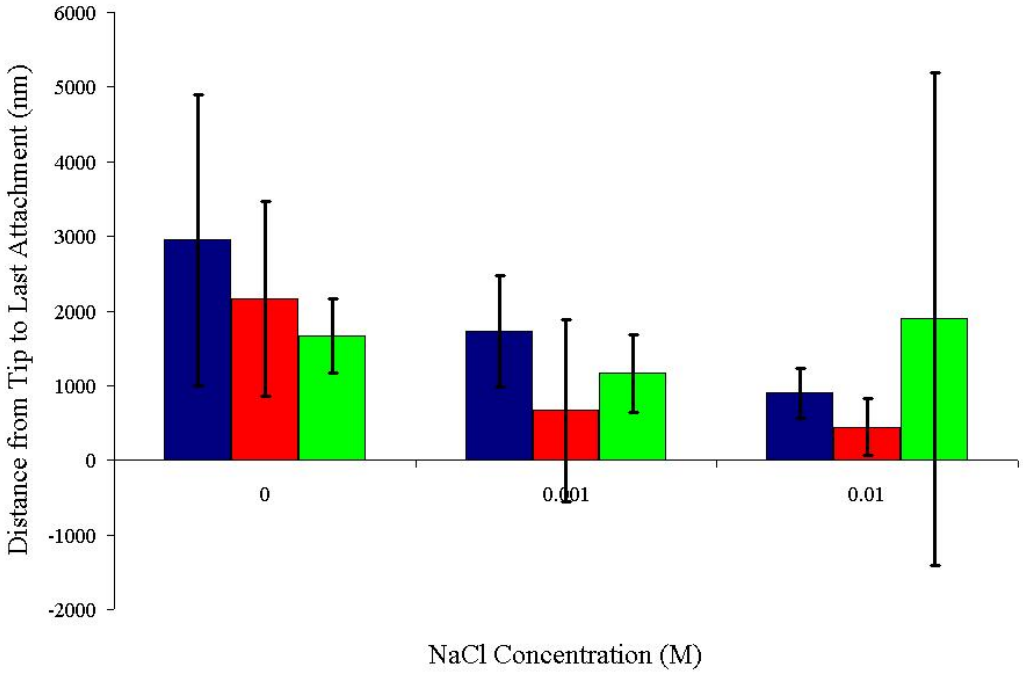

Figure 57: The average distance to the last polymer attachment point, in increasing NaCl concentrations on a mica surface, is shown for three different polymers.

It is apparent, from Figure 57, that the free tail portion of the adsorbed polymer is growing with increasing salt concentrations. However, the error bars can make this appear to be misleading. After evaluating all of the AFM data for the salt effect study, only 2 of 84 data points showed an increase with increasing salt concentration.

The two data points that showed a tail length growth were for the $0.01M$ category of the green trend in Figure 57. In this set of data, the previous longest distance to the last adsorption point measured was $2256.5nm$. The two of the distances, in the $0.01M$ condition, were $8273.7nm$ and $7011.3nm$. Because the number of data points

is small and the spread of results is large, it is difficult to analyze this using statistics. The two large loop lengths were the first two tests of the polymer at this particular condition. Following this the values obtained were around the low hundreds. If these initial points were discarded, the plot would be changed to that shown in Figure 58.

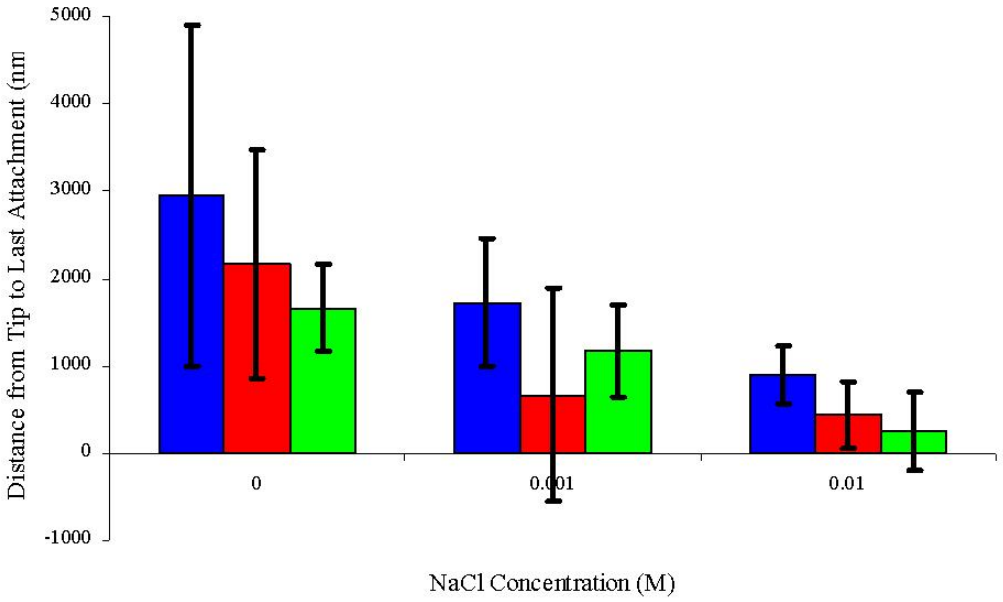

Figure 58: The average distance to the last polymer attachment point, in increasing NaCl concentrations on a mica surface, is shown for three different polymers. Here the two outlying points of Figure 57 were excluded.

It is important to keep in mind that, even if there is salt in the solution which was competing for adsorption sites and screening the electrostatics between charged sites on the polymer backbone, there is still no reason why it was not possible for a polymer to relax on the surface in a conformation similar to that of a lower salt concentration.

As in the previous section, it is not expected that the ion size, for salts of identical valence charge, of the salt cation should have much effect on the tail length of the adsorbed polymer's conformation because of the small difference in size of the ions

evaluated. This was investigated, however, in order to support the trend of polymer tail length increase with salt concentration. Figures 59 and 60 illustrate the continuance of this trend.

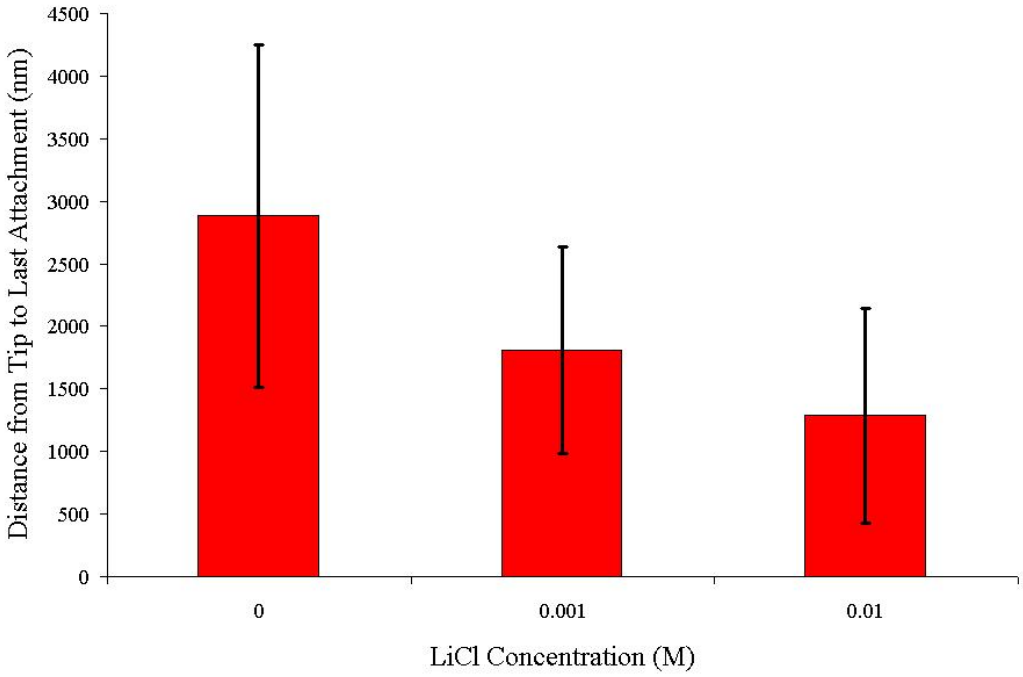

Figure 59: The average distance to the last polymer attachment point, in increasing LiCl concentrations on a mica surface.

Different ions can affect the adsorbed polymer conformation if their valence charge differs. It is possible that an ion with a *+2* charge would adsorb on the surface and still retain a *+1* charge. This would allow electrostatic repulsion of the polymer as it approaches this filled adsorption site. Alternatively, these magnesium ions could also fill the Stern layer creating electrostatic repulsion to the polymer but not being directly adsorbed to a point on the surface. To investigate the possibility of the valence charge of a salt ion to affect and adsorbed polymer's tail length test were run at different concentrations of $MgCl_2$, a divalent cation. This is shown in Figure 61. As with the other salts, increases in $MgCl_2$ concentration result in longer tail portions of adsorbed polymers.

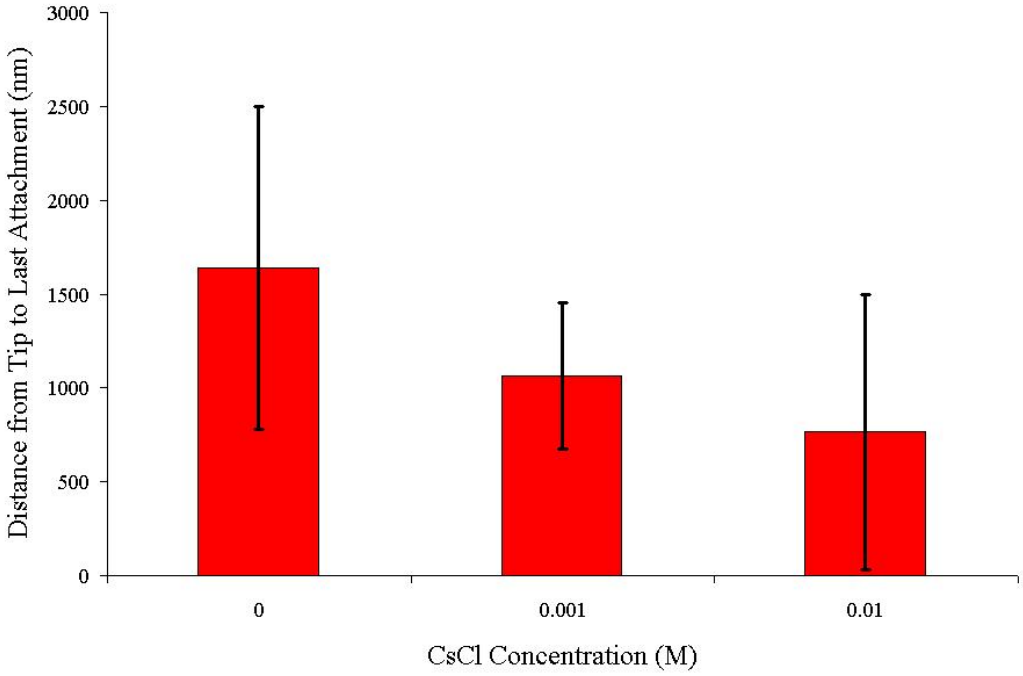

Figure 60: The average distance to the last polymer attachment point, in increasing CsCl concentrations on a mica surface.

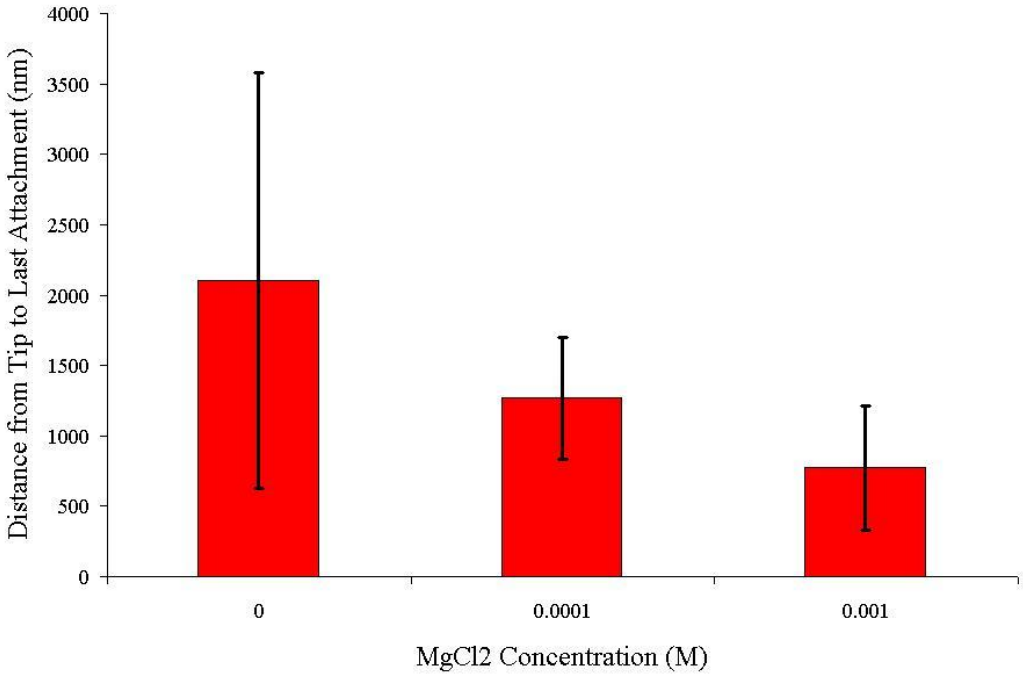

Figure 61: The average distance to the last polymer attachment point, in increasing $MgCl_2$ concentrations on a mica surface.

The figures, in this section, show that the average tail length of an adsorbed polymer does increase with increasing salt concentration. However, without the use of a single polymer, controlled surface, and a preponderance of force curves, an average tail length growth percentage is meaningless. As cations adsorb and desorb from the surface, the locations of specific adsorption sites change. As the AFM tip is retracted and brought back to the surface, the polymer can move through endless conformation changes, similar to those shown in Figures 46 and 47, thus affecting the adsorbed polymer conformation. In addition to the conformation of the polymer on the tip, Douglas *et al.* have discussed the heterogeneity of the conformations of adsorbed polymer layers[85]. They have shown that as a polymer adsorbs from solution, it will constantly change, thereby not allowing the use of equilibrium states for comparison of conformations[85]. Another problem with using average tail lengths is that the distribution is predicted to be very broad[234]. While the inability to predict an average tail length increase is present, the value of these results is still very high. Prior to this work, no other research has been able to experimentally confirm that the tail length of an adsorbed polymer increases with increasing salt concentration.

6.3.3 Polymer Loop Length

Adsorbed polymer loop lengths are an important component of an adsorbed polymer's conformation. Most theory deals with this portion of an adsorbed polymer's conformation. However, very little direct evidence of an adsorbed polymer's loop lengths has been developed. When analyzing the effect of salt concentration on adsorbed polymer loop lengths, no direct experimental evidence has been reported.

As in Chapter V, the loop lengths of adsorbed polymers will be compared by investigating their distribution and the weighted average loop length for each condition. It is important to note, in these results only the distributions of the same polymer on the same substrate will be compared due to the possible effects variance in polymer

backbone structure. This is the best method to obtain meaningful results, Figure 62 displays the loop length distribution of the MAPTAC/acrylamide copolymer in different concentrations of a NaCl/water medium.

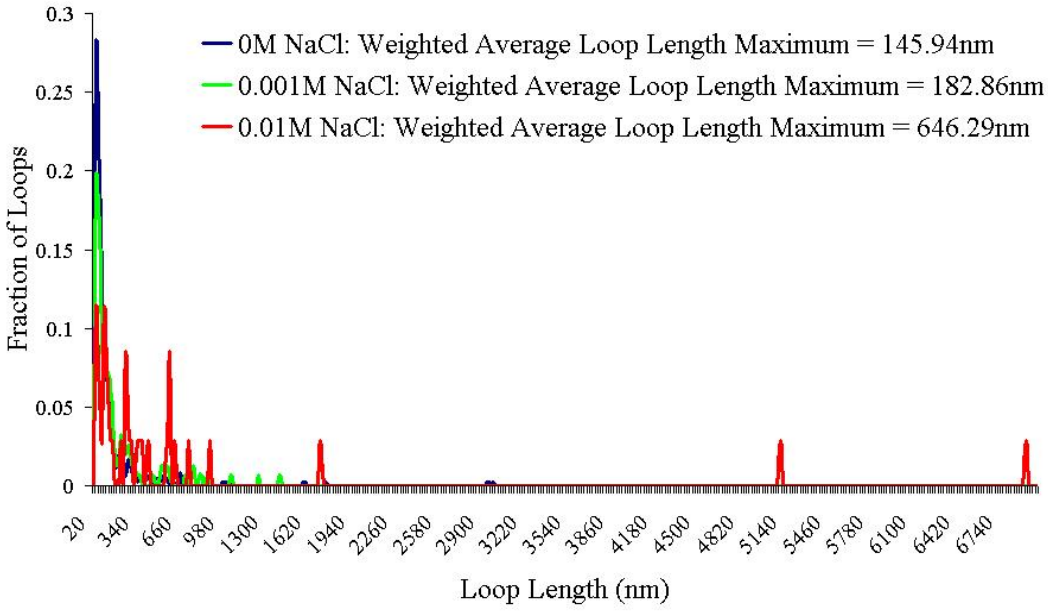

Figure 62: The effect of NaCl concentration on the loop length distribution of the same MAPTAC/acrylamide copolymer on a mica surface.

Shubin and Linse predicted that along with the tail length, the loop lengths of an adsorbed polymer should increase with increasing salt concentration[245]. This is supported by the decrease in the number of attachment points with increasing salt concentrations. However, this decrease does not mean that both the loop and tail lengths have to increase. Through analysis of the different distributions in Figure 62 this trend is difficult to determine. The weighted average maximum loop lengths, for increasing salt concentrations, illustrated this effect. While it can be contested that the weighted average maximum loop lengths will be skewed by a few large loops, it is important to remember that the minimum number of loops used to calculate this value was 35 loops obtained from 35 force curves. While this was for the highest NaCl concentration, it is expected that the number of events and loops should decrease for this condition. As with the previous AFM techniques used to evaluate the salt effect

on adsorbed polymer conformation, the effects of electrolytes with different ionic radii were also tested. Again, no large difference in conformation was expected here due to the small difference in ion size. Figures 63 and 64 show the effects of a smaller and larger ion, respectively.

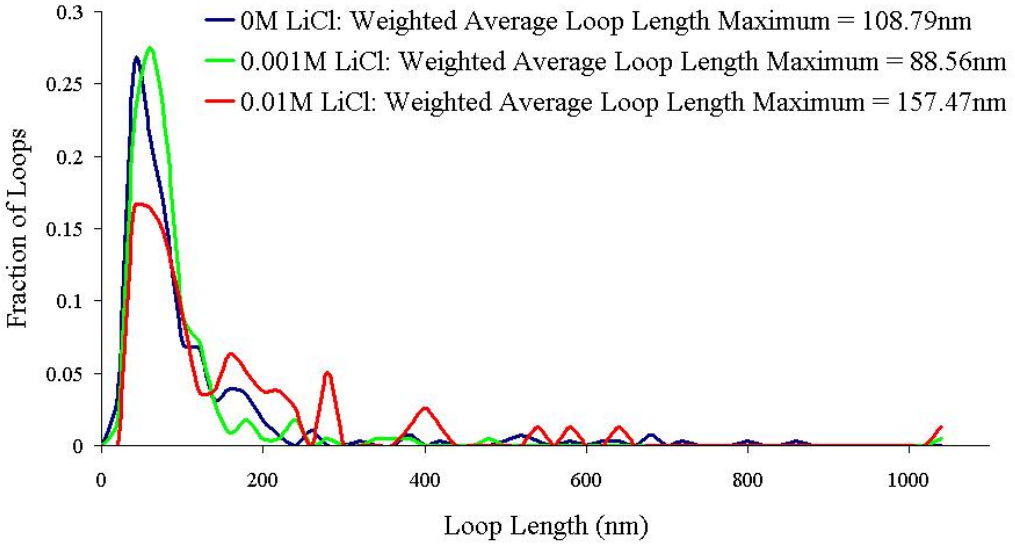

Figure 63: The effect of LiCl concentration on the loop length distribution of the same MAPTAC/acrylamide copolymer on a mica surface.

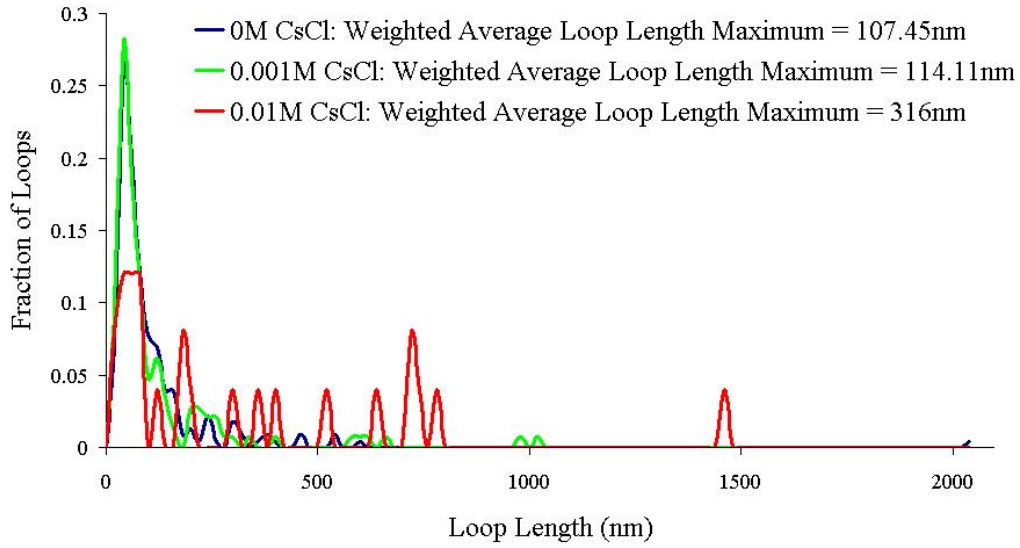

Figure 64: The effect of CsCl concentration on the loop length distribution of the same MAPTAC/acrylamide copolymer on a mica surface.

Again, it is shown for these two salts that the adsorbed polymer loop lengths increase with increasing salt concentration. However, Figure 63 does have a decrease from the $0M$ LiCl to the $0.001M$ conditions. Although this is unexpected, it is plausible that the polymer could adsorb with shorter loop lengths in any of these conditions. As was mentioned previously, the available adsorption sites could have shifted in a manner which made smaller loops more favorable. Although it is unlikely that this type of shift would cause this change, it is possible. The highest concentration of LiCl gave an expected trend and result, allowing the declaration that this trend is valid.

As stated previously, by testing a divalent salt, it is possible to show different, and expected, changes in the adsorbed polymer loop length distributions. This is due to the electrostatic repulsion that would be present between the adsorbed salt ion and the cationic groups on the unadsorbed polymer. Figure 65 displays these results.

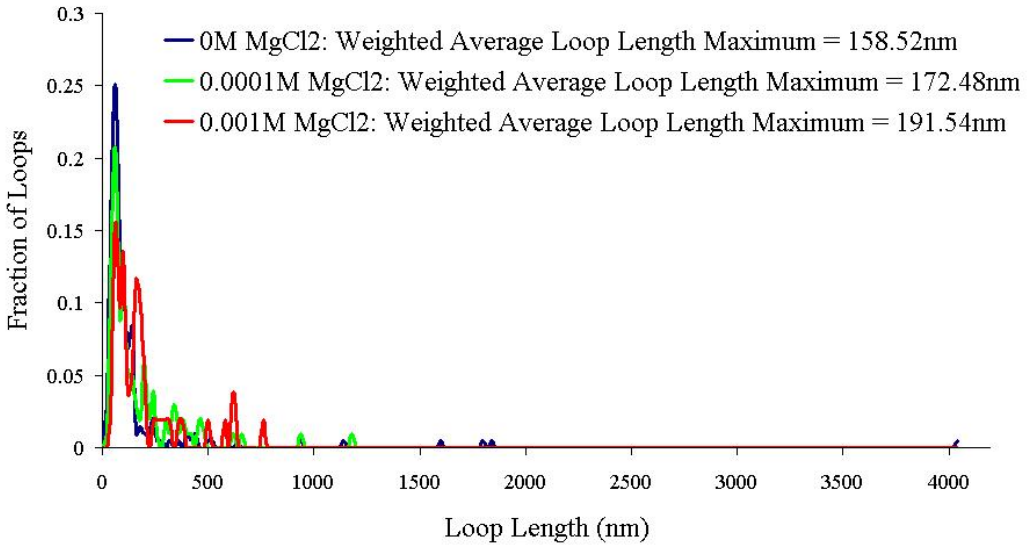

Figure 65: The effect of $MgCl_2$ concentration on the loop length distribution of the same MAPTAC/acrylamide copolymer on a mica surface.

Figure 65 does not show any noticeable difference in the adsorbed polymer loop length distributions relative to the other salts. As expected it shows the increase in weighted average maximum loop length. The lack of a definitive difference in loop length increases could be due to the size of the magnesium ion. This ion has a radius

smaller than any of the other salts used. If the remaining positive charge on the adsorbed ion is hidden intimately adjacent to the surface that the polymer is not largely affected by it, it is likely the results would be similar to those found in Figure 65.

6.3.4 Strength of Polymer Attachment

In the literature review of this thesis, questions regarding polymer desorption force measurement were explained. However, in order to compare the work found in this research to the work done by others, it is necessary to address the desorption force when pulling the MAPTAC/acrylamide copolymer off of the surface.

First, it is important to briefly discuss force measurement using atomic force microscopy. Forces, measured using an AFM, are determined by quantifying changes in deflection of the cantilever as it is pulled from, or approaches, a surface. In most common commercial AFMs, this is done using a split, or quad, photodiode. Using published knowledge of beam deflection, this change in light can be related to the distance in which the cantilever deflects during a measurement.

Using the distance a cantilever deflects, from the AFM photodiode, and knowledge of the beam shape and properties, the force necessary to deflect the beam can be calculated[206]. The technique of Sader *et al.* is commonly used to calculate the spring constant of a rectangular cantilever using the resonant frequency of the the lever[228]. Poggi *et al.* reported that the most commercial AFM cantilevers have beams which resemble a trapezoid more than a rectangle[206]. This was found to lead to an overestimate of the spring constant, using the Sader method, by 21-43%[206].

The Sader method was used for calculating the spring constants for cantilevers used for this project with full knowledge that the value may be significantly off from the actual spring constant. Because the forces were not a main focus of this work the use of th Sader method to determine the cantilever spring constant was allowed. It

is also important to mention, that for the study of the effects of salt concentration on polymer desorption force, in each of the experiments listed below, the same cantilever and polymer were used for each salt concentration. As the cantilevers were not damaged, the spring constant should remain relatively constant throughout the experiment. However, comparing the magnitude of the desorption force from experiment to experiment should be discouraged.

Haschke found that the force necessary to desorb polyacrylamide from a mica surface decreased with increasing ionic strength[109, 107]. This was attributed to the salt ions in solution screening the electrostatic attractive forces of the hydrogen bonds with the mica substrate[107]. Haschke stated that only small cations could adsorb on the mica surface and that ions as large as calcium were too large to block polymer adsorption[107].

This research found that the ionic strength of the medium does not affect the strength of polymer adsorption to a mica substrate. Table 8 shows this result.

Table 8: Effect of NaCl concentration on the average force to pull a polymer attachment point from a mica surface.

Experiment	**Force (nN)**	**Force (nN)**	**Force (nN)**
	0M NaCl	**0.001M NaCl**	**0.01M NaCl**
Salt Test 12/11/06	0.098884	0.097888976	0.096173345
Deviation	0.042	0.034	0.033
Salt Test 7/24/07	0.061002365	0.070620056	0.128599898
Deviation	0.033	0.032	0.066
Salt Test 7/27/07	0.173585012	0.121346197	0.108674491
Deviation	0.111	0.088	0.066

Table 8 lists the forces to desorb a MAPTAC/acrylamide copolymer from a mica surface in different concentrations of NaCl/water solutions. These forces were calculated from each of the attachment point desorption events in the NaCl salt study. Not only are the forces near constant, but the deviation of these forces, unlike Haschke's results, is of the same order of magnitude as the actual force[107]. It was also shown

that the radius of the salt cation did not have an effect on its ability to screen interactions with the mica surface.

The deviation of the results, in Table 8, is most likely due to the angle which the polymer is being pulled at from the tip, as described in the literature review. These results show that in these experiments, no evidence of electrostatic screening of the adsorption force of the MAPTAC/acrylamide copolymer was detected.

6.4 Conclusions

The effect of electrolyte concentration on a low charge density MAPTAC/acrylamide copolymer has been validated. In the following conclusions, the effect of salt concentration on the number of polymer attachment points, changes in adsorbed polymer tail length, changes in adsorbed polymer loop lengths, and the effect on adsorbed polymer attachment force will be discussed.

Similar to much of the published literature, it was found in this study that increasing salt concentration will decrease the number of attachment points a polymer has with a surface. Although this does not directly correlate to the adsorbed amount relations found in other research, it does follow the same trend. If more salt is added to the medium, the dissociated cations will compete with the polymer in solution for available surface sites. This increased competition will not only decrease the number of polymers which can be adsorbed, but will also decrease the number of attachment points each polymer has. In this research project, for the first time, this effect was seen on a single polymer.

The work of Shubin and Linse proposed a theory for adsorbed polymer conformation, predicting longer loop and tail lengths in increasing salt concentrations[245]. This prediction has never before been directly proven, experimentally. The results described above, illustrate a clear trend of increasing adsorbed polymer tail lengths with increasing salt concentration. Although there is a significant deviation around each

average value, this would be expected for the same reasons described in the previous chapter, and the results show what would be expected if an increase in tail length occurred. This information is extremely important for polymers used in industrial settings in which high salt concentrations are present. Using this information, the design of polymers can be tailored to give the best results in high electrolyte settings.

Similar to the evidence of increasing adsorbed polymer tail lengths, these AFM tests also confirmed an increase in the average loop lengths of an adsorbed polymer with increasing salt concentration. This again, was the first experimental proof of this theory. It was shown that neither the size of the salt cation or the valency of its charge have a significant effect on the loop length distribution. Divalent salts, as expected, show the same results as monovalent salts at lower salt concentrations. It is important to note, the increases in adsorbed polymer layer thickness appear to be due primarily to the increase in adsorbed polymer tail length, not the slight increase in the average loop lengths.

Contrary to previous AFM results, this research found no change in the force of desorption for an adsorbed polymer chain with increasing salt concentration. This is proposed to be mainly due to the geometric constraints put on the force measurements. However, this research has shown no reason to believe that the salt concentration would affect the strength of adsorption points. The problems associated with force spectroscopy are likely to have resulted in the changes in force found by Haschke[107].

CHAPTER VII

SITE BLOCKING EFFECT ON ADSORBED POLYMER CONFORMATION

7.1 Overview

For this work, two blocking additives were investigated: PDADMAC and cationic nanosilica. The effect of these additives on the hydrodynamic diameter, adsorbed polymer loop lengths, and adsorbed polymer tail length are discussed in the following sections.

7.2 Dynamic Light Scattering to Determine the Effect Site Blocking on Adsorbed Polymer Conformation

Dynamic light scattering was used to determine increases in the hydrodynamic diameter of particles in the small amount of previous literature which investigated the effect of site blocking additives on adsorbed polymer conformation[19, 20]. For this work, the same approach was taken and the results are presented below, divided by blocking additive.

7.2.1 PDADMAC

PDADMAC, a commonly used site blocking additive, is a high charge density cationic polymer. It is expected that this polymer will adsorb on the anionic latex surfaces in small patches. These patches should hinder the MAPTAC/acrylamide copolymer from adsorbing on top of, or intimately adjacent to, the PDADMAC patches. This effect is then expected to increase the adsorbed polymer layer thickness more than the increase from just adding a polymer. These results were found and illustrated in Figure 66.

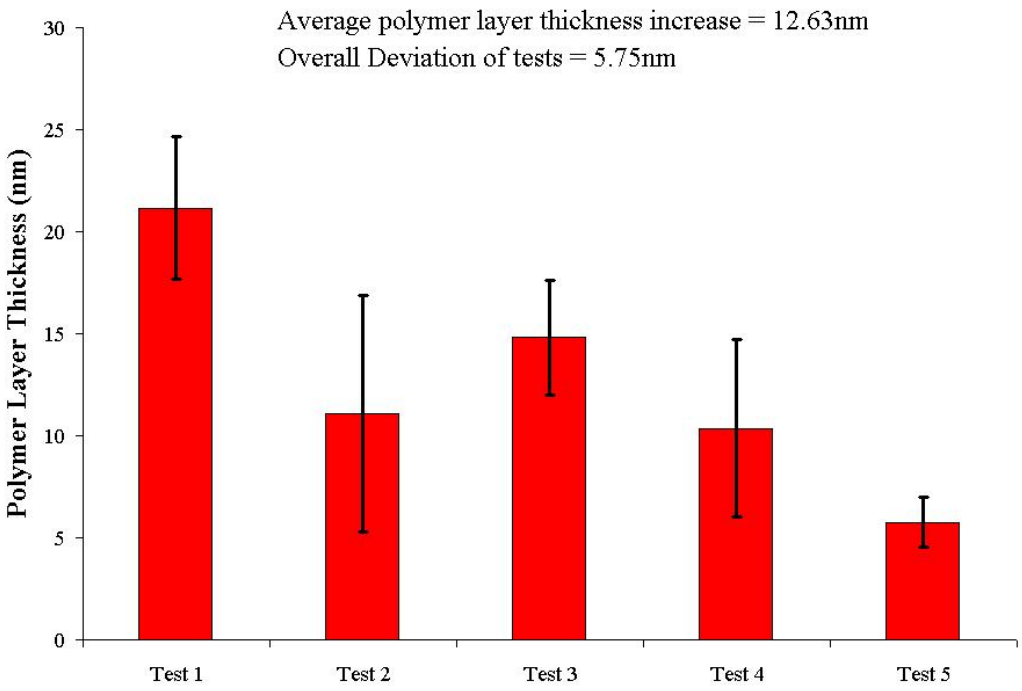

Figure 66: Dynamic light scattering adsorbed polymer layer thickness with $1.75ng$ of PDADMAC as a site blocking additive.

The increase in polymer layer thickness of around $12nm$ is slightly larger than the $9nm$ layer increase found using just the MAPTAC/acrylamide copolymer. However, the standard deviations of each of these average layer thicknesses overlap. This makes a definitive answer on the increase in adsorbed polymer layer thickness indeterminant.

7.2.2 Cationic Nanosilica

Cationic nanosilica was the next site blocking additive evaluated for this research. Similar to PDADMAC, these $12nm$ spheres have a cationic charge, which should act in a similar manner as the PDADMAC. However, unlike the PDADMAC this blocking additive is not polymeric and has well defined dimensions. As with PDADMAC, the use of cationic nanosilica as a blocking additive produced a slightly larger layer thickness than a polymer without any blocking additives. This is illustrated in Figure 67.

The increase in adsorbed polymer layer thickness was about $15nm$. This slightly

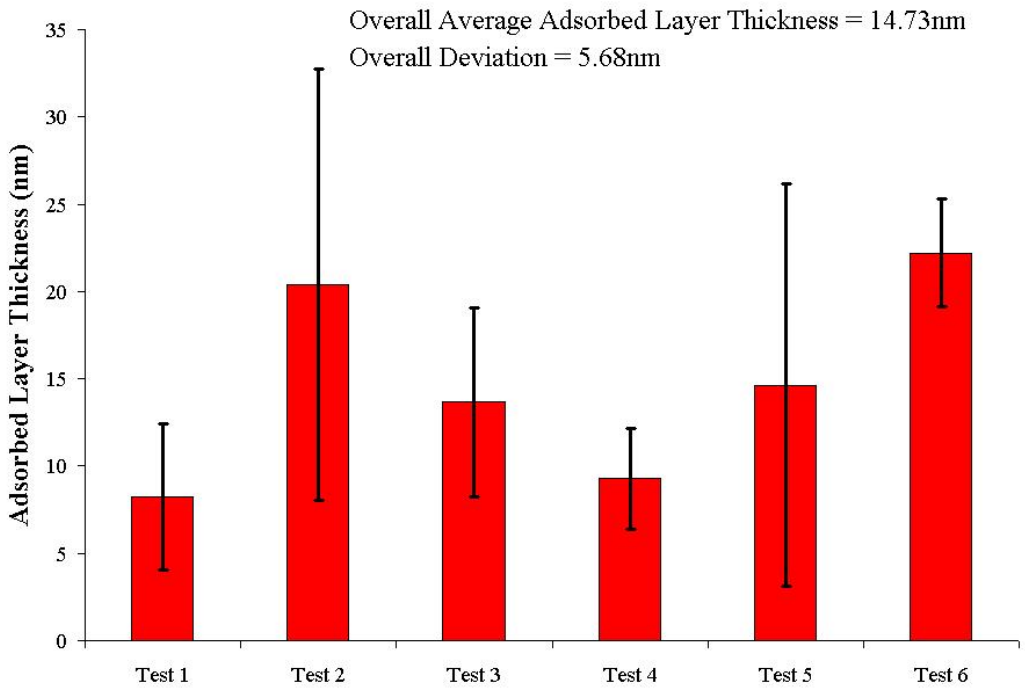

Figure 67: Dynamic light scattering adsorbed polymer layer thickness with $0.917ng$ of cationic nanosilica as a site blocking additive.

larger thickness is expected due to the blocking additive size. It was determined that the increase in adsorbed layer thickness is greater than the $12nm$ that would be measured for the addition of just the cationic nanosilica. In addition, it is apparent from the DLS data that the nanoparticles produce a better site blocking effect than the PDADMAC, or polymeric, additive. As with the PDADMAC DLS results, this data, due to the standard deviation of the results, can not conclusively prove an increase in adsorbed polymer layer thickness. However, the results show the expected increases and differences between different site blocking additives.

7.3 Atomic Force Microscopy to Determine the Effect Site Blocking on Adsorbed Polymer Conformation

In this work, for the first time, the effect of site blocking additives on adsorbed polymer conformation was measured directly. Two substrates, mica and glass, were used for these experiments. The results for the two site blocking additives, PDADMAC

and cationic nanosilica, are outlined in the following two sections.

7.3.1 PDADMAC

Polymeric site blocking additives have been used in much of the previous research on the effect of site blocking additives on adsorbed polymer conformation[251, 275, 174, 256, 164]. It is thought that the addition of a site blocking additive will increase a polymers adsorbed layer thickness by decreasing the area to which this polymer can adsorb. Consequently, it is expected that the number of polymer attachment points should decrease with increases in site blocking additives. Figure 68 illustrates that this does occur on a mica substrate.

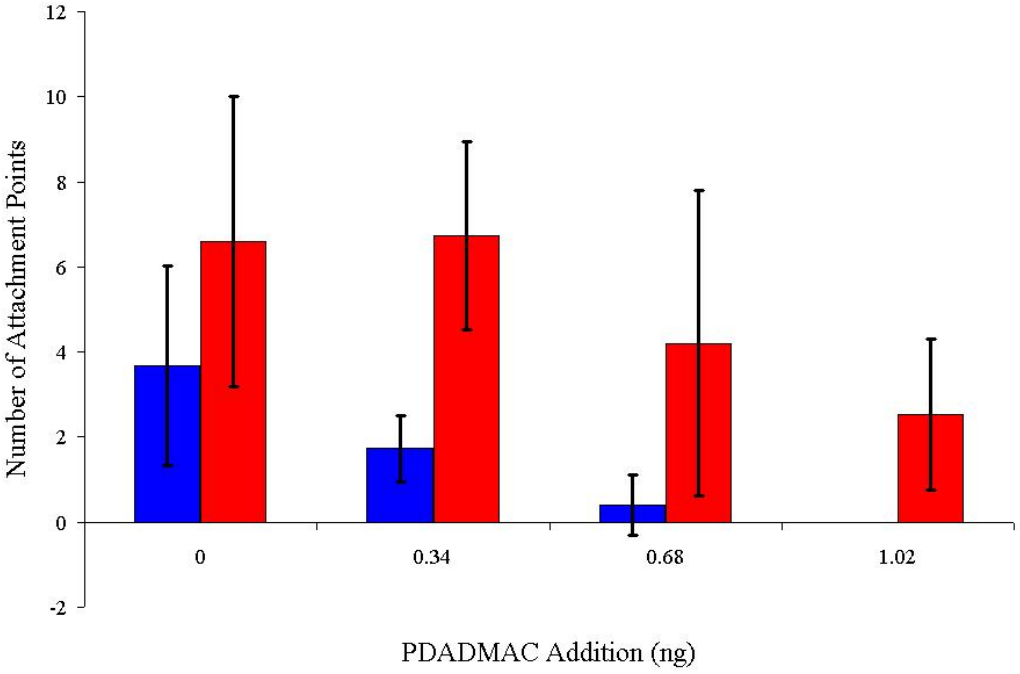

Figure 68: Number of attachments for polymer on mica substrate with different amounts of site blocking PDADMAC additions.

In Figure 68, the red and blue bars represent different repeats of the experiment. At the addition level of $0.34ng$ PDADMAC, the number of attachments for the red bars slightly increased. Although it is expected that the area available for polymer

adsorption should decrease at each step, it is unknown how many polymers are adsorbed around the retention polymer. The PDADMAC will continuously adsorb, desorb, and relax on the mica substrate. These occurances allow for this unexpected increase in the number of attachments. The expected decrease in the number of attachment points was obtained using a glass substrate, as shown in Figure 69.

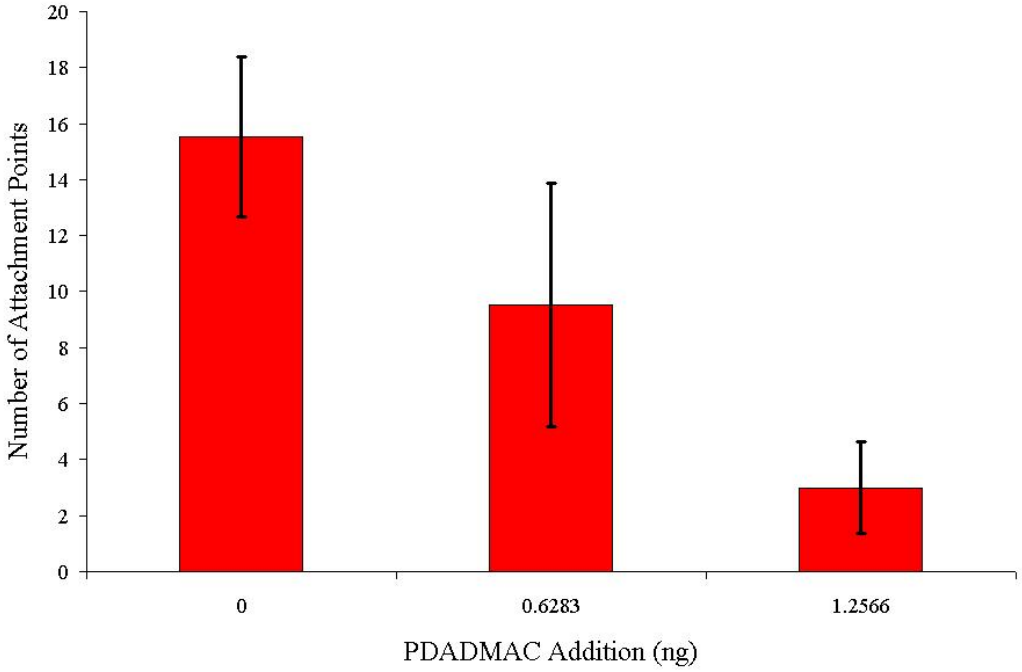

Figure 69: Number of attachments for polymer on glass substrate with different amounts of site blocking PDADMAC additions.

It has been proposed in previous literature that site blocking additives increase the loop lengths of adsorbed polymers. The histograms in Figures 70 and 71 illustrate the changes in adsorbed polymer loop length distributions found using atomic force microscopy.

Figures 70 and 71 do not show consistent increases in the adsorbed polymer's loop lengths with increasing amounts of PDADMAC. In fact, on the mica substrate the opposite trend was shown. This result does not support the previous results found from dynamic light scattering. This result shows that the changes in adsorbed

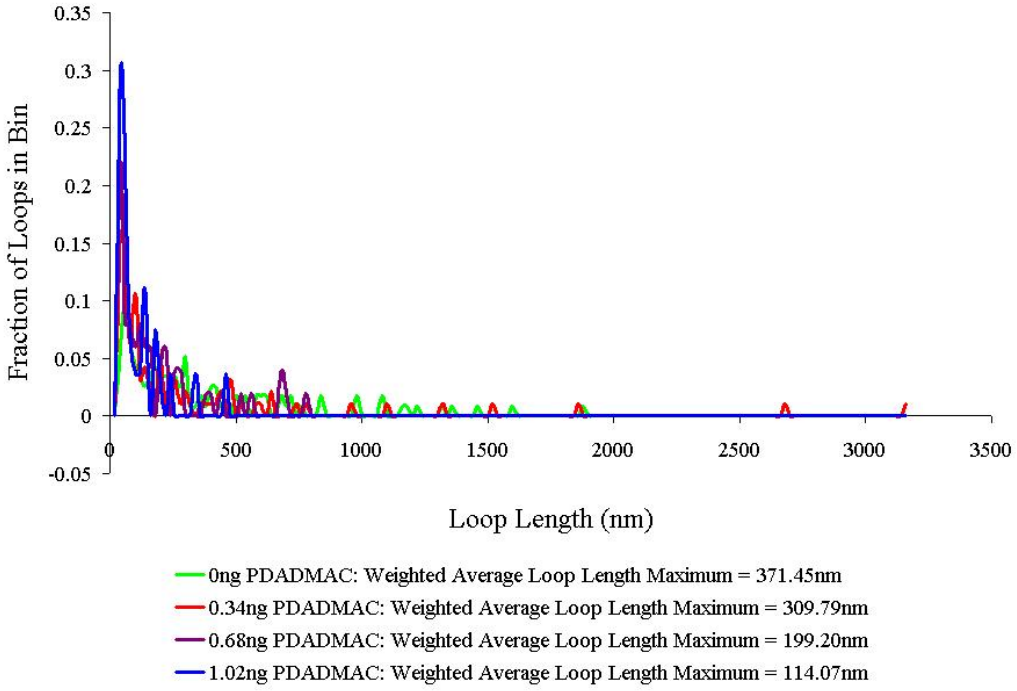

Figure 70: Loop length distributions of MAPTAC/acrylamide copolymer on mica with different amounts of PDADMAC used as a site blocking additive.

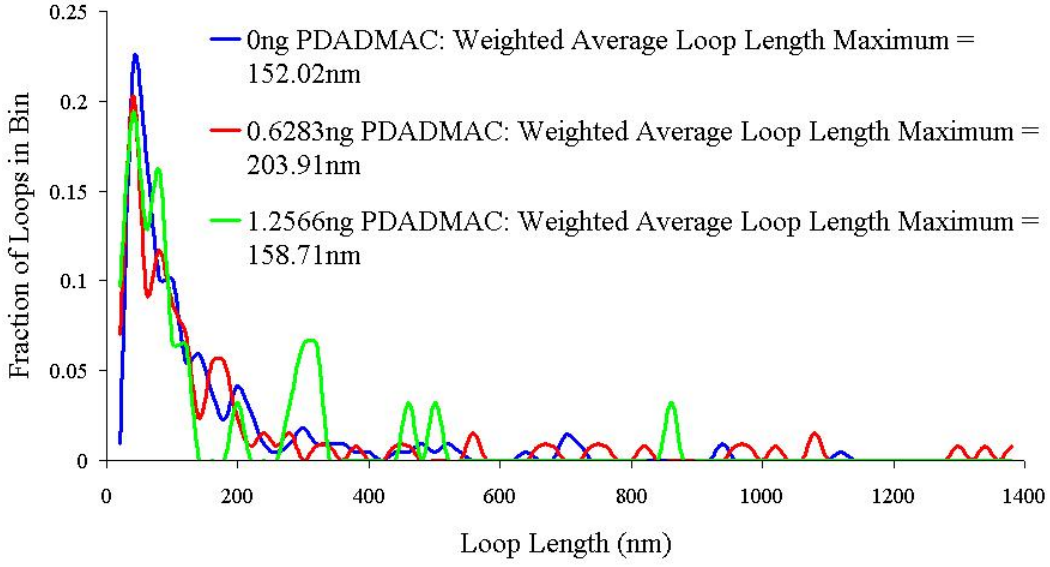

Figure 71: Loop length distributions of MAPTAC/acrylamide copolymer on glass with different amounts of PDADMAC used as a site blocking additive.

polymer loop lengths may not be the primary cause for the increase in hydrodynamic diameter. However, the electrostatic repulsion between the PDADMAC and the MAPTAC/acrylamide copolymer may cause these loops to extend further into the solution than the loops of the same size without site blocking additives. This actual adsorbed polymer thickness can not be directly measured using AFM. It can only be inferred using assumptions about the shape of the adsorbed polymer loops.

One aspect of the adsorbed polymer conformation which has not been accounted for yet in this chapter is the free polymer tail. The increases in hydrodynamic diameter could also be due to an increasing tail length. Figures 72 and 73 report the changes in tail length found in this research project for PDADMAC site blocking on glass and mica substrates.

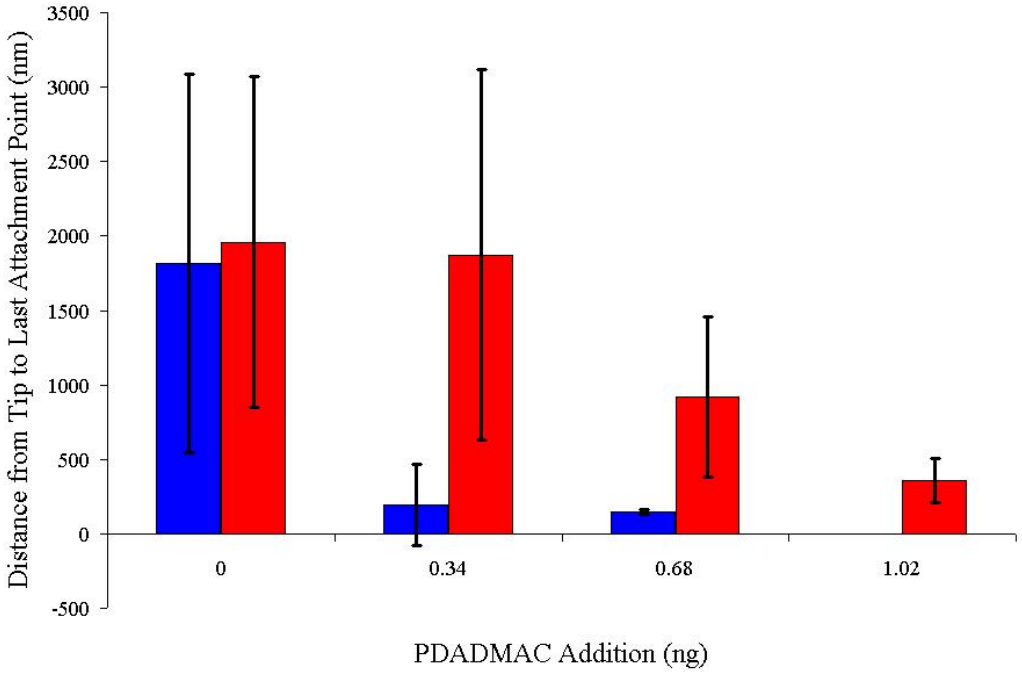

Figure 72: Change in distance to last polymer adsorption point using PDADMAC as a site blocking additive on a mica substrate.

Figures 72 and 73 clearly illustrate a distinct increase the adsorbed polymer's free tail length with increasing PDADMAC site blocking. This coupled with the relatively

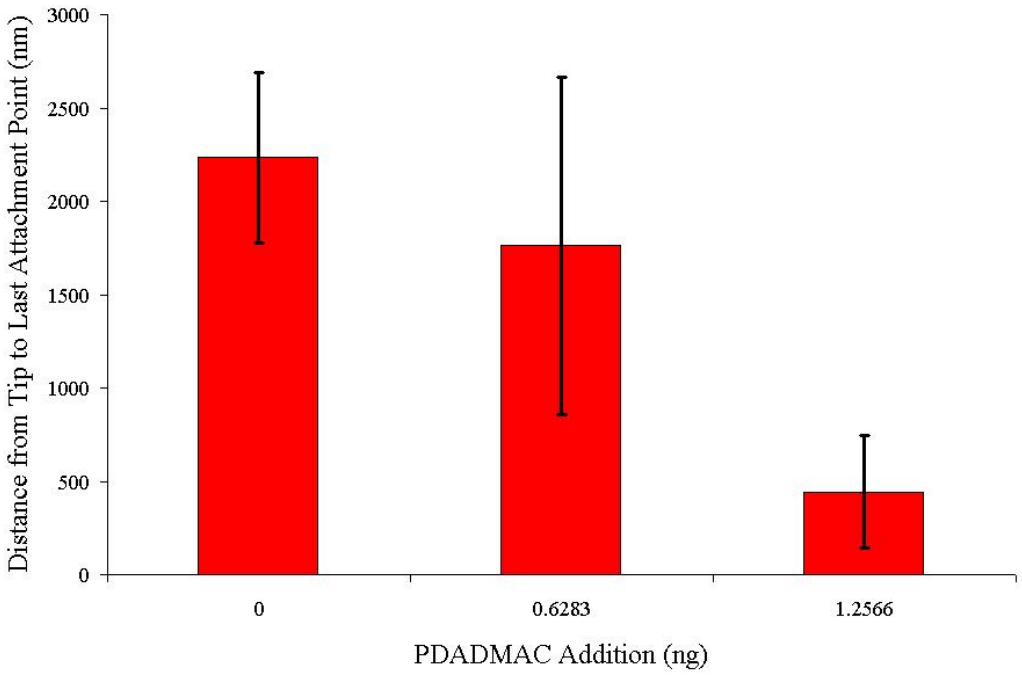

Figure 73: Change in distance to last polymer adsorption point using PDADMAC as a site blocking additive on a glass substrate.

constant adsorbed polymer loop lengths supports the notion that the tail portion of adsorbed polymers plays a large role in the hydrodynamic diameter found in dynamic light scattering measurements.

7.3.2 Cationic Nanosilica

The second site blocking additive used in this project is cationic nanosilica particles. These particles should not be as mobile on the substrate surfaces as the PDADMAC polymer. This is because the shape of these particles is constant and movement from one vacant site to another should not produce a noticeable decrease in energy. This does not mean that these particles will remain stationary, but it supports the idea that they should not be as mobile, across the substrate surface, as an adsorbed polymer. It is possible that these particles will more easily desorb from the substrate because the number of attachment points on the spheres is most likely significantly less than that of a PDADMAC polymer.

Another notable difference of the cationic nanosilica spheres is their size. These spheres have a diameter of $12nm$. The PDADMAC polymer molecules are expected to lay very close to the surface, in comparison to the nanosilica spheres which extend $12nm$ from the surface. The percentage of the substrate surface being blocked by cationic nanosilica is shown in Table 9. These values were calculated using the number of cationic nanosilica particles added for each level and multiplying this by the area of the circle which would be blocked by one of these spheres. The number of spheres was calculated from using the surface area per unit weight value given by Sigma Aldrich, $230\text{m}^2/\text{g}$.

Table 9: The percentage of the unavailable substrate surface areas for each substrate at each blocking condition.

Cationic Nanosilica Added (ng)	**% Mica**	**% Glass**
0.3264	0.00834	0.00579
0.6528	0.0167	0.0116
0.9792	0.025	
1.1328		0.0201
1.6128		0.0286
1.632	0.0417	

Table 9 reports that a very small portion of the available surface area is being blocked by the cationic nanosilica. Table 10 reports the distance between nanosilica spheres assuming all particles adsorb in a uniform lattice-like pattern on the surface. This portrays some spatial reference to the area in which the polymer can adsorb.

Another aspect to consider when reviewing Table 10, is how large of an area the polymer occupies as it moves to the surface. The diameter of gyration is approximately $300nm$. This shows that should the polymer make contact with the surface at the center of an unblocked area under all conditions there is enough space for it to adsorb. However, the electrostatic interactions between the polymer and the site blocking additives will most likely reduce this diameter of gyration.

As discussed previously, not all of the surface area of the mica or glass substrate is

Table 10: The distance between adsorbed cationic nanosilica spheres at different addition levels.

Cationic Nanosilica Added (ng)	**Mica (nm)**	**Glass (nm)**
0.3264	1152.12	1384.95
0.6528	811.16	975.79
0.9792	660.11	
1.1328		737.86
1.6128		616.44
1.632	508.61	

available for polymer adsorption. This is illustrated by analyzing the effect of cationic nanosilica particles on the number of retention polymer attachment points. Figures 74 and 75 illustrate these results for mica and glass, respectively.

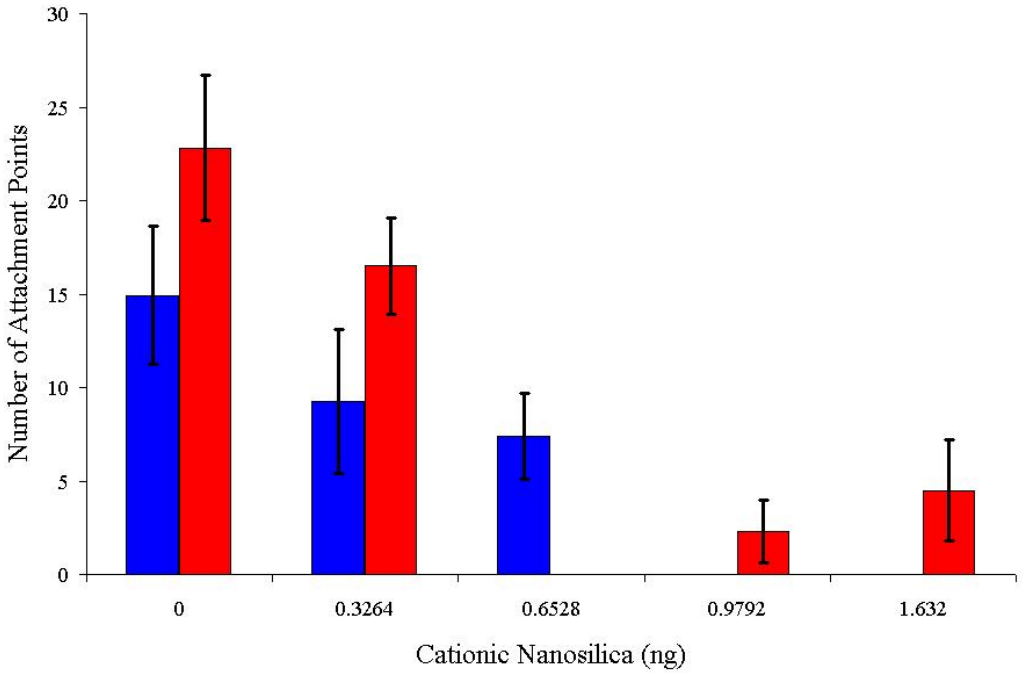

Figure 74: Number of attachments for polymer on mica substrate with different amounts of site blocking cationic nanosilica additions.

The decline in the number of attachment points as the cationic nanosilica concentration increases is shown in Figures 74 and 75. However, at the highest concentration of cationic nanosilica addition there is a small increase in the number of attachment

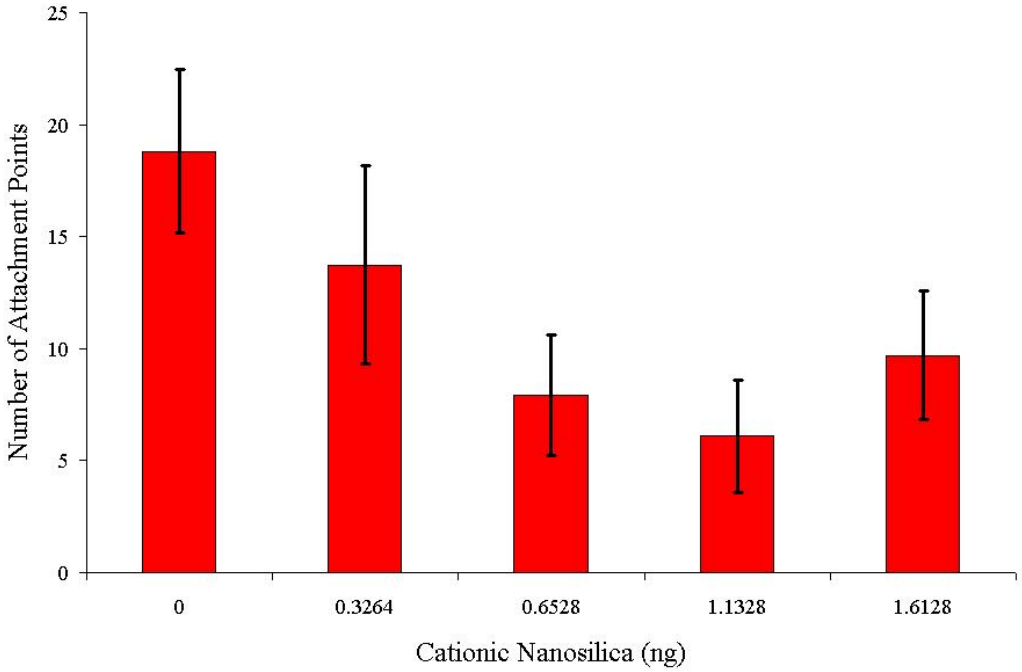

Figure 75: Number of attachments for polymer on glass substrate with different amounts of site blocking cationic nanosilica additions.

points. Although unexpected, it is possible for the cationic nanosilica spheres to desorb and move on the surface. This could be one possible explanation for the slight increase in the number of attachment points. Another could be that the number of nanoparticles added to the substrate is too high for them all to adsorb. This increase in the concentration of the cationic nanosilica spheres in the aqueous phase could raise the ionic strength of the medium. This could cause the polymer to contract upon itself by screening its electrostatic self-repulsion. Again, the anionic sites on both surface can change as different ionizable groups associate and dissociate.

The next aspect of adsorbed polymer conformation analyzed was the loop length distributions on both of the substrates. Figures 76 and 77 illustrate these changes. Tables 11 and 12 report the weighted average maximum loop lengths for each distribution.

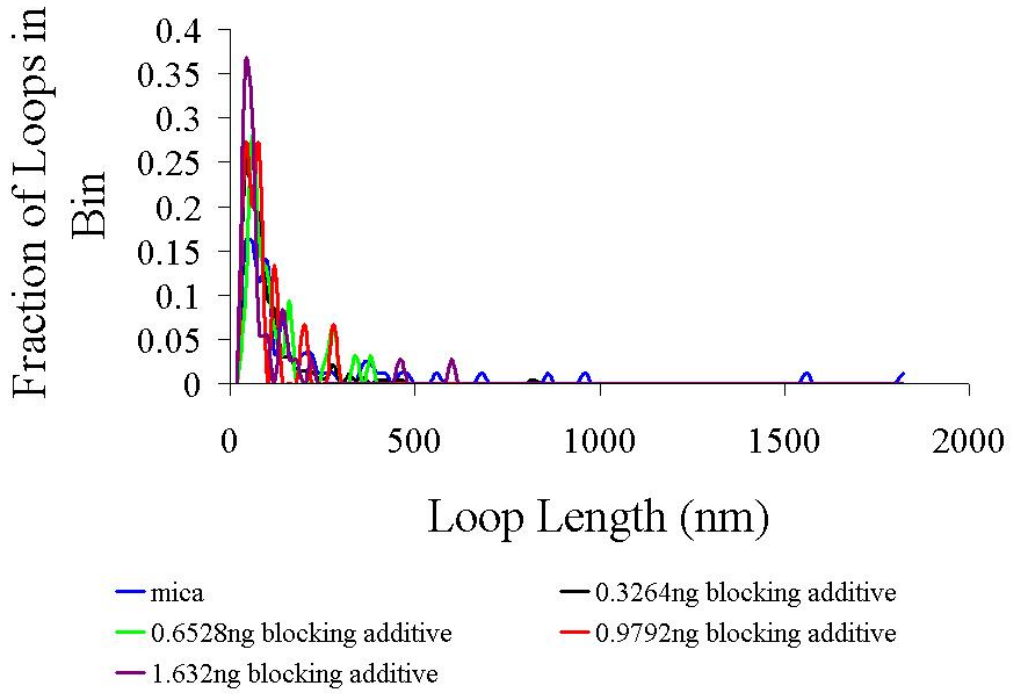

Figure 76: Loop length distributions of MAPTAC/acrylamide copolymer on mica with different amounts of cationic nanosilica used as a site blocking additive.

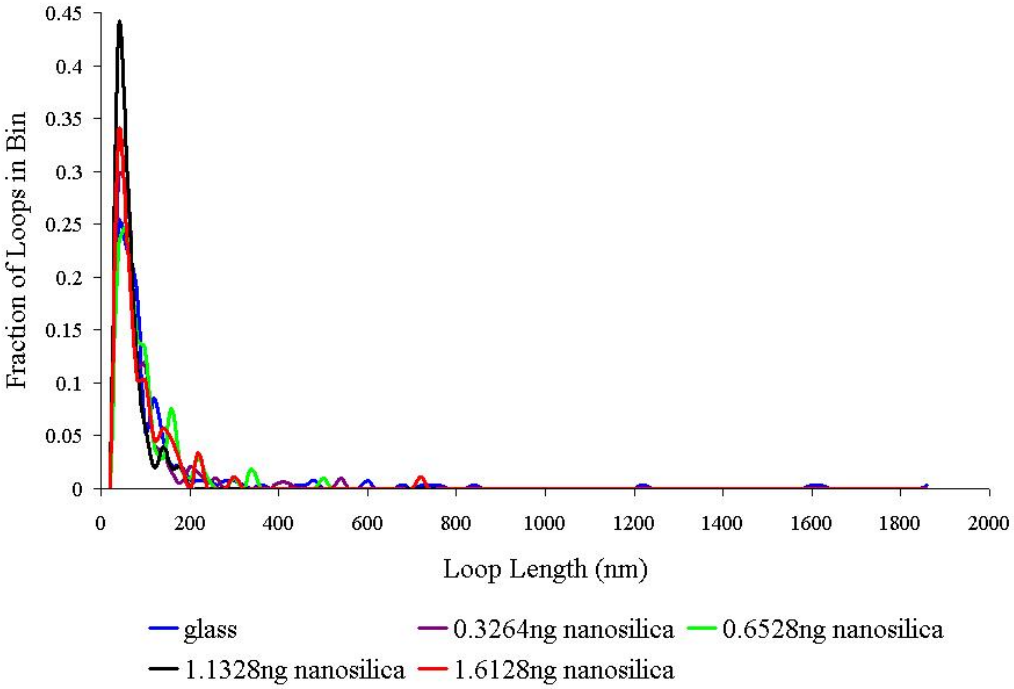

Figure 77: Loop length distributions of MAPTAC/acrylamide copolymer on glass with different amounts of cationic nanosilica used as a site blocking additive.

Table 11: Effect of cationic nanosilica concentration on the weighted average maximum loop length of MAPTAC/acrylamide copolymer on a mica substrate.

Cationic Nanosilica Added	**0ng**	**0.3264ng**	**0.6528ng**	**0.9792ng**	**1.632ng**
Average loop length(nm)	197.24	99.09	120.63	92.00	99.44

Table 12: Effect of cationic nanosilica concentration on the weighted average maximum loop length of MAPTAC/acrylamide copolymer on a glass substrate.

Cationic Nanosilica Added	**0ng**	**0.3264ng**	**0.6528ng**	**1.1328ng**	**1.6128ng**
Average loop length(nm)	130.26	88.33	97.52	64.71	90.11

From Figures 76 and 77 it is difficult to see any changes in the loop length distributions. Tables 11 and 12 confirm this as the weighted average loop length does not show any trend representing increasing or decreasing loop lengths.

The final aspect of an adsorbed polymer's conformation that will be investigated for this site blocking scenario is the change in adsorbed polymer free tail length. Figures 78 and 79 illustrate these results.

An interesting correlation between the change in the number of polymer adsorption points and the length of the free polymer tail can be seen when looking at Figures 78, 79, 74, and 75. It appears that the length of the free tail varies directly with the number of attachment points on the surface. This appears perfectly reasonable at first glance. However, there is no reason that these two aspects of an adsorbed polymer's conformation should be directly related. The free tail portion of a polymer can remain constant in length with many different combinations of polymer attachment points. Although it is reasonable to assume that if the polymer adsorbs linearly in one direction away from the tip, the tail length would shrink with increasing attachment points. This correlation fails to account for the loop lengths between these points.

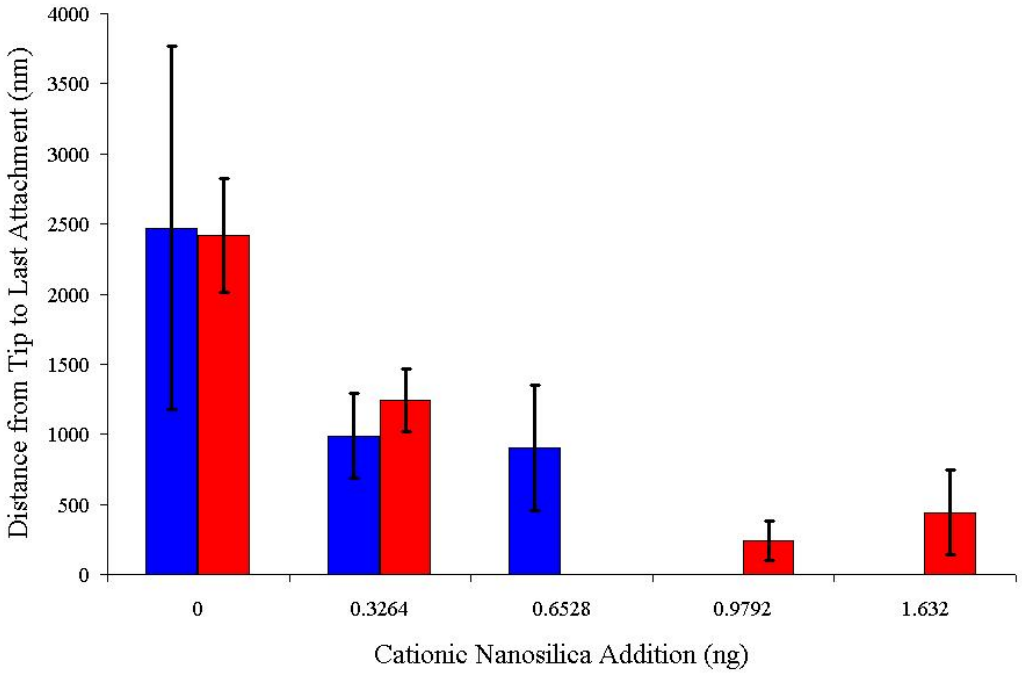

Figure 78: Change in distance to last polymer adsorption point using cationic nanosilica as a site blocking additive on a mica substrate.

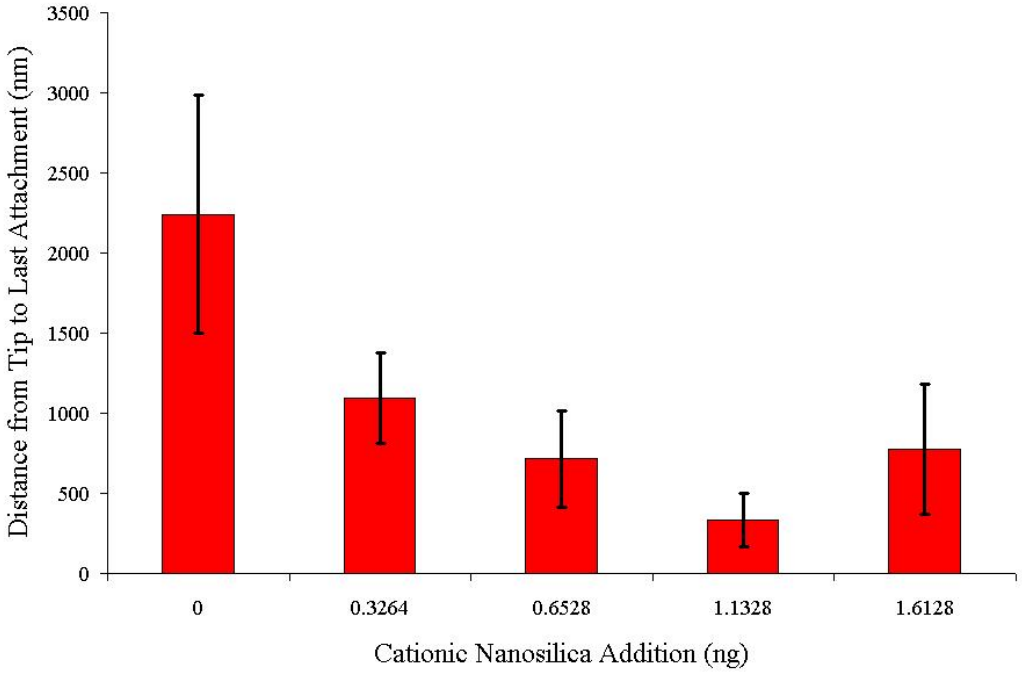

Figure 79: Change in distance to last polymer adsorption point using cationic nanosilica as a site blocking additive on a glass substrate.

7.4 Conclusions

For the first time, direct measurements have been performed to validate how an adsorbed polymer's conformation changes with the addition of site blocking additives. This research has shown that the hydrodynamic thickness of an adsorbed polymer layer on a latex sphere increases with the addition of site blocking additives. The addition of a polymeric additive, PDADMAC, resulted in a smaller adsorbed layer thickness increase than the addition of cationic nanosilica particles. This is expected as the nanosilica particles have a well defined shape and will not flatten out on the surface over time.

Similar to the addition of electrolytes to the media, which a polymer is surrounded by, the addition of site blocking additives tends to decrease the number of polymer attachment points. Although it was found that if the number of attachment points increased beyond a threshold value, the overall trend was a decrease in the number of attachment points. This is expected as the site blocking additives are expected to occupy possible polymer adsorption sites.

Contrary to current theory on site blocking, it was found that the adsorbed polymer loop length distribution does not change significantly for the conditions evaluated. This is most likely due to the location of site blocking additives on the surface. For theoretical calculations it is assumed that the site blocking additives are spread equally on the surface. For this work it is very unlikely that this is the case. This, coupled with the dependence on polymer tail length, is a probable cause of the results for adsorbed polymer loop lengths found using AFM. In one case these loop lengths were even found to decrease. This unexpected result was explained by the change in the adsorbed polymer's free tail length. This length value was found to increase with increasing site blocking additives. This not only explains the increase in hydrodynamic diameter of the adsorbed polymer with site blocking additives, but also validates the results found in industrial practice when using this method of flocculation.

Figure 80 illustrates a couple possible adsorption conformations within the length scales found in this research. A noteworthy observation is that the adsorbed portion of the polymer doesn't extend beyond the interstitial space of two lattice grid sections.

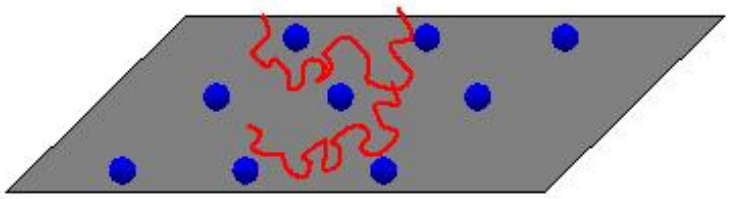

Figure 80: Illustration of possible adsorbed polymer conformations within an evenly spaced cationic nanosilica blocking arrangement.

The percentage of the surface area that was blocked, in the atomic force microscopy testing performed in this work, appears to be well below the predicted values for optimal site blocking efficiency[21]. However, this system is dynamic. The number of sites available for polymer adsorption and their locations are constantly changing. To determine the optimal surface area to block for flocculation a system with a less dynamic character must be studied.

CHAPTER VIII

COMPUTER SIMULATION WITH DISSIPATIVE PARTICLE DYNAMICS

The attempts, associated with this work, at using dissipative particle dynamics have been met with substantial difficulty. The use of dissipative particle dynamics, although not that new, to model experimental or industrial phenomena is still relatively unverified. Most of the work done, to date, deals with making empirical changes to the variable in order to match experimental results. Although information regarding the use of DPD parameterization can be obtained, a fundamental explanation of the application of DPD to actual phenomena has yet to be proposed. The approach of this project was to build, on fundamentally sound theory, a code which can give meaningful information on the conformation of adsorbed polymers. This type of work has only been performed by a few researchers, including Manke *et al.*, in the past[99]. However, this past work leaves many questions unanswered, including how polymer adsorption was simulated. For this project, unfortunately, simulations of adsorbed polymer conformation and the effects of site blocking on adsorbed polymer conformation were unable to be completed. This was due to the inability to parameterize the electrostatic values to describe the interactions of the MAPTAC/acrylamide copolymer with an anionic wall. With more time, however, the parameterization of the wall could be completed. This attempt to describe polymer adsorption on a wall using electrostatic interactions provides an excellent starting point for fitting DPD simulations to experimental and industrial phenomena. This chapter will report the results of the work done towards simulating the systems investigated experimentally for this project. These results involve the work done to simulate a polymer in solution and

what model parameters are reasonable for such a simulation.

8.1 Polymer Simulations

The dissipative particle dynamics model used in this work was parameterized to properly simulate a polymer's movement. The code written uses four main parameters to describe the constraints which will create a polymer: the cutoff radius, the bead/bead interaction parameter, a_{ii}, the spring constant of the bond holding beads together, and the equilibrium bond length between beads. In the code used, the a_{ii} parameter is not applied to directly bonded beads because the interaction is accounted for by a separate quadratic potential. However, this parameter is applied to non-neighboring beads. To begin these simulations, an a_{ii} parameter of 25, the same as used in verification of the DPD code, was used. Although this interaction parameter may not be accurate, a_{ii} is an assigned value to allow reproduction of experimental results and, by varying other variables, many reasonable values could be used. The cutoff radius, r_c, was always set equal to 1 to scale all distances in the simulation. This left only two parameters for adjusting the simulation of a polymer: the spring constant of the bond holding adjacent beads together and the equilibrium bond length between beads. Although these two parameters can be combined in many different ways to give acceptable results, the bond spring constant was set to 5. Nikunen *et al.* selected a bond length and then related the a_{ii} parameter to the spring constant by simply setting a_{ii} to one half the spring constant[182]. The spring constant values used by Nikunen *et al.* were two orders of magnitude greater than the value selected for this work. Again, this is acceptable because the weaker spring constant is accounted for by removing the conservative force between adjacent bonded beads. Equilibrium bond lengths of $0.001r_c$, $0.05r_c$, $0.1r_c$, $0.5r_c$, and $10r_c$ were evaluated for 100 bead polymers. All of these simulations displayed movement that would be expected for a polymer random coil in solution. However, the final

conformations, and the simulation path, were analyzed to see how well they represent the radius of gyration of a polymer in solution. Analysis of the simulation path involved watching for loss of control and unexpected movement of the polymer. If either of these conditions were found the simulation was not used. The results of these situations are illustrated in Figures 81 - 83. The box dimensions used in these figures were $100r_c$x$100r_c$x$200r_c$.

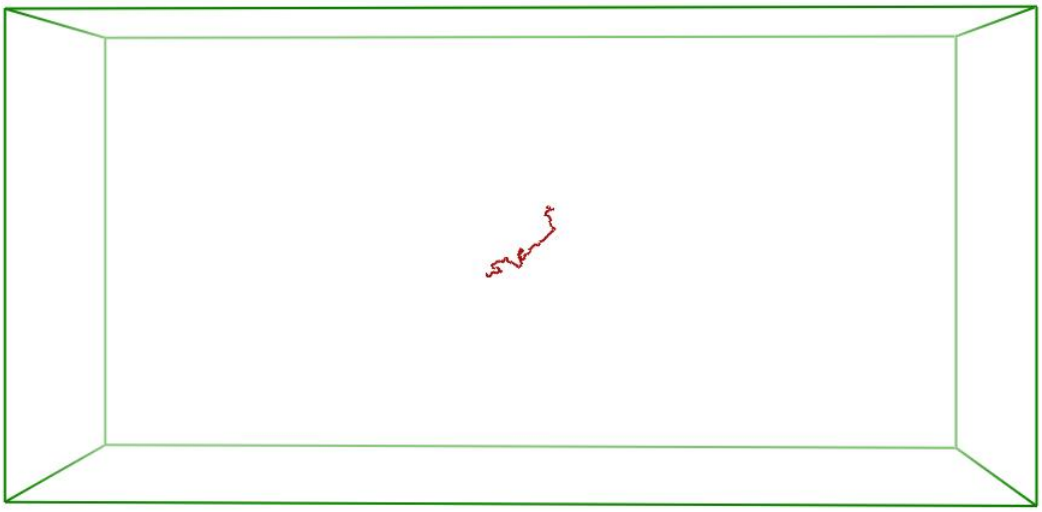

Figure 81: Polymer simulation using a bond spring constant of 5 and an equilibrium bond length of $0.001r_c$.

Figure 81 displays the effects of a $0.001r_c$ bond length set point on the conformation of a 100 bead polymer. Under these conditions, the directly connected polymer beads should be held closely together. Because the r_c is three orders of magnitude larger than this,the conservative force between any bead in the polymer and all the other beads is applied, except for the one or two beads directly bonded to it. This caused a great deal of strain to be placed on the bonds. For the spring constant chosen to describe the bonds, the conservative force is too great resulting in the bond lengths between the beads to be almost two orders of magnitude higher than the set point. The resulting R_g of this simulation was approximately $10r_c$.

Figure 83 illustrates the effect of a bond length being too large. In this example,

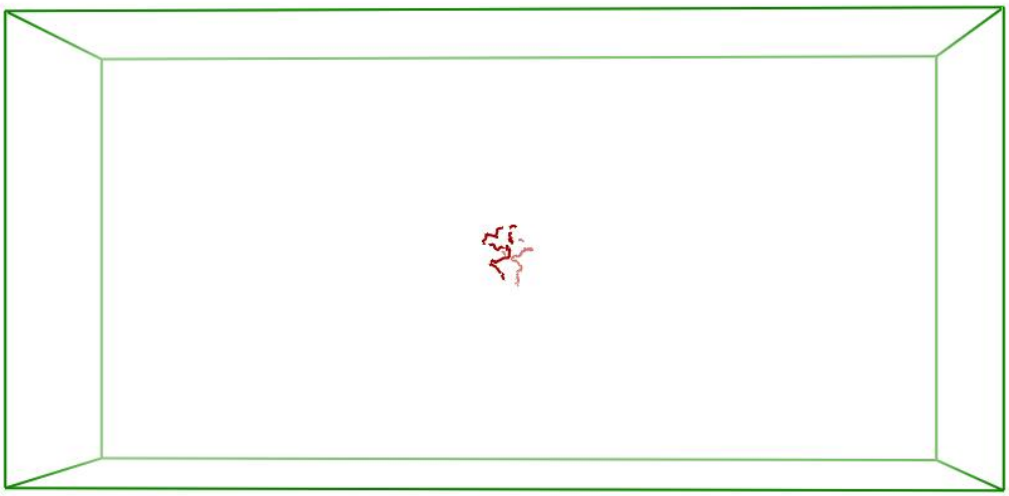

Figure 82: Polymer simulation using a bond spring constant of 5 and an equilibrium bond length of $0.5r_c$.

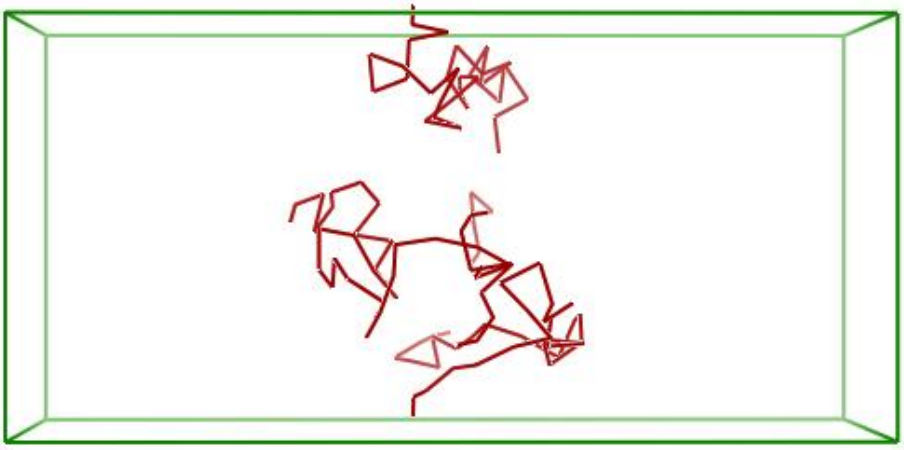

Figure 83: Polymer simulation using a bond spring constant of 5 and an equilibrium bond length of $10r_c$.

the conservative force is only applied in areas where the polymer has folded back near itself. Here the bond lengths are between $1r_c$ and $10r_c$. At distances greater than $10r_c$ the polymer spring constant pulled the beads back together. This large bond length resulted in an approximate R_g of $65r_c$.

The previous two bond length choices resulted in undesirable modeling situations. The choices of bond lengths of $0.05r_c$, $0.1r_c$, and $0.5r_c$ were designed to help pick an optimum bond length to use for this work. A bond length of $0.05r_c$ simulated a polymer with an approximate R_g of $4.5r_c$. As the bond length was increased to $0.1r_c$ the approximate R_g increased to $5r_c$ and the average bond length, found from the simulation, was around $0.75r_c$.

Figure 82 shows the effect of setting the bond length to $0.5r_c$. For this simulation, the closest match between the set point bond length($0.5r_c$) and the actual bond length($0.65r_c$) were found. The consistency of the calculated bond length and the bond length set point is essential to obtaining fundamentally sound simulations. Without this consistency the bonded beads in the simulated polymer will move well beyond reasonable distances from one another eliminating the ability of the simulation to be compared to experimental phenomena. The R_g of this simulation was shown to expand slightly to approximately $6.5r_c$. Because of this, the equilibrium bond length was chosen to be $0.5r_c$ for this work.

Now that an equilibrium bond length had been chosen, it was possible to determine the appropriate a_{ii} parameter of the polymer to allow reproduction of the experimentally determined R_g, $151nm$, of the MAPTAC/acrylamide copolymer. The first step in this process was to determine the number of beads necessary to represent the copolymer used for the AFM and DLS experimental studies. Assuming each bead to be two MAPTAC/acrylamide repeat unit this number was calculated to be 346 beads.

Because DPD code does not require a diameter of the beads used in simulations, a

method to relate the distances between beads and actual polymer length was required to extract information from these models. All lengths in DPD are scaled with the cutoff radius, r_c. This radius is the maximum distance from a bead which will produce interaction forces with other beads. It is unreasonable to assume that this r_c value could be used to directly quantify a beads size. If this was done the bead, or polymer repeat unit, would not feel any interactions with other beads unless they were in direct contact. It is well known that the electrostatic forces which most likely play an important role in a MAPTAC/acrylamide copolymer's configuration in solution, will extend large distances from the actual bead. To account for this, the beads diameter was set to $\frac{1}{3}$ the r_c value. While this assignment could be far from accurate when attempting to account for electrostatics it was a reasonable starting point for this work.

With the bead diameter, $11.7nm$, set to $\frac{1}{3}$ the r_c value, the length of r_c was calculated to be $35.1nm$. Figure 84 shows the configuration of the MAPTAC/acrylamide copolymer after a simulation of $1000ps$.

The R_g for the copolymer, simulated in Figure 84, was calculated to be $65.46nm$. A repeat of this simulation resulted in a R_g value of $61.78nm$. These values of R_g are about three times too small for the value obtained from static light scattering experiments performed. To help fit these simulations to the experimental results, the previously constant a_{ii} parameter was increased to assert more repulsion between beads. After increasing the a_{ii} parameter to 45, the radius of gyration was calculated to be $164.71nm$. This polymer configuration is shown in Figure 85.

Although the radius of gyration for a single polymer approximately matching the experimental results is good, that simulation and the experimental conditions are very different. In order to attempt to reproduce the correct R_g under experimental conditions, a simulation was done with six polymers in a smaller box. Figure 86 shows these results.

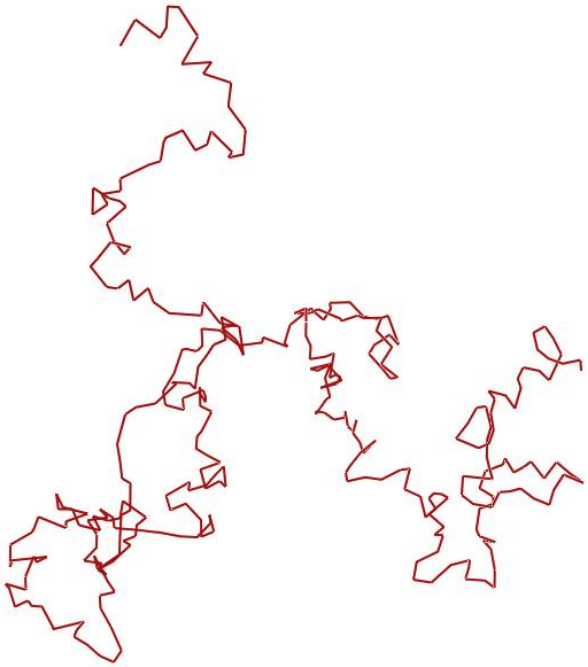

Figure 84: Polymer simulation of the MAPTAC/acrylamide copolymer using an a_{ii} parameter of 25.

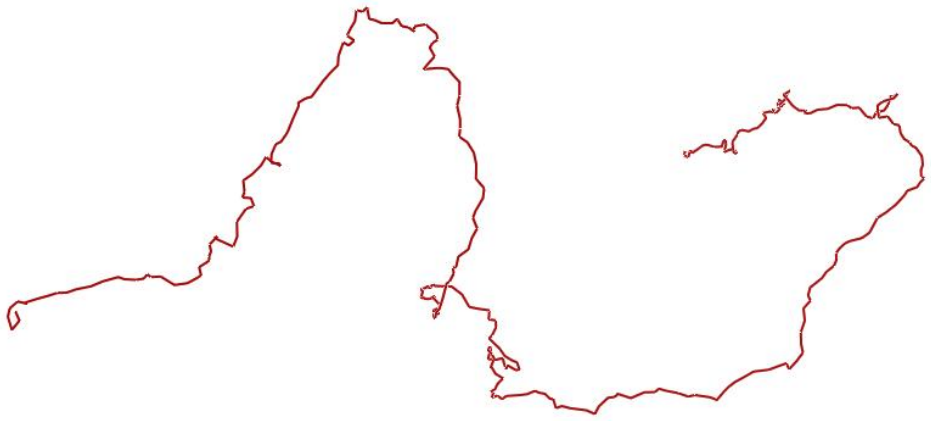

Figure 85: Polymer simulation of the MAPTAC/acrylamide copolymer using an a_{ii} parameter of 45.

Figure 86: Polymer simulation of six MAPTAC/acrylamide copolymers using an a_{ii} parameter of 45.

The six R_g values for the polymers in a simulation similar to that shown in Figure 86 are $137.84nm$, $176.03nm$, $185.50nm$, $168.23nm$, $134.30nm$, and $152.47nm$. The average R_g for these six polymers is $159.06nm$, again falling close to the experimental value found using static light scattering. It appears the box size must be reduced to approximately 1/3 its current size to see an influence of neighboring polymers on the respective polymer's radius of gyration. A box of this size would allow the polymers not to overlap, but be close enough to feel the effects of another polymer's movement.

8.2 Conclusions

Although simulations of an adsorbed polymer's conformation were unable to be completed, some significant steps were made in applying dissipative particle dynamics simulations to experimental data. Simulations of polymers in solution, using dissipative particle dynamics, were performed with little explanation as to the scaling of the variables used[182]. Although the radii of gyration of different polymers can be compared without ever giving the actual length, these simulations can not be compared to actual data without at least one additional assumption.

All length or distance values in the DPD simulations are scaled to r_c. However, without assigning a length to r_c the lengths in simulation can not be compared with experimental work. In this work, a closer look at what r_c actually signifies was taken. It is known that r_c is the distance from a bead in which it will feel interactions from other beads. For the MAPTAC/acrylamide copolymer, it is likely that electrostatics play a large role in the polymer's radius of gyration. It is also known that electrostatics act over fairly long distances. Because of this, it was assumed that the r_c value must be greater than the repeat unit diameter. For these simulations, as described in the previous section, it was assumed that r_c was three times the diameter of a bead. The diameter of a bead was roughly calculated knowing the straight chain length of the carbon/carbon bonds in the repeat unit backbone. With this information, it was possible to relate the DPD simulations to actual radius of gyration values obtained experimentally for the MAPTAC/acrylamide copolymer.

One aspect of DPD simulations which was not investigated, but should be, is the effect of the variation of the stochastic and viscous drag forces of the solvent as polymer is add to it. For this work these forces were kept at setpoints used by Frenkel and Smit[94]. Given more time, it should be possible to evaluate the effects of changes in these variables on the movement of a polymer in solution. However, this work has provided a reasonable starting point from which these effects can be investigated.

An important note to the methodology described above is that when altering the a_{ii} parameter to obtain the correct R_g value for the MAPTAC/acrylamide copolymer the equilibrium bond lengths change for the simulated polymer. With more time, it would have been important to again optimize the bond lengths by adjusting the spring constant of the polymer to account for the additional repulsive conservative force between beads.

The results presented in this chapter have shown reasonable values of the DPD parameters to simulate the conformation of a high molecular weight MAPTAC/acrylamide

copolymer in water. By using these values, further investigation of the effects of other DPD parameters can be analyzed and related to one another.

CHAPTER IX

OVERALL CONCLUSIONS AND RECOMMENDATIONS

This dissertation performed a fundamental analysis of an adsorbed polymers conformation on a surface. Using a well developed experimental method, dynamic light scattering, and developing a new experimental technique, using atomic force microscopy, specific information on adsorbed polymer conformation was reported. The verification of this new atomic force microscopy method opens up many possibilities for evaluating single adsorbed polymer properties. Many of these results were shown experimentally for the first time in this work.

Adsorbed MAPTAC/acrylamide copolymer conformations on different anionic substrates were analyzed. The dynamic light scattering results showed an increase in hydrodynamic radius, after the addition of the copolymer, most likely pertaining to an adsorbed polymer layer being deposited. Atomic force microscopy gave a direct measurement of an adsorbed polymer's loop lengths to determine its conformation. It was found through multiple tests that the average loop length of an adsorbed MAPTAC/acrylamide copolymer, with a molecular weight around $1\text{x}10^6 g/mol$, was around $174nm$. The loop length distribution showed the majority of the loops lengths were between 40 and $260nm$. These results could be manipulated to fit scaling predictions for adsorbed polymer conformations. However, these fits fail to illustrate the unique characteristics of an adsorbed polymer's conformation on a surface. For the first time, an adsorbed polymer's relaxation was shown using atomic force microscopy.

The second portion of this work examined the salt effect on adsorbed polymer conformations. Dynamic light scattering results showed increases in the adsorbed polymer layer thickness with increasing ionic strengths of the liquid medium. It was

verified that the addition of electrolytes to the liquid medium decreased the number of polymer attachment points to a surface. This is presumably due to a filling, or blocking, of available adsorption sites by salt counterions. Shubin and Linse's predictions for the salt effect on adsorbed polymer conformations was, for the first time, verified using this atomic force microscopy technique. It was shown that there may be a slight increase in loop length sizes with increasing ionic strength. However, the largest change in adsorbed polymer conformation is related to the increasing in the free tail length of an adsorbed polymer.

The final section of this work dealt with the effect of site blocking additives on adsorbed polymer conformation. Similar to past research, it was found that the use of site blocking additives increased the adsorbed polymer layer thickness on a surface. The dynamic light scattering results from this work showed a slightly greater increase in layer thickness when cationic nanosilica particles were used as a blocking additive compared with the use of PDADMAC as a blocking additive. The use of atomic force microscopy revealed surprising results regarding the actual adsorbed polymer conformation. Contrary to expected results, the adsorbed polymer loop length did not increase with increasing amounts of site blocking additives.

As was expected the number of attachment points did decrease with increasing amounts of site blocking additives. The free tail portion of an adsorbed polymer's conformation was found to increase with increasing site blocking additive concentrations. Due to the analysis of a single and different polymer, comparisons between the PDADMAC and cationic nanosilica blocking additives were not performed.

An interesting result from this work is the strikingly similar behavior between the addition of electrolytes and the addition of site blocking additives. Increasing amounts of both of these components decreases the number of polymer attachment points on the substrate. This supports the point that the salt ions are competing for adsorption points just as the site blocking additives are, and are actually blocking

possible adsorption points for the polymer on the substrate. Both of these components have only a slight effect, if any, on the adsorbed polymer's loop length distribution. This could be due to the truly random nature of polymer adsorption on a substrate. And finally the increase in the adsorbed polymer's free tail length with increasing concentrations of these components is very interesting.

The increase in adsorbed polymer tail length could have profound effects on the understanding of flocculation. It is known that the addition of site blocking additives increases the amount of flocculation with smaller additions of retention polymers. This could signify that the free tail portion of the adsorbed polymer's conformation plays the dominant role in flocculation. If true, this gives a new tool to retention polymer manufacturers to tailor their molecules to capitalize on this phenomena.

Overall, this research project has resulted in the development of a novel atomic force microscopy technique which allows the investigation of the properties of a single adsorbed polymer. Information regarding an adsorbed polymers conformation has been detailed. The effects of salt concentration and site blocking additives on a single adsorbed polymer's conformation were, for the first time, reported and analyzed. With future work these methods and findings may help researchers develop a better understanding of how polymers interact with surfaces and the factors influencing this.

9.1 Recommendations For Future Work

This work has added key pieces of experimental evidence to support predictions for adsorbed polymer conformation. This thesis provides an introduction for new techniques to characterize polymer's conformations, with these techniques it is possible to now investigate more complex polymer phenomena. The following areas, listed below, are some of the many possible paths this research can be continued on:

- **Further verification of the single molecule assumption made for the AFM portion of this work.** Although significant steps were taken to ensure

a single polymer was being analyzed, no direct proof was ever provided. It is possible that by placing a fluorescent or luminescent tag on the other terminal end of the polymer being tested, the assumption of a single polymer could be proven. One method for this is possibly attaching a quantum dot to the other terminal end of the polymer. This could be seen with currently available microscopy systems coupled with the AFM.

- **Removal of the variance in the substrate adsorption site location and number.** The use of a well characterized, stable, substrate could allow more information on how exactly an adsorbed polymer is adsorbing on a surface relative to the available number of adsorption sites. Using a substrate, such as silicon, which can be cleaved to give a known number and spacing of charged sites would help take some of the ambiguity out of the data obtained.

- **Testing on well characterized, constant, structured polymers.** By evaluating block copolymers with known repeat units and molecular weights, the factors of polymer structure which affect adsorbed polymer conformation can be investigated. This work used a random copolymer with a substantial polydispersity complicating conclusions on adsorbed polymer conformation and tail length.

- **Study of site blocking additive's size, surface affinity, and structure effects on adsorbed polymer conformation.** This study of the site blocking effect of two additives has raised questions into what actually happens with other changes in the site blocking additive's properties. By using different blocking additives of different sizes and surface affinities more information, regarding this system, can be obtained.

- **Analysis of the fundamentals of flocculation.** Very little is known on how flocculation actually occurs. By using the results of this study and some of the

paths described previously, it is possible to outline an experimental plan aimed at determining the actual mechanism of flocculation and the role of different types of polymers in this process.

- **Further development of dissipative particle dynamics program.** With this work a reasonable approach to applying DPD to a real system was developed. By continuing this work it is likely that polymer adsorption on a wall can be simulated. This would allow the use of simulations to aid in the design of new polymer modified surfaces.

APPENDIX A

DPD SVL CODE

```
#svl
    #set main DPD
        // Write data to database
    local function WriteDB [mdb, time, kbT, acc, vel, init]
        local molsys = mol_Extract Atoms[];
        // setup data and write to database      local data = [time:time, mol:molsys, kbT:kbT, accx:acc(1), accy:acc(2), accz:acc(3), velx:vel(1), vely:vel(2), velz:vel(3), init:init];
    db_Write [mdb, 0, data];
    db_Flush mdb;
    endfunction
        // DPD_Force solves the force equations for DPD. Returns the total force.
    local function DPD_Force [n, pos, box, vel, rc, gamma, sigma, aij,      element, bond, bond_spring, blength, inv_sqrt_dt, es]
        local k, i, j, rij, rijmag, eij, vij, wr, wd, a;      local fci, fdi, fri, fwi;      local bond_rij, bond_rijmag, bond_eij, fsi;      local y, sgny, ekd;
        local f = rep[[0,0,0], n];
        // loop over all beads      for i = 1, n loop
    for j = i+1, n-1 loop
        // get distance between beads for pair interactions      rij = pos(i) - pos(j);
        // Minimum Image Convention      rij = rij - box * round ( rij * invz box);
        // magnitude of bead distance (rij)      rijmag = sqrt add sqr rij;
```

// random, dissipative, and conservative forces are only calculated // if they are within rc

if rc > rijmag then

// make unit vector for rij eij = rij * invz rijmag;

// determine the interaction parameter for conservative force a = select [select[aij.aii, aij.ajj, element(i)=='Ar'], aij.aij, element(i) == element(j)];

// calculate velocity difference for dissipative force vij = vel(i) - vel(j);

// calculate omega_r and omega_d used in f_r and f_d wr = 1 - rijmag * invz rc; wd = sqr wr;

// conservative force fci = a * (1 - rijmag) * eij;

// dissipative force fdi = - gamma * wd * add (vij*eij) * eij;

//random force fri = sigma * wr * randN(1) * eij * inv_sqrt_dt;

// add up the forces and assign properly to the force vector f(i) = f(i) + (fci + fdi + fri); f(j) = f(j) - (fci + fdi + fri);

endif

endloop

endloop

// spring (bond) force calculations (f_s)

bond_rij = pos[bond.i] - pos[bond.j]; bond_rij = bond_rij - [box] * round (bond_rij * invz [box]); bond_rijmag = sqrt app add sqr bond_rij; bond_eij = bond_rij * invz bond_rijmag;

fsi = bond_spring * (blength - bond_rijmag) * bond_eij; f[bond.i] = f[bond.i] + fsi; f[bond.j] = f[bond.j] - fsi;

// force due to electrostatic attraction to the wall (f_w)

y = (tr pos)(2); sgny = sign y; y = abs y; ekd = exp(-es.kr*y); fwi = tr [0, (-1.04765e-4*es.br*es.kr*invz sqr es.ns * es.P2P2) * (es.SPP2P2*(-ekd * invz (1-ekd) * invz (1+ekd)) + sqr ekd *invz (1-sqr ekd)) - es.ea * // LJ (12 * pow[es.cd

/ y, 12] / y), // repulsive 0]; fwi = fwi * sgny; f = f + fwi;

return f;

endfunction

// This function places the molecule (Ar, He = A, B) in a periodic // cube in a random position

local function placemolecules3d [NA, NA_beads, NB, NB_beads, box, rc, blength]

local chainsA, polyA, atomsA, posA, chainsB, polyB, atomsB, posB; local k, new_pos, rho, theta, phi, new_chains; local poly_chains, pos, x_mask, y_mask, z_mask, y, new_y;

// Center the original coordinates and then place randomly next to an atom // get Ar atom keys and places the first atom by changing the atom name, // the mass, and the color based on element color. Does the same with He.

atomsA = app sm_Build rep['[Ar]',NA]; aSetName [atomsA, tok_cat ['A',totok ((igen NA - 1) * NA_beads + 1)]]; posA = tr (randU rep [box, NA] - rep [box/2,NA]); aSetPos [atomsA, posA]; polyA = atomsA; chainsA = aChain atomsA;

atomsB = app sm_Build rep['[He]',NB]; aSetName [atomsB, tok_cat ['B',totok ((igen NB - 1) * NB_beads + 1)]]; posB = tr (randU rep [box, NB] - rep [box/2,NB]); aSetPos [atomsB, posB]; polyB = atomsB; chainsB = aChain atomsB;

// make the polymer. The previous loops put all of the atoms in the box for // the first bead in a polymer. These loops finish the polymers

for k=2, NA_beads loop

rho = blength * (1 + randU rep[0.2,NA] - 0.1); theta = randU rep[2*PI,NA]; phi = randU rep[2*PI,NA]; new_pos = [rho * cos theta * sin phi, rho * sin theta * sin phi, rho * cos phi]; posA = new_pos + posA;

atomsA = app sm_Build rep['[Ar]',NA]; aSetName [atomsA, tok_cat ['A',totok ((igen NA - 1) * NA_beads + k)]]; aSetPos [atomsA, posA]; Bond [polyA, atomsA];

polyA = atomsA; new_chains = aChain atomsA; oReparent [aResidue atomsA,chainsA]; oDestroy new_chains;

endloop

for k=2, NB_beads loop

rho = blength * (1 + randU rep[0.2,NB] - 0.1); theta = randU rep[2*PI,NB]; phi = randU rep[2*PI,NB]; new_pos = [rho * cos theta * sin phi, rho * sin theta * sin phi, rho * cos phi]; posB = new_pos + posB;

atomsB = app sm_Build rep['[He]',NB]; aSetName [atomsB, tok_cat ['B',totok ((igen NB - 1) * NB_beads + k)]]; aSetPos [atomsB, posB]; Bond [polyB, atomsB]; polyB = atomsB; new_chains = aChain atomsB; oReparent [aResidue atomsB,chainsB]; oDestroy new_chains;

endloop

// Move any chains that cross the y axis to above/below the y axis // (whichever is closest). Used so that polymers cannot cross the wall

poly_chains = Chains[] |app length oChildren Chains[] > 1; pos = cat app aPos cAtoms poly_chains; x_mask = cat rep[[1,0,0],(length pos)/3]; y_mask = cat rep[[0,1,0],(length pos)/3]; z_mask = cat rep[[0,0,1],(length pos)/3]; y = pos |y_mask; new_y = cat select [y, select[y + abs app min y + 1, y - abs app max y - 1, abs app max y > abs app min y], sign app max y == sign app min y]; aSetPos [cat cAtoms poly$_c$hains, [cat (pos|x_mask), new_y, cat (pos|z_mask)]];

endfunction

// The setup function makes commonly used variables and sets up the system. // It adds the periodic cell and colors the atoms. // Variables that are returned: // i and j (pair interaction indices for all atoms) // mass (vector of masses) // a (stores interaction parameters aii, ajj, and aij) // bond (stores bond indices for bonded atoms with tags i and j) // es (stores all electrostatics parameters)

local function setup [massA, massB, box, aii, aij, ajj, energy_attraction, collision_diameter, ns, np, ps, pp, kappa, bead_radius]

local n, atoms, element, I, J, mass, a, A, B, bond, es;

// enable the box CellParameters['P1', box, [90,90,90]]; CellEnable 1;

// get total number of beads n = length Atoms[]; atoms = Atoms[]; element = aElement atoms;

// Color the atoms aSetColorBy [atoms,'rgb']; aSetRGB [atoms, select[0x990000,0x999999,element=='Ar']];

// Create the mass vector mass = select [massA, massB, element=='Ar'];

// make a vector of interaction parameters aij = [aii:aii, ajj:ajj, aij:aij];

// create a vector to collect bond information // dummy variables are used first, then assigned to the tagged bond variable if add aBondCount atoms > 0 then A = cat apt rep [x_id atoms, aBondCount atoms]; B = indexof [cat aBonds atoms, atoms]; [A,B] = [A,B] |||[A and B and A ¡ B]; bond.i = A; bond.j = B; endif

// setup electrostatic parameters es.ea = energy_attraction; es.cd = collision_diameter; es.P2P2 = sqr ns * sqr ps + sqr np * sqr pp; es.ns = ns; es.SPP2P2 = 2*ns*np*ps*pp * invz es.P2P2; es.kr = kappa * bead_radius; es.br = bead_radius;

return [element, mass, aij, bond, es];

endfunction

// MD integration function

local function MD [mdb, vel, acc, mass, sigma, kbT, rc, box, iter, dt, sample_time, sim_length, bond_spring, blength, element, aij, bond, init, es]

local pos, n, gamma, inv_sqrt_dt, total_steps; local time, trvel, kT;

// initialize necessary values pos = tr aPos Atoms[]; n = length Atoms[]; gamma = sqr sigma / (2 * kbT); inv_sqrt_dt = inv sqrt dt;

// total number of iterations total_steps = int ceil (sim_length / dt);

```
    loop
  // VV from Groot and Warren, which is VV since using lambda = 0.5 pos = pos
+ vel * dt + 0.5 * sqr dt * acc;
  // Periodic Boundary Conditions pos = pos - [box] * round (pos * invz [box]);
  aSetPos [Atoms[], tr pos];
  vel = vel + 0.5 * dt * acc;
  acc = DPD_Force [n, pos, box, vel, rc, gamma, sigma, aij, element, bond, bond_spring,
blength, inv_sqrt_dt, es] / mass;
  vel = vel + 0.5 * dt * acc;
  time = (iter = iter + 1) * dt;
  if mod [iter, sample_time] == 0 then    trvel = tr vel;    kT = add (mass * add
sqr trvel) / (3 * n - 3);    WriteDB [mdb, time, kT, tr acc, trvel, init]; endif
    until iter > total_steps    endloop
    db_Close mdb;
  endfunction
    // GetDPDSystem pulls a database entry from a given database and inserts
// it into the MOE window for viewing
  global function GetDPDSystem [dbname, entry_index]
    local mdb, values, chains;
   mdb = db_Open tok_cat[dbname,'.mdb'];   values = db_Read [mdb, (db_Entries
mdb)(entry_index), ['mol','init']];
   local [massA, massB, edgex, edgey, edgez, sigma, kbT, aii, aij, ajj, rc,   sim_length,
dt, sample_time, bond_spring, blength, bead_radius, kappa,    energy_attraction, col-
lision_diameter, ns, ps, np, pp] =    values.init;
    // Load current system into the MOE window    chains = mol_Create
values.mol;
    // Set colors for the atom types    aSetColorBy [Atoms[],'rgb'];    aSetRGB
```

[Atoms[], select[0x990000,0x999999,aElement Atoms[] == 'Ar']];

//Creates the box CellParameters ['P1', [edgex,edgey,edgez], [90,90,90]]; CellEnable 1;

db_Close mdb;

endfunction

// DPD_restart restarts a simulation that was ended prematurely

global function DPD_restart [dbname]

local mdb, last_entry, values, chains, box, vel, acc, iter;

mdb = db_Open [tok_cat[dbname,'.mdb'], 'read-write'];

last_entry = last db_Entries mdb;

// reads in values from the last entry values = db_Read [mdb, last_entry, ['mol', 'time', 'accx', 'accy', 'accz', 'velx', 'vely', 'velz', 'init']];

local [massA, massB, edgex, edgey, edgez, sigma, kbT, aii, aij, ajj, rc, sim_length, dt, sample_time, bond_spring, blength, bead_radius, kappa, energy_attraction, collision_diameter, ns, ps, np, pp] = values.init;

// Load current system into the MOE window chains = mol_Create values.mol;

// set up the system box = [edgex, edgey, edgez];

local [element, mass, a, bond, es] = setup [massA, massB, box, aii, aij, ajj, energy_attraction, collision_diameter, ns, np, ps, pp, kappa, bead_radius];

vel = tr [values.velx, values.vely, values.velz]; acc = tr [values.accx, values.accy, values.accz];

iter = int (values.time / dt);

MD [mdb, vel, acc, mass, sigma, kbT, rc, box, iter, dt, sample_time, sim_length, bond_spring, blength, element, a, bond, values.init, es];

endfunction

// Main Function

global function DPD [dbname, NA, massA, NA_beads, NB, massB, NB_beads, edgex, edgey, edgez, sigma, kbT, aii, aij, ajj, rc, sim_length, dt, sample_time, bond_spring, blength, bead_radius, kappa, energy_attraction, collision_diameter, ns, ps, np, pp]

// KBOLTZ = 0.00198722 kcal/K*mol // dbname = Database name as token (-.mdb extension) // NA = total number of A chains // massA = mass of an A bead (dimensionless mass units, generally 1) // NA_beads = the number of A beads in each A chain // NB = total number of B polymers // massB = mass of a B bead (dimensionless mass units) // NB_beads = the number of B beads in each B chain // edgex = the x dimension of the box (dimensionless units of Rc) // edgey = the y dimension of the box (dimensionless units of Rc) // edgez = the z dimension of the box (dimensionless units of Rc) // sigma = dimensionless value for sigma used in DPD force calculation // sigma**2 = 2*gamma*kbT (larger values of sigma = faster equilibration) // kbT = dimensionless value for energy. Should be assigned 1, where // E* = E/kbT // aii = interaction parameter of A-A Interactions (dimensionless E units) // aij = interaction parameter of A-B Interactions (dimensionless E units) // aij = interaction parameter of B-B Interactions (dimensionless E units) // rc = cutoff radius (dimensionless about 3*bead radius) // sim_length = total simulation time (dimensionless time units) // dt = time step (dimensionless units) // sample_time = number of time steps between samples // bond_spring = dimensionless value of the bond spring constant // blength = dimensionless equilibrium bond length // bead_radius = radius of a bead (assumes A & B beads are the same size) // (dimensionless units of Rc) // kappa = inverse debeye length (dimensionless units of Rc) // energy_attraction = // collision_diameter = // ns = nu_s, // ps = psi_s, // np = nu_p, // pp = psi_p,

local box, init, mdb, fields, n, pos, vel, inv_sqrt_dt, gamma, acc, kT, iter;

box = [edgex,edgey,edgez]; init = [massA, massB, edgex, edgey, edgez,

sigma, kbT, aii, aij, ajj, rc, sim_length, dt, sample_time, bond_spring, blength, bead_radius, kappa, energy_attraction, collision_diameter, ns, ps, np, pp];

// Creates the Data base mdb = db_Open [tok_cat[dbname,'.mdb'],'create']; db_EnsureField[mdb, 'mol', 'molecule'];

fields = ['time','kbT','accx','accy','accz','velx','vely','velz','init']; apt db_EnsureField[mdb, fields, 'float'];

//calls the random placement of atoms placemolecules3d [NA, NA_beads, NB, NB_beads, box, rc, blength];

//setup the system local [element, mass, a, bond, es] = setup [massA, massB, box, aii, aij, ajj, energy_attraction, collision_diameter, ns, np, ps, pp, kappa, bead_radius];

n = length Atoms[]; pos = tr aPos Atoms[];

// initial guess for the velocities (also removes linear momentum) vel = randN rep[sqrt (kbT/mass), 3]; vel = vel - app add (vel * [mass]) / add mass; vel = tr (vel * sqrt ((3 * n - 3) * kbT / add (mass * add sqr vel)));

// get variables needed for first force calculation inv_sqrt_dt = inv sqrt dt; gamma = sqr sigma / (2 * kbT);

acc = DPD_Force [n, pos, box, vel, rc, gamma, sigma, a, element, bond, bond_spring, blength, inv_sqrt_dt, es] / mass;

kT = add (mass * add sqr tr vel) / (3 * n - 3);

//output to database WriteDB [mdb, 0, kT, tr acc, tr vel, init];

iter = 0;

MD [mdb, vel, acc, mass, sigma, kbT, rc, box, iter, dt, sample_time, sim_length, bond_spring, blength, element, a, bond, init, es];

endfunction

REFERENCES

[1] Adachi, Y. and Wada, T., "Initial stage dynamics of bridging flocculation of polystyrene latex spheres with polyethylene oxide," *Journal of Colloid and Interface Science*, vol. 229, pp. 148–154, 2000.

[2] Adriani, P. and Chakraborty, A., "Dynamics of relaxation at strongly interacting polymer-solid interfaces: Effects of chain architecture," *Journal of Chemical Physics*, vol. 95, pp. 4263–4274, 1993.

[3] Aksberg, R., Einarson, M., Berg, J., and Odberg, L., "Adlayer thickness of two cationic polyacrylamides adsorbed onto polystyrene latices," *Langmuir*, vol. 7, pp. 43–45, 1991.

[4] Aksberg, R. and Odberg, L., "Adsorption of an anionic polyacrylamide on cellulosic fibers with pre-adsorbed cationic polyelectrolytes," *Nordic Pulp and Paper Research Journal*, vol. 5, no. 4, pp. 168–171, 1990.

[5] Al-Maawali, S., Bemis, J., Akhremitchev, B., Leecharoen, R., Janesko, B., and Walker, G., "Study of the polydispersity of grafted poly(dimethylsiloxane) surfaces using single-molecule atomic force microscopy," *Journal of Physical Chemistry B*, vol. 105, pp. 3965–3971, 2001.

[6] Al-Maawali, S., Bemis, J., Akhremitchev, B., Liu, H., and Walker, G., "Single-molecule afm study of polystyrene grafted at gold surfaces," *Journal of Adhesion*, vol. 81, pp. 999–1016, 2005.

[7] Allen, M. and Tildesley, D., *Computer Simulation of Liquids*. Oxford Science Publications, 1989.

[8] Arita, T., Kanda, Y., and Higashitani, K., "In situ observation of single polymers adsorbed onto mica surfaces in water," *Journal of Colloid and Interface Science*, vol. 273, pp. 102–105, 2004.

[9] Ash, S., Everett, D., and Findenegg, G., "Multilayer theory for adsorption from solution," *Transactions of the Faraday Society*, vol. 66, pp. 708–722, 1970.

[10] Aubouy, M., "Organization of polymers at interfaces," *Physical Review E: Statistical Physics, Plasmas, Fluids, and Related Interdisciplinary Topics*, vol. 56, pp. 3370–3377, 1997.

[11] Aubouy, M., Guiselin, O., and Raphael, E., "Scaling description of polymer interfaces: Flat layers," *Macromolecules*, vol. 29, pp. 7261–7268, 1996.

[12] Avranas, A. and Iliou, P., "Interaction between hydroxypropylmethylcellulose and the anionic surfactants hexane-, octane-, and decanesulfonic acid sodium salts, as studied by dynamic surface tension measurments," *Journal of Colloid and Interface Science*, vol. 258, pp. 102–109, 2003.

[13] Backer, J., Lowe, C., Hoefsloot, H., and Iedema, P., "Combined length scales in dissipative particle dynamics," *Journal of Chemical Physics*, vol. 123, pp. 114905–1–114905–10, 2005.

[14] Baldwin, J. and Dempsey, B., "Effects of brownian motion and structured water on aggregation of charged particles," *Colloids and Surfaces A: Physicochemical and Engineering Aspects*, vol. 177, pp. 111–122, 2001.

[15] Barnett, K., Cosgrove, T., Vincent, B., Burgess, A., Crowley, T., King, T., Turner, J., and Tadros, T., "Neutron scattering, nuclear magnetic resonance, and photon correlation studies of polymers adsorbed at the solid-solution interface," *Polymer*, vol. 22, pp. 283–285, 1981.

[16] Barnett, K., Cosgrove, T., Vincent, B., Sissons, D., and Cohen Stuart, M., "The measurement of the polymer-bound fraction at the solid-liquid interface by pulsed nuclear magnetic resonance," *Macromolecules*, vol. 14, pp. 1018–1020, 1981.

[17] Bauer, D., Buchhammer, H., Fuchs, A., Jaeger, W., Killmann, E., Lunkwitz, K., Rehmet, R., and Schwarz, S., "Stability of colloidal silica, sikron and polystyrene latex influenced by the adsorption of polycations of different charge density," *Colloids and Surfaces A: Physicochemical and Engineering Aspects*, vol. 156, pp. 291–305, 1999.

[18] Bauer, D., Killmann, E., and Jaeger, W., "Adsorption of poly(diallyldimethyl-ammoniumchloride)(pdadmac)and copolymers of dadmac with n-methyl-n-vinyl-acetamide(nmva) on colloidal silica," *Progress in Colloid and Polymer Science*, vol. 109, pp. 161–169, 1998.

[19] Behl, S. and Moudgil, B. M., "Control of active sites in selective flocculation: Ii. role of site blocking agents," *Journal of Colloid and Interface Science*, vol. 161, pp. 422 – 429, 1993.

[20] Behl, S. and Moudgil, B. M., "Control of active sites in selective flocculation: Iii. mechanism of site blocking," *Journal of Colloid and Interface Science*, vol. 161, pp. 430 – 436, 1993.

[21] Behl, S., Moudgil, B., and Prakash, T., "Control of active sites in selective flocculation: I. mathematical model," *Journal of Colloid and Interface Science*, vol. 161, pp. 414 – 421, 1993.

[22] Behrens, S. H. and Grier, D. G., "The charge of glass and silica surfaces," *Journal of Chemical Physics*, vol. 115, pp. 6716–6721, 2001.

[23] Bellemans, A., "Statistical mechanics of chain molecules at an interface," *Journal of Colloid and Interface Science*, vol. 58, pp. 521–527, 1977.

[24] Bemis, J., Akhremitchev, B., and Walker, G., "Single polymer chain elongation by atomic force microscopy," *Langmuir*, vol. 15, pp. 2799–2805, 1999.

[25] Bhattacharjee, S. and Elimelech, M., "Surface element integration: A novel technique for evaluation of dlvo interaction between a particle and a flat plate," *Journal of Colloid and Interface Science*, vol. 193, pp. 273–285, 1997.

[26] Biggs, S. and Proud, A., "Forces between silica surfaces in aqueous solutions of a weak polyelectrolyte," *Langmuir*, vol. 13, pp. 7202–7210, 1997.

[27] Boek, E., Coveney, P., Lekkerkerker, H., and van der Schoot, P., "Simulating the rheology of dense colloidal suspensions using dissipative particle dynamics," *Physical Review E: Statistical Physics, Plasmas, Fluids, and Related Interdisciplinary Topics*, vol. 55, pp. 3124–3133, 1997.

[28] Bohmer, M., Evers, O., and Scheutjens, J., "Weak polyelectrolytes between two surfaces: Adsorption and stabilization," *Macromolecules*, vol. 23, pp. 2288–2301, 1990.

[29] Broseta, D., "Molecular weight and polydispersity effects at polymer-polymer interfaces," *Macromolecules*, vol. 23, pp. 132–139, 1990.

[30] Brotherson, B., Bottomley, L., Ludovice, P., and Deng, Y., "Cationic polyacrylamide conformation on mica studied by single molecule "pulling" with scanning probe microscopy," *Macromolecules*, vol. 40, pp. 4561–4567, 2007.

[31] Brotherson, B., Bottomley, L., Ludovice, P., and Deng, Y., "Observation of a single adsorbed polymers conformation on mica with scanning probe microscopy: effects of retraction rate and dwell time," in *233rd ACS National Meeting, Chicago, IL, March 25-29, 2007*, 2007.

[32] Bustamante, C., Smith, S., Liphardt, J., and Smith, D., "Single-molecule studies of dna mechanics," *Current Opinion in Structural Biology*, vol. 10, pp. 279–285, 2000.

[33] Cahn, J. and Hilliard, J., "Free energy of a nonuniform system. 1. interfacial free energy," *Journal of Chemical Physics*, vol. 28, pp. 258–267, 1958.

[34] Carnie, S. and Chan, D., "Interaction free energy between identical spherical colloidal particles: The linearized poisson-boltzmann theory," *Journal of Colloid and Interface Science*, vol. 155, pp. 297–312, 1993.

[35] Carrillo, J.-M. and Dobrynin, A., "Molecular dynamics simulations of polyelectrolyte adsorption," *Langmuir*, vol. 23, pp. 2472–2482, 2007.

[36] Carrion-Vazquez, M., Marszalek, P., Oberhauser, A., and Fernandez, J., "Atomic force microscopy captures length phenotypes in single proteins," *Proceedings of the National Academy of Science USA*, vol. 96, pp. 11288–11292, 1999.

[37] Carrion-Vazquez, M., Oberhauser, A., Fowler, S., Marszalek, P., Broedel, S., Clarke, J., and Fernandez, J., "Mechanical and chemical unfolding of a single protein: A comparison," *Proceedings of the National Academy of Science USA*, vol. 96, pp. 3694–3699, 1999.

[38] Chakraborty, A. and Adriani, P., "Glassy relaxation at polymer-solid interfaces," *Macromolecules*, vol. 25, pp. 2470–2473, 1992.

[39] Chang, S. and Chung, I., "Effect of shear flow on polymer desorption and latex dispersion stability in the presence of adsorbed polymer," *Macromolecules*, vol. 24, pp. 567–571, 1991.

[40] Chatellier, X., Senden, T., Joanny, J.-F., and Di Meglio, J.-M., "Detachment of a single polyelectrolyte chain adsorbed on a charged surface," *Eurphysics Letters*, vol. 41, pp. 303–308, 1998.

[41] Chibowski, S., Wiceniewska, M., and Opala Mazur, E., "The effect of temperature on the adsorption and conformation of polyacrylic acid macromolecules at the zro2-polymer solution interface," *Powder Technology*, vol. 141, pp. 12–19, 2004.

[42] Chowdanowski, P. and Stoll, S., "Polyelectrolyte adsorption on charged particles: Ionic concentration and particle size effects-a monte carlo approach," *Journal of Chemical Physics*, vol. 115, pp. 4951–4960, 2001.

[43] Chu, B., *Laser Light Scattering*. Academic Press, Inc., 1974.

[44] Clancy, T. and Webber, S., "Controlling adsorption of polymers at polymer-modified surfaces," *Macromolecules*, vol. 30, pp. 1340–1346, 1997.

[45] Clark, A. and Lal, M., "Monte carlo approach to the evaluation of the configurational free energy of chains," *Journal of Physics A: Mathematics and General*, vol. 11, pp. L11–L15, 1978.

[46] Clausen-Schaumann, H., Seitz, M., Krautbauer, R., and Gaub, H., "Force spectroscopy with single bio-molecules," *Current Opinion in Chemical Biology*, vol. 4, pp. 524–530, 2000.

[47] Cohen Stuart, M. A. and Tamai, H., "Dynamics of adsorbed polymers. 1. thickness relaxation of poly(vinylpyrrolidone) on glass," *Macromolecules*, vol. 21, pp. 1863–1866, 1988.

[48] Cohen Stuart, M., Fleer, G., and Scheutjens, J., "Displacement of polymers. 1. theory. segmental adsorption energy from polymer desorption in binary solvents," *Journal of Colloid and Interface Science*, vol. 97, pp. 515–525, 1984.

[49] Cohen Stuart, M., Scheutjens, J., and Fleer, G., "Polydispersity effects and the interpretation of polymer adsorption isotherms," *Journal of Polymer Science, Polymer Physics Edition*, vol. 18, pp. 559–573, 1980.

[50] Cohen Stuart, M. and Tamai, H., "Dynamics of adsorbed polymers. 2. thickness relaxation of poly(ethylene oxide) on glass as a function of segmental binding energy," *Langmuir*, vol. 4, pp. 1184–1188, 1988.

[51] Cohen Stuart, M. and Tamai, H., "A novel method to study polymer interfacial dynamics," *Colloids and Surfaces*, vol. 31, p. 265, 1988.

[52] Cohen Stuart, M., Waajen, F., Cosgrove, T., Vincent, B., and Crowley, T., "Hydrodynamic thickness of adsorbed polymer layers," *Macromolecules*, vol. 17, pp. 1825–1830, 1984.

[53] Conti, M., Bustanji, Y., Falini, G., Ferruti, P., Stefoni, S., and Samori, B., "The desorption process of macromolecules adsorbed on interfaces: the force spectroscopy approach," *ChemPhysChem*, vol. 2, pp. 610–613, 2001.

[54] Conti, M., Falini, G., and Samori, B., "How strong is the coordination bond between a histidine tag and ni-nitrilotriacetate? an experiment of mechanochemistry on single molecules," *Angewandte Chemie*, vol. 39, pp. 215–218, 2000.

[55] Cosgrove, T., "Estimates of the bound fraction of an adsorbed polymer at the solid-liquid interface. exact enumeration study of a self-avoiding walk model," *Macromolecules*, vol. 15, pp. 1290–1293, 1982.

[56] Cosgrove, T., "Polymer desorption by nmr," *Colloids and Surfaces*, vol. 31, p. 117, 1988.

[57] Cosgrove, T., "Volume-fraction profiles of adsorbed polymers," *Journal of the Chemical Society, Faraday Transactions*, vol. 86, pp. 1323–1332, 1990.

[58] Cosgrove, T., Crowley, T., Vincent, B., Barnett, K., and Tadros, T. F., "The configuration of adsorbed polymers at the solid-solution interface," *Faraday Symposia of the Chemical Society*, vol. 16, pp. 101–108, 1981.

[59] Cosgrove, T. and Fergie-Woods, J., "On the kinetics and reversibility of polymer adsorption," *Colloids and Surfaces*, vol. 25, pp. 91–99, 1987.

[60] Cosgrove, T. and Griffiths, P., "Nuclear magnetic resonance studies of adsorbed polymer layers," *Advances in Colloid and Interface Science*, vol. 42, pp. 175–204, 1992.

[61] Cosgrove, T. and Griffiths, P., "Characterisation of adsorbed polymer layers using nmr solvent diffusion studies," *Colloids and Surfaces A: Physicochemical and Engineering Aspects*, vol. 84, pp. 249–258, 1994.

[62] Cosgrove, T., Luckham, P., Richardson, R., Webster, J., and Zarbakhsh, A., "The measurement of volume fraction profiles for adsorbed polymers under compression using neutron reflectometry," *Colloids and Surfaces A: Physicochemical and Engineering Aspects*, vol. 86, pp. 103–110, 1994.

[63] Cosgrove, T., Phipps, J., Richardson, R., Hair, M., and Guzonas, D., "Surface force and neutron scattering studies on adsorbed poly(2-vinylpyridine)-b-polystyrene," *Colloids and Surfaces A: Physicochemical and Engineering Aspects*, vol. 86, pp. 91–101, 1994.

[64] Cosgrove, T. and Ryan, K., "Nmr relaxation studies on poly(ethylene oxide) terminally attached at the polystyrene/water interface," *Journal of the Chemical Society, Chemical Communications*, vol. 21, pp. 1424–1426, 1988.

[65] Cosgrove, T. and Ryan, K., "Nmr and neutron-scattering studies on poly(ethylene oxide) terminally attached at the polystyrene/water interface," *Langmuir*, vol. 6, pp. 136–142, 1990.

[66] Couture, L. and van de Ven, T., "Hydrodynamic layer thickness of poly(ethylene oxide) adsorbed on polystyrene latex," *Colloids and Surfaces*, vol. 54, pp. 245–260, 1991.

[67] Cui, S., Liu, C., Zhang, W., Zhang, X., and Wu, C., "Desorption force per polystyrene segment in water," *Macromolecules*, vol. 36, pp. 3779–3782, 2003.

[68] Dahlgren, M., Waltermo, A., Blomberg, E., Claesson, P., Sjostrom, L., Akesson, T., and Jonsson, B., "Salt effects on the interaction between adsorbed cationic polyelectrolyte layers-theory and experiment," *Journal of Physical Chemistry*, vol. 97, pp. 11769–11775, 1993.

[69] Daoulas, K. and Muller, M., "Single chain in mean field simulations: Quasi-instantaneous field approximation and quantitative comparison with monte carlo simulations," *Journal of Chemical Physics*, vol. 125, pp. 184904–1–184904–18, 2006.

[70] Daoulas, K., Muller, M., dee Pablo, J., Nealey, P., and Smith, G., "Morphology of multi-component polymer systems: Single chain in mean field simulation studies," *Soft Matter*, vol. 2, pp. 573–583, 2006.

[71] de Gennes, P.-G., *Scaling Concepts in Polymer Physics*. Cornell University Press, 1979.

[72] de Gennes, P.-G., "Polymer solutions near an interface. adsorption and depletion layers," *Macromolecules*, vol. 14, pp. 1637–1644, 1981.

[73] de Gennes, P.-G., "Polymers at an interface. 2. interaction between two plates carrying adsorbed polymer layers," *Macromolecules*, vol. 15, pp. 492–500, 1982.

[74] de Joannis, J., Park, C.-W., Thomatos, J., and Bitsanis, I., "Homopolymer physisorption: A monte carlo study," *Langmuir*, vol. 17, pp. 69–77, 2001.

[75] De Witt, J. and van de Ven, T., "The effect of neutral polymers and electrolyte on the stability of aqueous polystyrene latex," *Advances in Colloid and Interface Science*, vol. 42, pp. 41–64, 1992.

[76] Delle Site, L., Abrams, C., Alavi, A., and Kremer, K., "Polymers near metal surfaces: Selective adsorption and global conformations," *Physical Review Letters*, vol. 89, pp. 156103–1 – 156103–4, 2002.

[77] Deng, Y., Disxon, J., White, G., Loeppert, R., and Juo, A., "Bonding between polyacrylamide and smectite," *Colloids and Surfaces A: Physicochemical and Engineering Aspects*, vol. 281, pp. 82–91, 2006.

[78] Di Biasio, A., Bordi, F., and Cametti, C., "Effect of polymer adsorption on peo-coated latex particles during salt-induced aggregation," *Colloids and Surfaces A: Physicochemical and Engineering Aspects*, vol. 160, pp. 189–198, 1999.

[79] Diaz Barrios, A. and Howard, G., "Adsorption of polymers at the solution/solid interface. 15. styrene-vinylferrocene copolymers," *Makromolekulare Chemie*, vol. 182, pp. 1081–1096, 1981.

[80] Dickinson, E. and Euston, S., "Short-range structure of simulated flocs of particles with bridging polymer," *Colloids and Surfaces*, vol. 62, pp. 231–242, 1992.

[81] DiMarzio, E., "Proper accounting of conformations of a polymer near a surface," *Journal of Chemical Physics*, vol. 42, pp. 2101–2106, 1965.

[82] DiMarzio, E. and McCrackin, F., "One-dimensional model of polymer adsorption," *Journal of Chemical Physics*, vol. 43, pp. 539–547, 1965.

[83] Dobrynin, A., Deshkovski, A., and Rubinstein, M., "Adsorption of polyelectrolytes at oppositely charged surfaces," *Macromolecules*, vol. 34, pp. 3421–3436, 2001.

[84] Dorbrynin, A. and Rubinstein, M., "Theory of polyelectrolytes in solution and at surfaces," *Progress in Polymer Science*, vol. 30, pp. 1049–1118, 2005.

[85] Douglas, J., Schneider, H., Frantz, P., Lipman, R., and Granick, S., "The origin and characterization of conformational heterogeneity in adsorbed polymer layers," *Journal of Physics: Condensed Matter*, vol. 9, pp. 7699–7718, 1997.

[86] Eklund, D. and Lindstrom, T., *Paper Chemistry: An Introduction*. DT Paper Science Publications, 1991.

[87] Elaissari, A. and Pefferkorn, E., "Polyelectrolyte adsorption at solid/liquid interfaces: A simple model for the structural relaxation and excluded area effects," *Journal of Colloid and Interface Science*, vol. 143, pp. 85–91, 1991.

[88] Ermoshkin, A., Chen, J., and Lai, P.-Y., "Adsorption of a random copolymer at a lipid bilayer membrane," *Physical Review E*, vol. 66, pp. 051912–1 – 051912–6, 2002.

[89] Fleer, G., Stuart, M., Scheutjens, J., Cosgrove, T., and Vincent, B., *Polymers at Interfaces*. Chapman and Hall, 1993.

[90] Flood, C., Cosgrove, T., Howell, I., and Revell, P., "Effects of electrolytes on adsorbed polymer layers: Poly(ethylene oxide)-silica system," *Langmuir*, vol. 22, pp. 6923–6930, 2006.

[91] Flood, C., Cosgrove, T., Qiu, D., Espidel, Y., Howell, I., and Revell, P., "Influence of a surfactant and electrolytes on adsorbed polymer layers," *Langmuir*, vol. 23, pp. 2408–2413, 2007.

[92] Florin, E.-L., Moy, V., and Gaub, H., "Adhesion forces between individual ligand-receptor pairs," *Science*, vol. 264, pp. 415–417, 1994.

[93] Forsman, W. and Latshaw, B., "Conformation of polymer molecules at solid-liquid interfaces by small-angle neutron scattering," *Polymer Engineering and Science*, vol. 36, pp. 1114–1124, 1996.

[94] Frenkel, D. and Smit, B., *Understanding Molecular Simulation From Algorithms to Applications*. Academic Press, 2002.

[95] Fu, Z. and Santore, M., "Evolution of layer density and thickness during poly(thylene oxide) adsorption onto silica," *Langmuir*, vol. 13, pp. 5779–5781, 1997.

[96] Gao, S., Hahn, J., and Ho, W., "Adsorption induced hydrogen bonding by ch group," *Journal of Chemical Physics*, vol. 119, pp. 6232–6236, 2003.

[97] Garnier, L., Gauthier-Manuel, B., van der Vegte, E., Snijders, J., and Hadziioannou, G., "Covalent bond force profile and cleavage in a single polymer chain," *Journal of Chemical Physics*, vol. 113, pp. 2497–2503, 2000.

[98] Gess, J., ed., *Retention of Fines and Fillers During Papermaking*. TAPPI PRESS, 1975.

[99] Gibson, J., Zhang, K., Chen, K., Chynoweth, S., and Manke, C., "Simulation of colloid-polymer systems using dissipative particle dynamics," *Molecular Simulation*, vol. 23, pp. 1–41, 1999.

[100] Gilchrist, V., Lu, J., Staples, E., Garrett, P., and Penfold, J., "Adsorption of pentaethylene glycol monododecyl ether at the planar polymer/water interface studied by specular neutron reflection," *Langmuir*, vol. 15, pp. 250–258, 1999.

[101] Goel, T., Patra, C., Ghosh, S., and Mukherjee, T., "Structure of short polymers at interfaces: A combined simulation and theoretical study," *Journal of Chemical Physics*, vol. 121, pp. 4865–4873, 2004.

[102] Grandbois, M., Beyer, M., Rief, M., Clausen-Schaumann, H., and Gaub, H., "How strong is a covalent bond?," *Science*, vol. 283, pp. 1727–1730, 1999.

[103] Gregory, J., "Interaction of unequal double layers at constant charge," *Journal of Colloid and Interface Science*, vol. 51, pp. 44–51, 1975.

[104] Griebel, T., Kulicke, W.-M., and Hashemzadeh, A., "Characterization of water-soluble, cationic polyelectrolytes as exemplified by poly(acrylamide-co-trimethylammoniumethylethacrylate chloride) and the establishment of structure-property relationships," *Colloid and Polymer Science*, vol. 269, pp. 113–120, 1991.

[105] Grohens, Y., Carriere, P., Hamon, L., Castelein, G., Holl, Y., and Spevacek, J., "Adsorption of polymer/solvent complexes on silica surfaces," *Macromolecular Symposia*, vol. 166, pp. 59–70, 2001.

[106] Groot, R. and Warren, P., "Dissipative particle dynamics: Bridging the gap between atomistic and mesoscopic simulation," *Journal of Chemical Physics*, vol. 107, pp. 4423–4435, 1997.

[107] Haschke, H., *Force Spectroscopy and Microscopy of Single Molecules at the Solid-Liquid Interface*. PhD thesis, University of Bristol, 2003.

[108] Haschke, H., Miles, M., and Koutsos, V., "Conformation of a single polyacrylamide molecule adsorbed onto a mica surface studied with atomic force microscopy," *Macromolecules*, vol. 37, pp. 3799–3803, 2004.

[109] Haschke, H., Miles, M., and Sheppard, S., "Adsorption of individual polyacrylamide molecules studied by atomic force microscopy," *Single Molecules*, vol. 3, pp. 171–172, 2002.

[110] Hasegawa, R. and Doi, M., "Adsorption dynamics: Extension of self-consistent field theory to dynamical problems," *Macromolecules*, vol. 30, pp. 3086–3089, 1997.

[111] Hayashi, S., Abe, T., Higashi, N., Niwa, M., and Kurihara, K., "Polyelectrolyte brush layers studied by surface forces measurement: Dependence on ph and salt concentrations and scaling," *Langmuir*, vol. 18, pp. 3932–3944, 2002.

[112] Hecker, R., Fawell, P., and Jefferson, A., "The agglomeration of high molecular mass polyacrylamide in aqueous solutions," *Journal of Applied Polymer Science*, vol. 70, pp. 2241–2250, 1998.

[113] Heimenz, P. and Rajagopalan, R., *Principles of Colloid and Surface Chemistry*. Marcel Dekker Inc., 1997.

[114] Helfand, E., "Theory of inhomogeneous polymers: Lattice model for polymer-polymer interfaces," *Journal of Chemical Physics*, vol. 63, pp. 2192–2198, 1975.

[115] Helfand, E., "Theory of inhomogeneous polymers. lattice model for solution interfaces," *Mcaromolecules*, vol. 9, pp. 307–310, 1976.

[116] Hesselink, F., "Theory of stabilization of dispersions by adsorbed macromolecules. 1. statistics of the change of some configurational properties of adsorbed macromolecules on the approach of an impenetrable interface," *Journal of Physical Chemistry*, vol. 75, pp. 65–71, 1971.

[117] Higgins, J. and Benoit, H., *Polymers and Neutron Scattering*. Oxford University Press, 1994.

[118] Hoda, N. and Kumar, S., "Brownian dynamics simulations of polyelectrolyte adsorption onto charge patterned surfaces," *Langmuir*, vol. 23, pp. 1741–1751, 2007.

[119] Hoogendam, C., Peters, J., Tuinier, R., De Keizer, A., and Cohen Stuart, M., "Effective viscosity of polymer solutions: Relation to the determination of the depletion thickness and thickness of the adsorbed layer of cellulose derivatives," *Journal of Colloid and Interface Science*, vol. 207, pp. 309–316, 1998.

[120] Hoogerbrugge, P. and Koelman, J., "Simulating microscopic hydrodynamic phenomena with dissipative particle dynamics," *Europhysics Letters*, vol. 19, pp. 155–160, 1992.

[121] Hugel, T., Grosholz, M., Clausen-Shaumann, H., Pfau, A., Gaub, H., and Seitz, M., "Elasticity of single polyelectrolyte chains and their desorption from solid supports studied by afm based single molecule force spectroscopy," *Macromolecules*, vol. 34, pp. 1039–1047, 2001.

[122] Israelachvili, J., *Intermolecular and Surface Forces*. Academic Press, 1992.

[123] Israelachvili, J. and Adams, G., "Measurement of forces between two mica surfaces in aqueous electrolyte solutions in the range of 0-100nm," *Journal of the Chemical Society, Faraday Transactions 1: Physical Chemistry in Condensed Phases*, vol. 74, pp. 975–1001, 1978.

[124] Jakobsen, A., Besold, G., and Mouritsen, O., "Multiple time step update schemes for dissipative particle dynamics," *Journal of Chemical Physics*, vol. 124, pp. 094104–1–094104–6, 2006.

[125] Janshoff, A., Neitzert, M., Oberdorfer, Y., and Fuchs, H., "Force spectroscopy of molecular systems-single molecule spectroscopy of polymers and biomolecules," *Angewandte Chemie*, vol. 39, pp. 3212–3237, 2000.

[126] Jenkel, E. and Rumbach, B., "Adsorption of high polymers from solution," *Zeitschrift fuer Elektrochemie und Angewandte Physikalische Chemie*, vol. 55, pp. 612–618, 1951.

[127] Karlstrom, G., Carlsson, A., and Lindman, B., "Phase diagrams of nonionic polymer-water systems. experimental and theoretical studies of the effects of surfactants and other cosolutes," *Journal of Physical Chemistry*, vol. 94, pp. 5005–5015, 1990.

[128] Killmann, E., Sapuntzjis, P., and Maier, H., "Dynamic light scattering for characterization of latexes," *Makromolekulare Chemie, Macromolecular Symposia*, vol. 61, pp. 42–58, 1992.

[129] Kim, K. and Jo, W., "Effect of chain architecture of graft copolymer on the structure of adsorbed layer: A monte carlo simulation approach," *Polymer*, vol. 42, pp. 3205–3211, 2001.

[130] Klein, J. and Pincus, P., "Interaction between surfaces with adsorbed polymers: Poor solvents," *Macromolecules*, vol. 15, pp. 1129–1135, 1982.

[131] Klein Wolterink, J., Koopal, L., Cohen Stuart, M., and Van Riemsdijk, W., "Surface charge regulation upon polyelectrolyte adsorption, hematite, polystyrene sulfonate, surface charge regulation theoretical calculations and hematite-poly(styrene sulfonate) system," *Colloids and Surfaces A: Physicochemical Engineering Aspects*, vol. 291, pp. 13–23, 2006.

[132] Kong, Y., Manke, C., Madden, W., and Schlijper, A., "Simulation of a confined polymer in solution using the dissipative particle dynamics method," *International Journal of Thermophysics*, vol. 15, pp. 1093–1101, 1994.

[133] Krishantha, D. M. M., Rajapakse, R. M. G., Tennakoon, D. T. B., and Dias, H. V. R., "Ac impedance analysis of polyaniline-montmorillonite nanocomposites," *Ionics*, vol. 12, pp. 287–294, 2006.

[134] Kumaki, J. and Hashimoto, T., "Conformational change in an isolated single synthetic polymer chain on a mica surface observed by atomic force microscopy," *Journal of the American Chemical Society*, vol. 125, pp. 4907–4917, 2003.

[135] Kumaki, J., Nishikawa, Y., and Hashimoto, T., "Visualization of single-chain conformations of a synthetic polymer with atomic force microscopy," *Journal of the American Chemical Society*, vol. 118, pp. 3321–3322, 1996.

[136] Lapcik, L., Alince, B., and van de Ven, T., "Effect of poly(ethylene oxide) on the stability and flocculation of clay dispersions," *Journal of Pulp and Paper Science*, vol. 21, pp. 19–24, 1995.

[137] Lauw, Y., Leermakers, F., and Cohen Stuart, M., "Persistence length of wormlike micelles composed of ionic surfactants: Self-consistent-field predictions," *Journal of Physical Chemistry B*, vol. 111, pp. 8158–8168, 2007.

[138] Lax, M., "Configuratio of an adsorbed polymer molecule: Solvent effect," *Journal of Chemical Physics*, vol. 60, pp. 1931–1936, 1974.

[139] Lax, M., "A direct enumeration study of self-avoiding walks terminally attached to a surface," *Macromolecules*, vol. 7, pp. 660–666, 1974.

[140] Lax, M., "Numerical study of the statistical thermodynamic properties of a surface-interacting polymer chain," *Journal of Chemical Physics*, vol. 61, pp. 4133–4137, 1974.

[141] Lee, G., Chrisey, L., and Colton, R., "Direct measurement of the forces between complementary strands of dna," *Science*, vol. 266, pp. 771–773, 1994.

[142] Lee, G., Kidwell, D., and Colton, R., "Sensing discrete strptavidin-biotin interactions with atomic force microscopy," *Langmuir*, vol. 10, pp. 354–357, 1994.

[143] Leermakers, F., Ballauff, M., and Borisov, O., "On the mechanism of uptake of globular proteins by polyelectrolyte brushes: A two-gradient self-consistent field analysis," *Langmuir*, vol. 23, pp. 3937–3946, 2007.

[144] Levy, R. and Maaloum, M., "Probing adsorbed polymer chains using atomic force microscopy: Interpretation of rupture distributions," *Journal of Physics: Condensed Matter*, vol. 16, pp. 7199–7208, 2004.

[145] Levy, R. and Maaloum, M., "New tools for force spectroscopy," *Ultramicroscopy*, vol. 102, pp. 311–315, 2005.

[146] Li, H., Liu, B., Zhang, X., Gao, C., Shen, J., and Zou, G., "Single-molecule force spectroscopy on poly(acrylic acid) by afm," *Langmuir*, vol. 15, pp. 2120–2124, 1999.

[147] Li, H., Rief, M., Oesterhelt, F., and Gaub, H., "Single-molecule force spectroscopy on xanthan by afm," *Advanced Materials*, vol. 3, pp. 316–319, 1998.

[148] Li, H., Rief, M., Oesterhelt, F., and Gaub, H., "Force spectroscopy on single xanthan molecules," *Applied Physics A: Materials Science and Processing*, vol. 68, pp. 407–410, 1999.

[149] Li, H., Rief, M., Oesterhelt, F., Gaub, H., Zhang, X., and Shen, J., "Single-molecule force spectroscopy on polysaccharides by afm- nanomechnaical fingerprint of alpha-(1,4)-linked polysaccharides," *Chemical Physics Letters*, vol. 305, pp. 197–201, 1999.

[150] Li, H., Zhang, W., Xu, W., and Zhang, X., "Hydrogen bonding governs the elastic properties of poly(vinyl alcohol) in water: Single-molecule force spectroscopic studies of pva by afm," *Macromolecules*, vol. 33, pp. 465–469, 2000.

[151] Li, H., Zhang, W., Zhang, X., Shen, J., Liu, B., Gao, C., and Zou, G., "Single molecule force spectroscopy on poly(vinyl alcohol) by atomic force microscopy," *Macromolecular Rapid Communications*, vol. 19, pp. 609–611, 1998.

[152] Li, S. and Zhang, L., "Conformational structures and thermodynamic properties of compact polymer chains confined between two parallel plane boundaries," *Journal of Polymer Science: Part B: Polymer Physics*, vol. 44, pp. 2888–2901, 2006.

[153] Li, Y., Nagy, E., Esmail, M., and Horvolgyi, Z., "Weak flocculation of aqueous kaolin suspensions initiating by nacmc with different molecular weights," *Macromolecular Symposia*, vol. 202, pp. 307–323, 2003.

[154] Lide, D., ed., *CRC Handbook of Chemistry and Physics*. CRC Press, 1994.

[155] Linse, P., "Adsorption of weakly charged polyelectrolytes at oppositely charged surfaces," *Macromolecules*, vol. 29, pp. 326–336, 1996.

[156] Lipatov, Y. S. and Sergeeva, L. M., *Adsorption of Polymers*. Halsted, 1974.

[157] Lisal, M. and Nezbeda, I., "Conformations of attractive, repulsive, and amphiphilic polymer chains in a simple supercritical solvent: Molecular simulation study," *Journal of Chemical Physics*, vol. 119, pp. 4026–4034, 2003.

[158] Liu, H. and Chakrabarti, A., "Molecular dynamics study of adsorption and spreading of a polymer chain onto a flat surface," *Polymer*, vol. 40, pp. 7285–7293, 1999.

[159] Liufu, S.-C., Xiao, H.-N., and Li, Y.-P., "Adsorption of cationic polyelectrolyte at the solid/liquid interface and dispersion of nanosized silica in water," *Journal of Colloid and Interface Science*, vol. 285, pp. 33–40, 2005.

[160] Mackor, E. and van der Waals, J., "The statistics of the adsorption of rod-shaped molecules in connection with the stability of certain colloidal dispersions," *Journal of Colloid Science*, vol. 7, pp. 535–550, 1952.

[161] Malfreyt, P. and Tildesley, D., "Dissipative particle dynamics simulations of grafted polymer chains between two walls," *Langmuir*, vol. 16, pp. 4732–4740, 2000.

[162] Mao, Y., Burin, A., Ratner, M. A., and Jarrold, M., "A first-order transition in the charge-induced conformational changes of polymers," *Journal of Chemical Physics*, vol. 116, pp. 9964–9974, 2002.

[163] Masters, A. and Warren, P., "Kinetic theory for dissipative particle dynamics: The importance of collisions," *Europhysics Letters*, vol. 48, pp. 1–7, 1999.

[164] Mathur, S., Singh, P., and Moudgil, B., "Advances in selective flocculation technology for solid-solid separations," *International Journal of Mineral Processing*, vol. 58, pp. 201–222, 2000.

[165] Mavrantzas, V., Beris, A., Leermakers, F., and Fleer, G., "Continuum formulation of the scheutjens-fleer lattice statistical theory for homopolymer adsorption from solution," *Journal of Chemical Physics*, vol. 123, pp. 174901–1–174901–11, 2005.

[166] Meadows, J., Williams, P., Garvey, M., Harrop, R., and Phillips, G., "Enhanced polyelectrolyte adsorption," *Colloids and Surfaces*, vol. 32, pp. 275–288, 1988.

[167] Mears, S., Cosgrove, T., Obey, T., Thompson, L., and Howell, I., "Dynamic light scattering and small-angle neutron scattering studies on the poly(ethylene oxide)/sodium dodecyl sulfate/plystyrene latex system," *Langmuir*, vol. 14, pp. 4997–5003, 1998.

[168] Mears, S., Cosgrove, T., Thompson, L., and Howell, I., "Solvent relaxation nmr measurements on polymer, particle, surfactant systems," *Langmuir*, vol. 14, pp. 997–1001, 1998.

[169] Min, G., Bevan, M., Prieve, D., and Patterson, G., "Light scattering characterization of polystyrene latex with and without adsorbed polymer," *Colloids and Surfaces A: Physicochemical and Engineering Aspects*, vol. 202, pp. 9–21, 2002.

[170] Minko, S. and Roiter, Y., "Afm single molecule studies of adsorbed polyelectrolytes," *Current Opinion in Colloid and Interface Science*, vol. 10, pp. 9–15, 2005.

[171] Mishra, P., Kumar, S., and Singh, Y., "Force-induced desorption of a linear polymer chain adsorbed on an attractive surface," *Europhysics Letters*, vol. 69, pp. 102–108, 2005.

[172] Miyamoto, T. and Cantow, H., "Nuclear magnetic resonance study on the adsorption of poly(methyl methacrylate) at a solid/liquid interface," *Makromolekulare Chemie*, vol. 162, pp. 43–51, 1972.

[173] Moudgil, B., Mathur, S., and Behl, S., "Dolomite-dolomite separation by a selective flocculation technique," *Transactions of Scoiety for Mining, Metallurgy, and Exploration, Inc.*, vol. 298, pp. 24–27, 1996.

[174] Moudgil, B. and Prakash, T., "Competitive adsorption of polymer surfactants on solid substrates," *Colloids and Surfaces A: Physicochemical and Engineering Aspects*, vol. 133, pp. 93–97, 1998.

[175] Nanko, H. and Pan, S., "Visualization of polymer adsorption on pulp fiber 1: Polyacrylamide," 2003.

[176] Nanko, H. and Pan, S., "Visualization of polymer adsorption on pulp fiber 1: Polyacrylamide, part 2," 2003.

[177] Nanko, H., Pan, S., and McNeal, M., "Polymer adsorption on cellulose substrate visualized by transmission electron microscopy," 2003.

[178] Neimo, L., ed., *Papermaking Chemistry*. Fapet Oy, 1999.

[179] Nelson, A. and Cosgrove, T., "Dynamic light scattering studies of poly(ethylene oxide) adsorbed on laponite: Layer conformation and its effect on particle stability," *Langmuir*, vol. 20, pp. 10382–10388, 2004.

[180] Nelson, A., Jack, K., Cosgrove, T., and Kozak, D., "Nmr solvent relaxation in studies of multicomponent polymer adsorption," *Langmuir*, vol. 18, pp. 2750–2755, 2002.

[181] Nicolai, T., Clarke, C., Jones, R., and Penfold, J., "Segment density profiles of end-adsorbed polymers in chemically identical melts," *Colloids and Surfaces, A: Physicochemical and Engineering Aspects*, vol. 86, pp. 153–163, 1994.

[182] Nikunen, P., Vattulainen, I., and Karttunen, M., "Reptational dynamics in dissipative particle dynamics simulations of polymer melts," *Physical Review E*, vol. 75, pp. 036713–1–036713–7, 2007.

[183] Noskov, B., Akentiev, A., Bilibin, A., Grigoriev, D., Loglio, G., Zorin, I., and Miller, R., "Adsorption kinetics of non-ionic polymers: An ellipsometric study," *Mendeleev Communications*, vol. 5, pp. 198–200, 2005.

[184] Oberhauser, A., Marszalek, P., Carrion-Vazquez, M., and Fernandez, J., "Single protein misfolding events captured by atomic force microscopy," *Nature Structural Biology*, vol. 6, pp. 1025–1028, 1999.

[185] Omarjee, P., Hoerner, P., Riess, G., Cabuil, V., and Mondain-Monval, O., "Diblock copolymers adsorbed at a water-oil interface," *European Physical Journal E: Soft Matter*, vol. 4, pp. 45–50, 2001.

[186] Ono, H. and Deng, Y., "Cationic microparticle retention aids: The mechanism study and laboratory evaluation," in *Transactions of the 11th Fundamental Research Symposium in The Fundamentals of Papermaking Materials Held at Cambridge: September 1997*, pp. 1097 – 1119, 1997.

[187] Ortiz, C. and Hadziioannou, G., "Entropic elasticity of single polymer chains of poly(methacrylic acid) measured by atomic force microscopy," *Macromolecules*, vol. 32, pp. 780–787, 1999.

[188] O'Shaughnessy, B. and Vavylonis, D., *Theoretical and Mathematical Models in Polymer Science*. Academic, 1998.

[189] O'Shaughnessy, B. and Vavylonis, D., "Kinetic regimes and cross-over times in many-particle reacting systems," *Europhysics Letters*, vol. 45, pp. 653–658, 1999.

[190] O'Shaughnessy, B. and Vavylonis, D., "Reactive polymer interfaces: How reaction kinetics depend on reactivity and density of chemical groups," *Macromolecules*, vol. 32, pp. 1785–1796, 1999.

[191] O'Shaughnessy, B. and Vavylonis, D., "Irreversible adsorption from dilute polymer solutions," *European Physical Journal E*, vol. 11, pp. 213–230, 2003.

[192] O'Shaughnessy, B. and Vavylonis, D., "Non-equilibrium in adsorbed polymer layers," *Journal of Physics: Condensed Matter*, vol. 17, pp. R63–R99, 2005.

[193] Oulanti, O., Pefferkorn, E., Champ, S., and Auweter, H., "Relaxation phenomena of hydrolyzed polyvinylamine molecules adsorbed at the silica/water interface i. saturated homogeneous polymer layers," *Journal of Colloid and Interface Science*, vol. 291, pp. 98–104, 2005.

[194] Oulanti, O., Pefferkorn, E., Champ, S., and Auweter, H., "Relaxation phenomena of hydrolyzed polyvinylamine molecules adsorbed at the silica/water interface ii. saturated heterogeneous polymer layers," *Journal of Colloid and Interface Science*, vol. 291, pp. 105–111, 2005.

[195] Oulanti, O., Pefferkorn, E., Champ, S., and Auweter, H., "Relaxation phenomena of hydrolyzed polyvinylamine molecules adsorbed at the silica/water interface iii. interfacial exchange and transfer processes," *Journal of Colloid and Interface Science*, vol. 291, pp. 112–119, 2005.

[196] Oulanti, O., Widmaier, J., Pefferkorn, E., Champ, S., and Auweter, H., "Destabilization of polystyrene latex particles induced by adsorption of polyvinylamine: Mass, size and structure characteristics of the growing aggregates," *Journal of Colloid and Interface Science*, vol. 294, pp. 95–103, 2006.

[197] Pashley, R., "Hydration forces between mica surfaces in aqueous electrolyte solutions," *Journal of Colloid and Interface Science*, vol. 80, pp. 153–162, 1981.

[198] Pecora, R., "Dynamic light scattering measurement of nanometer particles in liquids," *Journal of Nanoparticle Research*, vol. 2, pp. 123–131, 2000.

[199] Pefferkorn, E. and Elaissari, A., "Adsorption-desorption processes in charged polymer/colloid systems; structural relaxation of adsorbed macromolecules," *Journal of Colloid and Interface Science*, vol. 138, pp. 187–194, 1990.

[200] Pelssers, E., Cohen Stuart, M., and Fleer, G., "Kinetic aspects of polymer bridging: Equilibrium flocculation and nonequilibrium flocculation," *Colloids and Surfaces*, vol. 38, pp. 15–25, 1989.

[201] Pelssers, E., Cohen Stuart, M., and Fleer, G., "Kinetics of bridging flocculation," *Journal of the Chemical Society Faraday Transactions*, vol. 86, pp. 1355–1361, 1990.

[202] Pelton, R., "Electrolyte effects in the adsorption and desorption of a cationic polyacrylamide on cellulose fibers," *Journal of Colloid and Interface Science*, vol. 111, pp. 475–485, 1986.

[203] Perkins, T., Smith, D., Larson, R., and Chu, S., "Stretching of a single tethered polymer in a uniform flow," *Science*, vol. 268, pp. 83–87, 1995.

[204] Peters, E. and Barenbrug, T., "Efficient brownian dynamics simulation of particles near walls: Ii. sticky walls," *Physical Review E*, vol. 66, pp. 056702–1 – 056702–11, 2002.

[205] Pivkin, I. and Karniadakis, G., "Coarse-graining limist in open and wall-bounded dissipative particle dynamics systems," *Journal of Chemical Physics*, vol. 124, pp. 184101–1–184101–7, 2006.

[206] Poggi, M., McFarland, A., Colton, J., and Bottomley, L., "A method for calculating the spring constant of atomic force microscopy cantilevers with a nonrectangular cross section," *Analytical Chemistry*, vol. 77, pp. 1192–1195, 2005.

[207] Polverari, M. and van de Ven, T., "Dynamic light scattering of suspensions of peo-coated latex particles," *Colloids and Surfaces, A: Physicochemical and Engineering Aspects*, vol. 86, pp. 209–228, 1994.

[208] Polverari, M. and van de Ven, T., "Electrostatic and steric interactions in particle deposition studied by evanescent wave light scattering," *Journal of Colloid and Interface Science*, vol. 173, pp. 343–353, 1995.

[209] Poncet, C., Tiberg, F., and Audebert, R., "Ellipsometric study of the adsorption of hydrophobically modified polyacrylates at hydrophobic surfaces," *Langmuir*, vol. 14, pp. 1697–1704, 1998.

[210] Premilat, S. and Hermans Jr., J., "Conformational statistics of short chains of poly(l-alanine) and poly(glycine) generated by monte carlo method and the partition function of chains with constrained ends," *Journal of Chemical Physics*, vol. 59, pp. 2602–2612, 1973.

[211] Radeva, T., Netzel, J., Petkanchin, I., and Stoylov, S., "Electrooptic study of neutral polymer adsorption on mica," *Journal of Colloid and Interface Science*, vol. 160, pp. 493–495, 1993.

[212] Radoslovich, E., "The structure of muscovite, kal2(si3al)o10(oh)2," *Acta Crystallographica*, vol. 13, pp. 919–932, 1960.

[213] Raucci, R. and Vacatello, M., "Monte carlo studies of the conformational statistics of polymers. polyethylene," *Makromolekulare Chemie, Theory and Simulations*, vol. 2, pp. 875–888, 1993.

[214] Ravi, M. and Hopfinger, A., "Molecular modeling of polymers. 10. characterization of conformational transitions of poly(acrylic acid) and poly(methacrylic acid) using dyad structures," *Journal of Polymer Science, Part B: Polymer Physics*, vol. 32, pp. 1033–1047, 1994.

[215] Ray, C., Brown, J., and Akhremitchev, B., "Correction of systematic errors in single-molecule force spectroscopy with polymeric tethers by atomic force microscopy," *Journal of Physical Chemistry B*, vol. 111, pp. 1963–1974, 2007.

[216] Rehmet, R. and Killmann, E., "Adsorption of cationic poly(diallyl-dimethyl-ammoniumchloride), poly(diallyl-dimethyl-ammoniumchloride-co-n-methyl-n-vinylactamide) and poly(n-methyl-n-vinyl-acetamide) on polystyrene latex," *Colloids and Surfaces A: Physicochemical and Engineering Aspects*, vol. 149, pp. 323–328, 1999.

[217] Rennie, A., Crawford, R., Lee, E., Thomas, R., Crowley, T., Roberts, S., Qureshi, M., and Richards, R., "Adsorption of poly(ethylene oxide) at the air-solution interface studied by neutron reflection," *Macromolecules*, vol. 22, pp. 3466–3475, 1989.

[218] Revenga, M., Zuniga, I., and Espanol, P., "Boundary conditions in dissipative particle dynamics," *Computer Physics Communications*, vol. 121-122, pp. 309–311, 1999.

[219] Richmond, P., "Electrical force between particles with arbitrary fixed surface charge distributions in ionic solution," *Journal of the Chemical Society, Faraday Transactions 2: Molecular and Chemical Physics*, vol. 70, pp. 1066–1073, 1974.

[220] Rief, M., Clausen-Schaumann, H., and Gaub, H., "Sequence-dependent mechanics of single dna molecules," *Nature Structural Biology*, vol. 6, pp. 346–349, 1999.

[221] Rief, M., Gautel, M., Oesterhelt, F., Fernandez, J., and Gaub, H., "Reversible unfolding of individual titin immunoglobulin domains by afm," *Science*, vol. 276, pp. 1109–1112, 1997.

[222] Ringenbach, E., Chauveteau, G., and Pefferkorn, E., "Aggregation/fragmentation of colloidal alumina," *Journal of Colloid and Interface Science*, vol. 172, pp. 208–213, 1995.

[223] Roe, R., "Conformation of an isolated polymer molecule at an interface," *Proceedings of the National Academy of Sciences of the United States of America*, vol. 53, pp. 50–57, 1965.

[224] Roiter, Y., Jaeger, W., and Minko, S., "Conformation of single polyelectrolyte chains vs. salt concentration: Effects of sample history and solid substrate," *Polymer*, vol. 47, pp. 2493–2498, 2006.

[225] Roiter, Y. and Minko, S., "Afm single molecule experiments at the solid-liquid interface: In situ conformation of adsorbed flexible polyelectrolyte chains," *Journal of the American Chemical Society*, vol. 127, pp. 15688–15689, 2005.

[226] Roiter, Y. and Minko, S., "Adsorption of polyelectrolyte versus surface charge: In situ single-molecule atomic force microscopy experiments on similarly, oppositely, and heterogeneously charged surfaces," *Journal of Physical Chemistry B*, vol. 111, pp. 8597–8604, 2007.

[227] Rojas, O., Claesson, P., Muller, D., and Neuman, R., "The effect of salt concentration on adsorption of low-charge-density polyelectrolytes and interactions between polyelectrolyte-coated surfaces," *Journal of Colloid and Interface Science*, vol. 205, pp. 77–88, 1998.

[228] Sader, J., Chon, J., and Mulvaney, P., "Calibration of rectangular atomic force microscope cantilevers," *Review of Scientific Instruments*, vol. 70, pp. 3967–3969, 1999.

[229] Samoshina, Y., Diaz, A., Becker, Y., Nylander, T., and Lindman, B., "Adsorption of cationic, anionic, and hydrophobically modified polyacrylamides on silica surfaces," *Colloids and Surfaces, A: Physicochemical and Engineering Aspects*, vol. 231, pp. 195–205, 2003.

[230] Samoshina, Y., Nylander, T., Shubin, V., Bauer, R., and Eskilsson, K., "Equilibrium aspects of polycation adsorption on silica surface: How the adsorbed layer responds to changes in bulk solution," *Langmuir*, vol. 21, pp. 5872–5881, 2005.

[231] Santore, M. and Fu, Z., "Direct measurement of molecular-weight driven competition during polymer adsorption," *Macromolecules*, vol. 30, pp. 8515–8516, 1997.

[232] Scheutjens, J. and Fleer, G., "Statistical theory of the adsorption of interacting chain molecules. 1. partition function, segment density distribution, and adsorption isotherms," *Journal of Physical Chemistry*, vol. 83, pp. 1619–1635, 1979.

[233] Scheutjens, J. and Fleer, G., "Statistical theory of the adsorption of interacting chain molecules. 2. train, loop, and tail size distribution," *Journal of Physical Chemistry*, vol. 84, pp. 179–190, 1980.

[234] Scheutjens, J., Fleer, G., and Cohen Stuart, M., "End effects in polymer adsorption: A tale of tails," *Colloids and Surfaces*, vol. 21, pp. 285–306, 1986.

[235] Schlijper, A., Hoogerbrugge, P., and Manke, C., "Computer simulation of dilute polymer solutions with the dissipative particle dynamics method," *Journal of Rheology*, vol. 39, pp. 567–579, 1995.

[236] Schneider, H., Frantz, P., and Granick, S., "The bimodal energy landscape when polymers adsorb," *Langmuir*, vol. 12, pp. 994–996, 1996.

[237] Scott, W., *Principles of Wet End Chemistry*. TAPPI Press, 1996.

[238] Seitz, W. and Klein, D., "Excluded volume effects for branched polymers: Monte carlo results," *Journal of Chemical Physics*, vol. 75, pp. 5190–5193, 1981.

[239] Senden, T., "Force microscopy and surface interactions," *Current Opinion in Colloid and Interface Science*, vol. 6, pp. 95–101, 2001.

[240] Senden, T., di Meglio, J.-M., and Auroy, P., "Anomalous adhesion in adsorbed polymer layers," *The European Physical Journal B*, vol. 3, pp. 211–216, 1998.

[241] Senden, T., di Meglio, J.-M., and Silberzan, I., "The conformation of adsorbed polyacrylamide and derived polymers," *Comptes Rendus de l'Academie des Sciences, Serie IV: Physique, Astrophysique*, vol. 1, pp. 1143–1152, 2000.

[242] Sennerfors, T., Solberg, D., and Tiberg, F., "Adsorption of polyelectrolyte-nanoparticle systems on silica: Influence of ionic strength," *Journal of Colloid and Interface Science*, vol. 254, pp. 222–226, 2002.

[243] Shafir, A. and Andelman, D., "Polyelectrolyte adsorption: Chemical and electrostatic interactions," *Physical Review E*, vol. 70, pp. 061804–1–061804–12, 2004.

[244] Shubin, V., "Adsorption of cationic polyacrylamide onto monodisperse colloidal silica from aqueous electrolyte solutions," *Journal of Colloid and Interface Science*, vol. 191, pp. 372–377, 1997.

[245] Shubin, V. and Linse, P., "Effect of electrolytes on adsorption of cationic polyacrylamide on silica: ellipsometric study and theoretical modeling," *Journal of Physical Chemistry*, vol. 99, pp. 1285–1291, 1995.

[246] Singh, Y., Giri, D., and Kumar, S., "Crossover of a polymer chain from bulk to surface states," *Journal of Physics A: Mathematical and General*, vol. 34, pp. L67–L74, 2001.

[247] Siqueira, L. and Ribeiro, M., "Molecular dynamics simulation of the polymer electrolyte poly(ethylene oxide)/liclo4: I. structural properties," *Journal of Chemical Physics*, vol. 122, pp. 194911/1–194911/8, 2005.

[248] Sperling, L., *Introduction to Physical Polymer Science*. Wiley-Interscience, 2001.

[249] Sprakel, J., Besseling, N., Leermakers, F., and Cohen Stuart, M., "Micellization of telechelic associative polymers: Self-consistent field modeling and comparison with scaling concepts," *Journal of Physical Chemistry B*, vol. 111, pp. 2903–2909, 2007.

[250] Stemme, S., Odberg, L., and Malmsten, M., "Effect of colloidal silica and electrolyte on the structure of an adsorbed cationic polyelectrolyte layer," *Colloids and Surfaces, A: Physicochemical and Engineering Aspects*, vol. 155, pp. 145–154, 1999.

[251] Stemme, S. and Odberg, L., "Layer thickness for high molecular weight cationic polyacrylamides adsorbed on a surface with a preadsorbed polydiallyldimethylammonium chloride," *Colloids and Surfaces A: Physicochemical and Engineering Aspects*, vol. 157, pp. 307–313, 1999.

[252] Stromberg, R., Tutas, D., and Passaglia, E., "Conformation of polystyrene adsorbed at the theta-temperature," *Journal of Physical Chemistry*, vol. 69, pp. 3955–3963, 1965.

[253] Strunz, T., Oroszlan, K., Schafer, R., and Guntherodt, H.-J., "Dynamic force spectroscopy of single dna molecules," *Proceeding of the National Academy of Science USA*, vol. 96, pp. 11277–11282, 1999.

[254] Sukhishvili, S. and Granick, S., "Polyelectrolyte adsorption onto an initially-bare solid surface of opposite electrical charge," *Journal of Chemical Physics*, vol. 109, pp. 6861–6868, 1998.

[255] Swerin, A. and Odberg, L., "Some aspects of retention aids," in *Transactions of the 11th Fundamental Research Symposium in The Fundamentals of Papermaking Materials Held at Cambridge: September 1997*, pp. 265–350, 1997.

[256] Swerin, A., Odberg, L., and Wagberg, L., "An extended model for the estimation of flocculation efficiency factors in multicomponent flocculant

systems," *Colloids and Surfaces A: Physicochemical and Engineering Aspects*, vol. 113, pp. 25–38, 1996.

[257] Swerin, A., Sjodin, U., and Odberg, L., "Flocculation of cellulosic fiber suspensions by model microparticulate retention aid systems. effect of polymer charge density and type of microparticle," *Nordic Pulp and Paper Research Journal*, vol. 8, pp. 389–398, 1993.

[258] Symeonidis, V., Karniadakis, G., and Caswell, B., "Dissipative particle dynamics simulations of polymer chains: Scaling laws and shearing response compared to dna experiments," *Physical Review Letters*, vol. 95, pp. 076001–1–076001–4, 2005.

[259] Takahashi, A., Kawaguchi, M., and Kato, T., "Ellipsometric study of adsorption of polyelectrolyte onto a metal surface," *ACS Symposium Series*, vol. 240, pp. 39–52, 1984.

[260] Tanaka, H., "Copolymerization of cationic monomers with acrylamide in an aqueous solution," *Journal of Polymer Science: Polymer Chemistry Edition*, vol. 24, pp. 29–36, 1986.

[261] Taunton, H., Toprakcioglu, C., Fetters, L., and Klein, J., "Forces between surfaces bearing terminally anchored polymer chains in good solvents," *Nature*, vol. 332, pp. 712–714, 1988.

[262] Taunton, H., Toprakcioglu, C., Fetters, L., and Klein, J., "Interactions between surfaces bearing end-adsorbed chains in a good solvent," *Macromolecules*, vol. 23, pp. 571–580, 1990.

[263] Taunton, H., Toprakcioglu, C., and Klein, J., "Direct measurement of the interaction between mica surfaces with adsorbed diblock copolymer in a good solvent," *Macromolecules*, vol. 21, pp. 3333–3336, 1988.

[264] ter Horst, J., Wong Fong Sang, K., de Vreugd, C., Geertman, R., Witkamp, G., and van Rosmalen, G., "Adsorption behaviour of polyelectrolytes on calcium fluoride part ii: Molecular modeling of the adsorption behaviour," *Colloids and Surfaces A: Physicochemical and Engineering Aspects*, vol. 154, pp. 273–284, 1999.

[265] Torrie, G., Middlemiss, K., Bly, S., and Whittington, S., "Self-avoiding walks interacting with an interface," *Journal of Chemical Physics*, vol. 65, pp. 1867–1871, 1976.

[266] van de Steeg, H., Cohen Stuart, M., De Keizer, A., and Bijsterbosch, B., "Polyelectrolyte adsorption: A subtle balance of forces," *Langmuir*, vol. 8, pp. 2538–2546, 1992.

[267] van de Ven, T., "Filler and fines retention in papermaking," in *Transactions of the 13th Fundamental Research Symposium in The Fundamentals of Papermaking Materials Held at Cambridge: September 2005*, pp. 1193–1224, 2005.

[268] van der Beek, G. and Cohen Stuart, M., "The hydrodynamic thickness of adsorbed polymer layers measured by dynamic light scattering: Effects of polymer concentration and segmental binding strength," *Journal de Physique*, vol. 49, pp. 1449–1454, 1988.

[269] van der Beek, G., Cohen Stuart, M., and Cosgrove, T., "Polymer adsorption and desorption studies via h nmr relaxation of the solvent," *Langmuir*, vol. 7, pp. 327–334, 1991.

[270] van der Beek, G., Cohen Stuart, M., Fleer, G., and Hofman, J., "A chromatographic method for the determination of segmental adsorption energies of polymers. polystyrene on silica," *Langmuir*, vol. 5, pp. 1180–1186, 1989.

[271] van der Beek, G., Cohen Stuart, M., Fleer, G., and Hofman, J., "Segmental adsorption energies for polymers on silica and alumina," *Macromolecules*, vol. 24, pp. 6600–6611, 1991.

[272] van Dyck J. van Landuyt G. van Tendeloo, S. A. D., ed., *Electron Microscopy: Principles and Fundamentals*. VCH, 1997.

[273] van Eijk, M. and Cohen Stuart, M., "Polymer adsorption kinetics: Effects of supply rate," *Langmuir*, vol. 13, pp. 5447–5450, 1997.

[274] van Eijk, M., Cohen Stuart, M., Rovillard, S., and DeConinck, J., "Adsorption and spreading of polymers at plane interfaces; theory and molecular dynamics simulations," *The European Physical Journal B*, vol. 1, pp. 233–244, 1998.

[275] Wagberg, L. and Eriksson, J., "New equipment for detection of polymer induced flocculation of cellulosic fibres by using image analysis-application to microparticle systems," *Chemical Engineering Journal*, vol. 80, pp. 51–63, 2000.

[276] Walldal, C. and Wall, S., "Coil-to-globule-type transition of poly(n-isopropylacrylamide) adsorbed on colloidal silica particles," *Colloid and Polymer Science*, vol. 278, pp. 936–945, 2000.

[277] Walter, H., Harrats, C., Muller-Buschbaum, P., Jerome, R., and Stamm, M., "Adsorption of ampholytic diblock copolymers from dilute aqueous solution at the solid/liquid interface," *Langmuir*, vol. 15, pp. 1260–1267, 1999.

[278] Wang, C., Shi, W., Zhang, W., and Zhang, X., "Force spectroscopy study on poly(acrylamide) derivatives: Effects of substitutes and buffers on single-chain elasticity," *Nano Letters*, vol. 2, pp. 1169–1172, 2002.

[279] Wang, T. and Audebert, R., "Adsorption of cationic copolymers of acrylamide at the silica-water interface: Hydrodynamic layer thickness measurements," *Journal of Colloid and Interface Science*, vol. 121, pp. 32–41, 1988.

[280] Wang, Y. and Rajagopalan, R., "Dynamic properties of homopolymer layers adsorbed on a solid surface," *Journal of Chemical Physics*, vol. 105, pp. 696–705, 1996.

[281] Wang, Y., Rajagopalan, R., and Mattice, W., "Kinetics of detachment of homopolymers from a solid surface," *Physical Review Letters*, vol. 74, pp. 2503–2506, 1995.

[282] Wang, Z., Luo, M., and Xu, J., "Conformational entropy of self-avoiding polymer chains," *European Polymer Journal*, vol. 35, pp. 973–975, 1999.

[283] Weber, T. and Helfand, E., "Theory of inhomogeneous polymers. solutions for the interfaces of the lattice model," *Macromolecules*, vol. 9, pp. 311–316, 1976.

[284] Widmaier, J., Shulga, A., Pefferkorn, E., Champ, S., and Auweter, H., "Reconformation of polyvinylamine adsorbed on glass fibers," *Journal of Colloid and Interface Science*, vol. 264, pp. 277–283, 2003.

[285] Wind, B. and Killmann, E., "Adsorption of polyethylene oxide on surface modified silica-stability of bare and covered particles in suspension," *Colloid and Polymer Science*, vol. 276, pp. 903–912, 1998.

[286] Wu, C. and Gao, J., "A simple scaling of the density profile of long linear polymer chains adsorbed on a hydrophobic surface," *Macromolecules*, vol. 32, pp. 1704–1705, 1999.

[287] Xu, Q., Zhang, W., and Zhang, X., "Oxygen bridge inhibits conformational transition of 1,4-linked alpha-d-galactose detected by single-molecule atomic force microscopy," *Macromolecules*, vol. 35, pp. 871–876, 2002.

[288] Yamamoto, S., Tsujii, Y., and Fukuda, T., "Atomic force microscopic study of stretching a single polymer chain in a polymer brush," *Macromolecules*, vol. 33, pp. 5995–5998, 2000.

[289] Yang, S., Yan, D., and Shi, A., "Structure of adsorbed polymers on a colloid particle," *Macromolecules*, vol. 39, pp. 4168–4174, 2006.

[290] Yu, K.-Q., Li, Z.-S., and Sun, J., "Polymer structures and glass transition: A molecular dynamics simulation study," *Macromolecular Theory and Simulations*, vol. 10, pp. 624–633, 2001.

[291] Zhang, L., Wang, X., Ma, H., and Huang, Y., "Conformational behavior of short adsorbed polymer chains," *European Polymer Journal*, vol. 35, pp. 167–172, 1999.

[292] Zhang, R., Liu, C., and Somasundaran, P., "A model for the cooperative adsorption of surfactant mixtures on solid surfaces," *Journal of Colloid and Interface Science*, vol. 310, pp. 377–384, 2007.

[293] Zhang, W., Xu, Q., Zou, S., Li, H., Xu, W., and Zhang, X., "Single-molecule force spectroscopy on bombyx mori silk fibroin by atomic force microscopy," *Langmuir*, vol. 16, pp. 4305–4308, 2000.

[294] Zhang, W. and Zhang, X., "Single molecule mechanochemistry of macromolecules," *Progress in Polymer Science*, vol. 28, pp. 1271–1295, 2003.

[295] Zhang, W., Zou, S., Wang, C., and Zhang, X., "Single polymer chain elongation of poly(n-isopropylacrylamide) and poly(acrylamide) by atomic force microscopy," *Journal of Physical Chemistry B*, vol. 104, pp. 10258–10264, 2000.

[296] Zhao, J. and Brown, W., "Dynamic light scattering study of adsorption of a nonionic surfactant (c12e7) on polystyrene latex particles: Effects of aromatic amino groups and the surface polymer layer," *Journal of Colloid and Interface Science*, vol. 179, pp. 281–289, 1996.

[297] Zhao, J. and Granick, S., "How polymer surface diffusion depends on surface coverage," *Macromolecules*, vol. 40, pp. 1243–1247, 2007.

[298] Zhu, P. and Napper, D., "The effect of polymer concentration on the dynamics of adsorbed poly(n-isopropylacrylamide) at particle surfaces in water," *Journal of Colloid and Interface Science*, vol. 214, pp. 389–394, 1999.

[299] Zweistra, H. and Besseling, N., "Adsorption and desorption of reversible supramolecular polymers," *Physical Review E*, vol. 74, pp. 021806–1–021806–10, 2006.